The Islamic University of Gaza
Deanship of Research and
graduate students
Faculty of Engineering
Master of Electrical Engineering

الجامعة الإسلامية بغزة
عمادة البحث العلمي
والدراسات العليا
كلية الهندسة
ماجستير الهندسة الكهربائية

A Comparative Study of Photovoltaic Solar Systems Installed in Gaza Strip

دراسة مقارنة لأنظمة الطاقة الكهروضوئية المستخدمة في قطاع غزة

By

Tamer I. Abu Dabousa

Supervised by

Prof. Mohamed M. Abdelati

Professor in Electrical Engineering

A Thesis Submitted in Partial Fulfillment
of the Requirements for the Degree of
Master of Science in Electrical Engineering

February-2018

إقـــــرار

أنا الموقع أدناه مقدم الرسالة التي تحمل العنوان:

A Comparative Study of Photovoltaic Solar Systems Installed in Gaza Strip

دراسة مقارنة لأنظمة الطاقة الكهروضوئية المستخدمة في قطاع غزة

أقر بأن ما اشتملت عليه هذه الرسالة إنما هو نتاج جهدي الخاص، باستثناء ما تمت الإشارة إليه حيثما ورد، وأن هذه الرسالة ككل أو أي جزء منها لم يقدم من قبل الاخرين لنيل درجة أو لقب علمي أو بحثي لدى أي مؤسسة تعليمية أو بحثية أخرى.

Declaration

I understand the nature of plagiarism, and I am aware of the University's policy on this.

The work provided in this thesis, unless otherwise referenced, is the researcher's own work, and has not been submitted by others elsewhere for any other degree or qualification.

Student's name:	تامر عيسى أبو دبوسه	اسم الطالب:
Signature:		التوقيع:
Date:	----/2/2018	التاريخ:

بسم الله الرحمن الرحيم

الجامعة الإسلامية غزة
The Islamic University of Gaza
عمادة البحث العلمي والدراسات العليا
هاتف داخلي: 1150

الرقم: Ref: ج س غ/35/
التاريخ: Date: 2018/03/28م

نتيجة الحكم على أطروحة ماجستير

بناءً على موافقة عمادة البحث العلمي والدراسات العليا بالجامعة الإسلامية بغزة على تشكيل لجنة الحكم على أطروحة الباحث/ **تامر عيسى احمد ابودبوسه** لنيل درجة الماجستير في كلية **الهندسة**/ قسم **الهندسة الكهربية/أنظمة الاتصالات** وموضوعها:

دراسة مقارنة لأنظمة الطاقة الكهروضوئية المستخدمة في قطاع غزة

A Comparative Study of Photovoltaic Solar Systems Installed in Gaza Strip

وبعد المناقشة التي تمت اليوم **الاربعاء** 11 **رجب** 1439هـ الموافق 2018/03/28م الساعة **الحادية عشرة صباحاً**، في قاعة مبنى **القدس** اجتمعت لجنة الحكم على الأطروحة والمكونة من:

أ. د. محمد محمد عبد العاطي	**مشرفاً ورئيساً**	.....
د. عمار محمد رمضان/ أبو هدروس	**مناقشاً داخلياً**	.....
د. محمد طه عمر الأسطل	**مناقشاً خارجياً**	.....

وبعد المداولة أوصت اللجنة بمنح الباحث درجة الماجستير في **كلية الهندسة/قسم الهندسة الكهربية/أنظمة الاتصالات**.

واللجنة إذ تمنحه هذه الدرجة فإنها توصيه بتقوى الله تعالى ولزوم طاعته وأن يسخر علمه في خدمة دينه ووطنه.

والله ولي التوفيق،،،

عميد البحث العلمي والدراسات العليا

أ. د. مازن إسماعيل هنية

E

3106480 المواد المصاحبة :

التاريخ: 30 / 5 / 2018م

الموضوع/ مطابقة مواصفات النسخة الإلكترونية

بعد الإطلاع على الأسطوانات التي تحتوي على رسالة الطالب/ ساهر عيسى أبو دبوسة

رقم جامعي: 120132152 كلية: الهندسة قسم: الهندسة المدنية

فإننا نحيطكم علماً بأنها مطابقة للمواصفات المطلوبة المبينة أدناه:

66

جميع فصول الرسالة في ملف (WORD) واحد وليست ملفات متفرقة.

تحتوي الأسطوانة على ملف (PDF + WORD).

مطابقة التنسيق في جميع الصفحات (نوع وحجم الخط) بين النسخة الورقية والإلكترونية.

مطابقة النص في الصفحة الورقية مع النص في الصفحة الإلكترونية لجميع صفحات الرسالة.

ملاحظة: ستقوم عمادة المكتبات بنشر الرسالة العلمية كاملة (PDF) على موقع المكتبة.

والله ولي التوفيق،

توقيع المكتبة المركزية

Central Library

توقيع الطالب تم استلام نسخة الكترونية فقط

ساهر

Abstract

Solar energy is one of the most important types of renewable energy. It is environmentally friendly where it does not emit greenhouse gases that harm the environment. Recently, the use of PV solar systems has been deployed here in the Gaza Strip as a solution to the problem of the frequent electricity outage. PV systems have different types and each type has its own advantages and disadvantages. So, PV systems have been selected as cases of study to compare the electrical and economic characteristics of each system in proposed conditions. The selected systems represent the different types of PV systems installed in Gaza strip. The selected systems were The Islamic University of Gaza (IUG), Al Azhar University (AAU) and Deir Elatin School (DES) PV solar systems.

For the purposes of work, HOMER software was used to simulate the selected systems as cases of study. The steps of using HOMER software include obtain the solar radiation and temperature data of the case study geographical location, provide the software with the load profile data of the electrical loads connected to the system, modelling and finally simulating of the system. The simulation results of IUG system showed mainly that the rated power of the system inverters was oversized. In the case of DES system, The simulation results showed that the system has a valid economic feasibility during permanent availability of the utility grid and has no benefit during utility grid outage periods. Regarding AAU system, there was no practical method to obtain an accurate load data so, the simulation could not performed and it was suggested as a future work.

In order to confirm HOMER simulation results, PVsyst was used. the procedure that followed in using PVsyst software is the same procedure followed in using HOMER software. PVsyst simulation results for both the IUG and DES systems were compared with those obtained from HOMER. The results from the two software tools were close.

الملخص

تعتبر الطاقة الشمسية من أهم أنواع الطاقة المتجددة وتتميز بأنها صديقة للبيئة فلا ينبعث منها غازات تضر بالبيئة. وفي الآونة الاخيرة، انتشر استخدام الأنظمة الكهروضوئية هنا في قطاع غزة كحل لمشكلة الانقطاع المتكرر للكهرباء العمومية. وحيث أن للأنظمة الكهروضوئية أنواع مختلفة وكل نوع له مميزاته وعيوبه، تم اختيار أنظمة كهروضوئية كحالات دراسة لمقارنة الخصائص الكهربائية والاقتصادية لكل نظام في ظروف مقترحة. وتمثل تلك الأنظمة المختارة الأنواع المختلفة للأنظمة الكهروضوئية التي تم تركيبها في القطاع. والأنظمة المختارة هي: النظام الكهروضوئي للجامعة الإسلامية والنظام الكهروضوئي لجامعة الأزهر والنظام الكهروضوئي لمدرسة دير اللاتين. وقد تم التعرف على مكونات كل نظام ووظيفة كل مكون من تلك المكونات.

في هذه الرسالة، استُخدم برنامج يسمى هومر في عمل محاكاه للأنظمة المختارة كحالات دراسة. وقد تضمنت خطوات استخدام البرنامج الحصول على بيانات الاشعاع الشمسي والحرارة للموقع الجغرافي لحالة الدراسة وتزويد البرنامج ببيانات الحمل الكهربائي الموصول على النظام وعمل نموذج ثم محاكاه للنظام. وقد تبين من نتائج محاكاه نظام الجامعة الإسلامية أن قدرة العواكس في النظام أعلى من القدرة المناسبة للحمل الكهربائي الموصول على النظام. وبالنسبة لنظام مدرسة دير اللاتين فقد اظهرت النتائج أن النظام بدون فترات قطع للكهرباء العمومية ذو جدوى اقتصادية جيدة وأنه لا فائدة للنظام في فترات قطع الكهرباء العمومية. أما بالنسبة لنظام جامعة الأزهر فلم يتم عمل محاكاه للنظام لعدم وجود طريقة دقيقة لمعرفة الحمل الكهربائي الموصول على النظام وتم اقتراح عمل محاكاه للنظام كعمل مستقبلي.

ولتأكيد نتائج المحاكاة ببرنامج هومر تم استخدام برنامج بي في سست. وتم اتباع نفس الخطوات المتبعة في استخدام برنامج هومر لاستخدام برنامج بي في سست. وبمقارنة نتائج برنامج بي في سست لكلاً من نظام الجامعة الاسلامية ونظام مدرسة دير اللاتين مع النتائج التي تم الحصول عليها من برنامج هومر لِكِلا النظامين تبين ان نتائج البرنامجين متقاربة.

Dedication

I dedicate this thesis to

The soul of my father Issa Abu Dabousa

my beloved mother Boshra

and my darling wife Rasha.

Acknowledgment

Praise be to Allah the lord of the worlds and may the blessings and peace of Allah be upon the most honored of messengers our master Muhammad and upon all his family and companions.

I would like to express my thanks and gratitude to my wife who helped and supported me all the time.

I would like to extend my thanks and appreciation to my supervisor Prof. Mohamed M. Abdelati for his continuous and valuable guidance. Besides my supervisor, I would like to thank the discussion committee members, Dr. Ammar Abu-Hudrouss and Dr. Mohammed Taha El Astal for their comments and recommendations.

My thanks are also dedicated to the dean of the University College of Science and Technology, deputy deans and department head for providing me with necessary facilities to finish this work.

Special thanks to Dr. Jamal Alattar, Mr. Hanibal Najjar, engineers of the Attala Company and the engineers of the Gaza Electricity Distribution Company for their cooperation that greatly assisted my work.

Table of Contents

List of Tables

List of Figures

Chapter One

Introduction

1.1 Introduction to renewable energy

Gaza Strip suffers from frequent electricity outage for long periods of time because of the political situation. Therefore, the need for alternative sources of energy became highly imperative. Among these sources, backup generators were a good choice. Recently, the use of PV solar systems began to widely spread due to their merits. As they are environmentally friendly and do not need fuel to operate whereas PV systems depend on sunlight to generate electricity. PV systems became an open research area where many researches have been made in that field.

1.2 Thesis organisation

This document is organized as follows: Chapter One presents an introduction of the thesis. This chapter also includes the problem statement, contribution, objectives, literature review of the thesis and the electricity situation in Gaza Strip. In Chapter Two, the different components used in PV systems, their characteristics and functions were discussed. Different types of each component are also described. Chapter Three presents the types of PV solar systems. In such chapter, solar irradiance and irradiation were described also, sizing of PV system components and their associated losses were stated in mathematical forms. The selected cases of study were presented in Chapter Four. The component types and specifications were fully described. In addition, the components connecting diagrams in the system were depicted. In Chapter Five, Modelling, simulation and optimization of each case of study were performed using HOMER software. This was started with obtaining the load profile of the case of study, importing meteorological data of the location of the case study, modelling and simulating the system. Finally, obtaining and discussing the results. Chapter Six has the same procedure of Chapter Five except that the used software was PVsyst instead of HOMER. The results of PVsyst software were discussed and then compared with the results obtained from HOMER software.

1.3 Problem statement

Recently, the installation of PV solar systems has increased here in Gaza Strip. There are several types of PV systems, some types are connected to the grid, the other types are isolated from the grid. Furthermore, PV systems may or may not have backup batteries. It is worth to mention that, the available electricity amount in Gaza Strip is not enough to meet the demand of electricity. So, the electricity is distributed

according to a distribution schedule, which is often 4 hours "On" followed by 12 hours "Off". Accordingly, the effect of that electricity situation reflects on the performance of PV systems. In another context, most of the followed procedures in designing a PV system are not applied according to the design standards. Furthermore, most if not all PV system designers do not use PV systems design software. Although of the advantage of using design tools in obtaining the optimal design. The study of each type of PV systems has a great importance in knowing the components of the system. In the same time, using design software to simulate PV systems will help to determine the advantages and disadvantages of each system from the electrical and economic aspects.

1.4 Contribution

This thesis aims to determine the electrical and economic characteristics of the different types of PV systems installed in Gaza strip. Thereby, finding out the advantages and disadvantages of the varies types of PV systems. The main contribution of this thesis is the optimization of IUG PV system. The optimization was carried out in a paper entitled "Modelling, simulation and optimization of a PV solar system" presented in the third international conference on basic and applied sciences (ICBAS III) in Al-Azhar University-Gaza on 19-20 March, 2018. In addition to the thesis contributions, the results showed the economic feasibility of DES PV system which is classified as on-grid system. Furthermore, based on the simulation results, the customer who wants to install PV system will have the adequate knowledge to choose the type of PV system that is suitable for his own application.

1.5 Objectives

The main aim of this work is to find out the electrical and economic characteristics of each PV system of those systems selected as cases of study, as well as their advantages and disadvantages. The work objectives are to study each system of the systems selected as cases of study in order to identify the components of the system and their functions. Also to use software tools such as HOMER and PVsyst which accounted as powerful tools in PV systems design, in system optimization or simulation under proposed conditions.

1.6 Literature review

1.6.1 PV solar system components

Kibria, Ahammed, Sony, Hossain and Shams-Ul-Islam have presented comparative studies on different generation solar cells technology. The comparison was done according to material types used in the manufacture, efficiency and price. Based on the authors classification, solar cells are classified into three generations. First generation solar cells are made from crystalline silicon, they have low efficiency, and their production is relatively expensive. Most of second generation solar cell are amorphous silicon based thin film cells, their efficiency is lower than the efficiency of 1st generation cells, their manufacture cost is cheap with respect to the cost of 1st generation cells manufacture. The most developed third generation solar cells are dye sensitized and concentrated cell, their efficiency is high and their cost is relatively low (Kibria, Ahammed, Sony, Hossain, & Shams-Ul-Islam, 2015).

A simple mathematical model of a PV module was introduced by Park, Kim, Cho and Shin in their paper published in 2014. The input parameters to the model are the solar radiation and the temperature while the simulated output is the $I-V$ characteristics curves. The proposed model require the module manufacture data such as open circuit voltage, short circuit current, voltage and current at maximum power point and temperature coefficients of voltage and current (Park, Kim, Cho, & Shin, 2014).

Jakhrani, Samo, Kamboh, Labadin and Rigit have developed an improved mathematical model for computing PV module output power. The purpose of the article was to find a mathematical model using numerical and analytical methods in order to overcome the limitation of the pervious methods which mostly depend on numerical methods only. The required parameters of $I-V$ curve were computed analytically. While the PV module output current was determined by Lambert W function and the PV module output voltage was computed numerically by Newton-Raphson method. The model was found to be a practical model in determining the output power of the PV module (Jakhrani, Samo, Kamboh, Labadin, & Rigit, 2014).

A comprehensive overview of grid interfaced solar PV systems was presented by Mahela and Shaik. The aim of the paper was to provide the researchers, designers and engineers with a wide knowledge of grid connected PV systems, their

components and types. The authors also presented a comparison of MPPT techniques from several aspects, advantages and disadvantages of solar inverters topologies and a comparison of DC to DC converters. Information considered in the paper was derived from more than 100 research publications (Mahela & Shaik, 2017).

1.6.2 Solar radiation

PV system design requires monthly average radiation data. For more precise design, the radiation data should be given for tilt surfaces facing to the sun not for horizontal surfaces. In fact solar radiation data on horizontal surfaces are available while it is generally not available on tilt surfaces. Klein has described a simplified method to estimate the average daily solar radiation on surfaces oriented directly toward the equator and he has extended the method to estimate the solar radiation on surfaces east or west of south (Klein, 1976).

Jakhrani, Othman, Rigit, Samo and Kamboh have presented an estimation of incident solar radiation on tilted surface using different empirical models. In general, no difference between authors about estimating the beam and reflected radiation, the difference is in estimating the diffuse radiation. The proposed empirical models are Liu and Jordan, Hay and Davies, Reindl et al., Koronakis, Badescu and HDKR. The authors concluded that the better model to estimate the solar radiation in cloudy weather was Liu and Jordan model (Jakhrani, Othman, Rigit, Samo, & Kamboh, 2012).

1.6.3 Simulation using HOMER and PVsyst

A comparative study of on-grid and off-grid PV solar systems is presented by Okedu, Uhunmwangho and Ngang. The authors have proposed two scenarios. One scenario was a hybrid off-grid system consists of a PV system with backup battery bank and a backup generator. The other scenario was on-grid system which has the same components of the first scenario in addition to the grid. The comparative study was done using HOMER software. The results showed that superiority is for on-grid systems (Okedu, Uhunmwangho, & Ngang, 2015).

Singh, Baredar and Gupta have presented a simulation and optimization of a hybrid PV solar system using HOMER pro. The selected area of study was the Maulana Azad National Institute of Technology in India. The solar radiation and temperature data of the study area location was obtained from surface meteorology

and solar energy website of the National Aeronautics and Space Administration (NASA). The electrical load included lighting, ceiling fans, small appliances and computer devices with a 5 kW maximum load demand. The system components were biomass gasifier generator set, solar PV and fuel cell. The results showed that the optimal configuration of the system contains 5 kW biomass gasifier generator set, 5 kW solar PV and 5 kW fuel cell. For the optimal configuration, the cost of energy and the net present cost were 15.064 Rs/kWh and Rs5189003 respectively (Singh, Baredar, & Gupta, 2015).

In the fish farming business, improving fishery production capacity depends on maintaining water quality which decreases as the dissolved oxygen increases. The solution of the dissolved oxygen problem is to aerate the water using aeration blower. Based on the previous solution, Prasetyaningsari, A. Setiawan and A. A. Setiawan have presented a design optimization of solar powered aeration system for fish pond using HOMER software. The primary load demand was 450 kW/d while the peak load was 1.692 kW/d. The results showed that the optimal configuration of the system consists of 1 kW PV array, 8 batteries of 200 Ah and 0.2 kW inverter. The optimal configuration was the most economically feasible (Prasetyaningsar, Setiawan, & Setiawan, 2012).

A designing of a 2 kW stand-alone PV System was presented in a paper authored by Morshed, Ankon, Chowdhury and Rahman. The paper was published in 2015. The design was carried out using SolarMAT, HOMER and PVsyst software. The purpose of the paper was to design the 2 kW system and evaluate the three software used in the design. The authors of the paper are the developers of SolarMAT software. The results data of SolarMAT was closer to the practical data while a small extend difference was between PVsyst results data and the practical data. The authors found that HOMER is preferred for hybrid system design, optimization and sensitivity analysis. While PVsyst is a good choice for detailed design and economic analysis of standalone and grid tie systems. Moreover, SolarMAT is a reliable choice for simple design (Morshed, Ankon, Chowdhury, & Rahman, 2015).

A grid tie PV solar system was presented by Nand and Raturi. Different sizes of the system were proposed in order to determine the optimal size of the system.

The system was designed using PVsyst and the economic feasibility analysis was performed using HOMER software. The authors concluded that PVsyst is a useful tool for designing a PV system and HOMER software is a very good tool in economic analysis. The results showed that the optimal size of the grid tie system is 5 kW. In the other hand, the high capital cost of PV systems makes them non-competitive with the available conventional energy systems (Nand & Raturi, 2013).

1.7 Gaza Strip electricity

The electricity resources in the Gaza Strip are Gaza Power Generating Company (GPGC) with a capacity of 140 MW, the feed lines from the Israel occupation with a total power of 120 MW and the Egyptian feed lines with a capacity of 22 MW. In fact, GPGC generates about 60 MW for most the time. Therefore, the available amount of electricity is 200 MW. Actually, the required amount of electricity to meet the Gaza Strip demand is 500 MW. This means that the electricity shortage is more the half of the electricity demand. Electricity shortage yields to long periods of electricity outage in the electricity distribution schedule. The electricity distribution schedule is often 4 hour of electricity connecting followed by 12 hour of electricity disconnecting.

Chapter Two

Photovoltaic Solar System Components

2.1 Introduction

PV system components vary as the system type varies. Each component of the system has a specific function that completes the system operation. No doubt that the common component of PV systems is the PV array, where it converts the solar energy into electric energy. In this chapter, various components of PV systems are described, their characteristics and functions.

2.2 Photovoltaic cell

Photovoltaic is a term comes from the Greek φῶς (phōs) meaning "light", and from "volt", the unit of electrical voltage, its abbreviation is PV. A PV effect phenomenon is the generation of electric voltage or current in a material when it is exposed to light. A solar PV cell is a PV cell when the sun is the source of light.

2.2.1 PV cell basics

A PV cell is a semiconductor material in the form of P-N junction. The backside of the material is the positive side and the other (the side towards the sun) is the negative one. The N-type material is kept thin to allow passing of light through to the P-N junction.

A solar PV cell converts solar energy into electrical energy. As shown in Figure (2.1), when a PV cell is exposed to sun light, the semiconductor material of the PV cell absorbs the photons of light rays. This gives the electrons of the semiconductor material more energy to jump to higher energy levels then to break their atomic bonds and become free. These free electrons flow into metal contacts as an electrical current. Each PV cell is capable of generating 4 A of direct current at 0.5 V resulting in 2 W of electrical power.

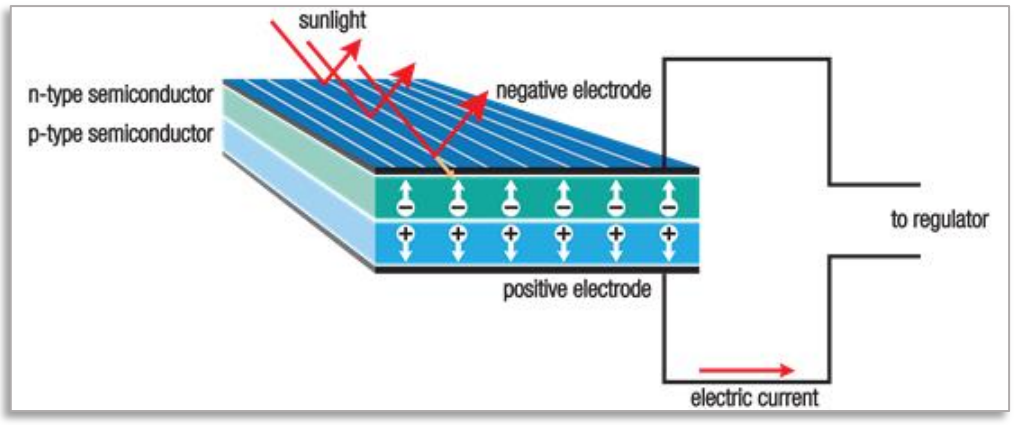

Figure (2.1): How a solar PV cell works (Wolinsky, 2010).

The mostly used material in manufacturing PV cells is silicon. The diameter of a typical silicon PV cell is about 12 cm with thickness of about 0.25 mm (Ventura, 2011). Figure (2.2) shows a silicon PV cell.

Figure (2.2): Silicon PV cell.

2.2.2 Different generations of solar cells

Solar cells are generally classified into categories called generations. Normally, there are three main generations: First, second and third. First generation solar cells have low efficiency. Their production is relatively expensive. They represent 85-90% of the global annual market today. Second generation solar cells also have low efficiency but their cost of production is lower. They currently represent 10-15% of the global PV module sales. Third generation solar cells have high efficiency. They are still under research and they have not entered commercial markets yet (Kibria et al., 2015).

First generation solar cells: These solar cells are the most commonly used cells due to their high efficiency compared to the second generation solar cells. They are produced from silicon in the form of wafers. Figure (2.3) shows the structure of first generation solar cell.

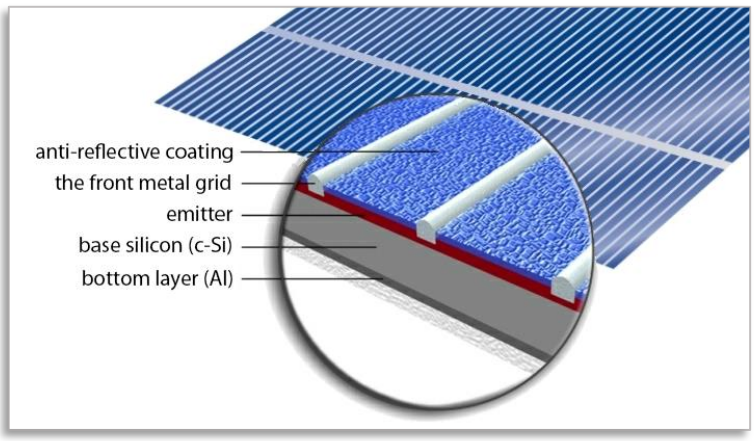

Figure (2.3): First generation solar cell structure (ProEnerga company, 2016).

First generation solar cells are of two types: Mono (or single) crystalline and poly (or multi) crystalline solar cells. The efficiency of a mono crystalline solar cell is about 24%. It is higher than the efficiency of a poly crystalline one which is about 20%. However, producing poly crystalline cell is easier and less in cost. Figure (2.4) shows the actual shapes of mono and poly crystalline cells.

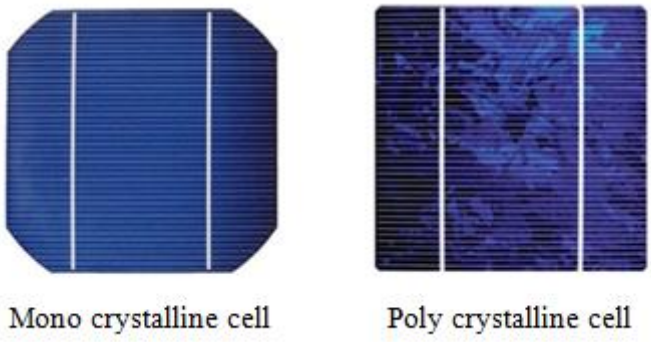

Figure (2.4): Mono and poly crystalline cell shapes

(Solaris Technology Industry, 2014).

To increase the power produced by solar cells, they are connected together to form a module. A solar panel consists of multiple modules connected to each other. Arranging solar panels in rows and columns forms an array. Sometimes modules connected in a same connecting box (forming a sub-array) are called string. Figure (2.5) shows how a PV array is configured from solar cells.

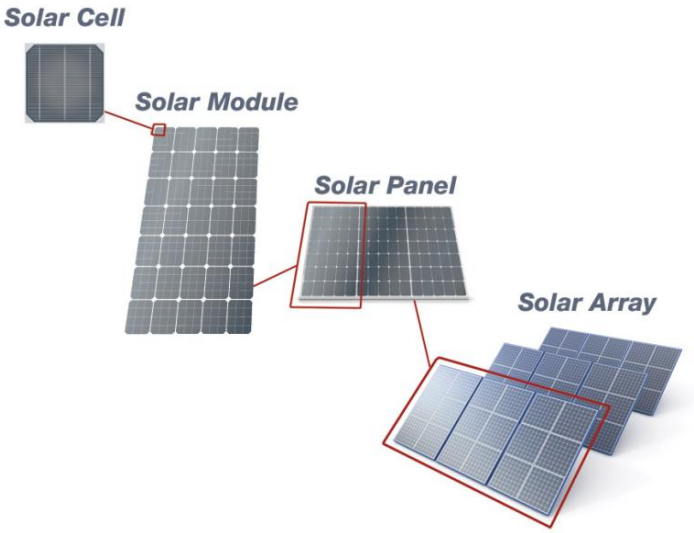

Figure (2.5): Configration of a PV array from solar PV cells (Vijay, 2014).

Second generation solar cells: The efficiency of these cells is less than that of the first generation solar cells. However, they have an advantage that their

manufacture enables them to be laid on flexible substrate. Hence, they are more applicable for installing on curved surfaces and in photovoltaic-integrated buildings. Figure (2.6) shows the structure and actual view of a thin film solar cell.

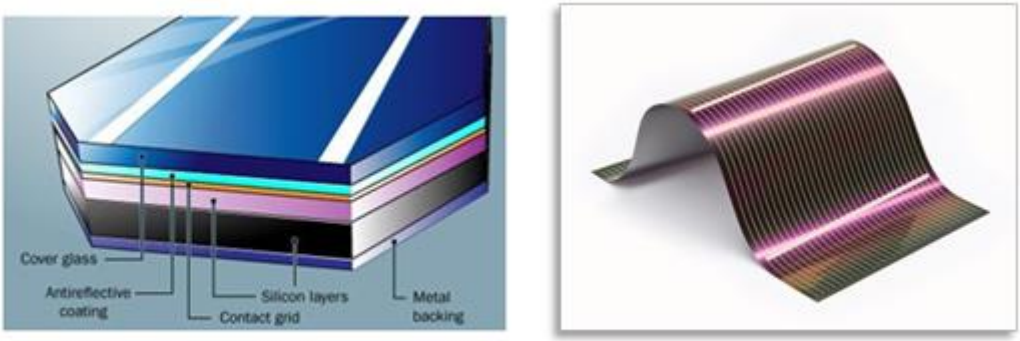

Structure of a thin film solar cell Actual view of a thin film solar cell

Figure (2.6): Structure and actual view of a thin film solar PV cell (Çelik, Teke, & Yıldırım, 2015).

Second generation solar cells include amorphous Si (a-Si) based thin film solar cells, Cadmium Telluride/Cadmium Sulfide (CdTe/CdS) solar cells and Copper Indium Gallium Selenide (CIGS) solar cells.

Third generation solar cells: The technologies used in this generation are promising technologies. Most of third generation solar cells are dye sensitized and concentrated solar cells. The idea of dye-sensitized solar cells (DSSC) is based on the transportation of the electron hole pairs which occur in the dye molecules through Titanium dioxide (TiO_2) nanoparticles. See Figure (2.7). DSSC has low efficiency, its cost is also low due to the ease of production compared to other third generation technologies.

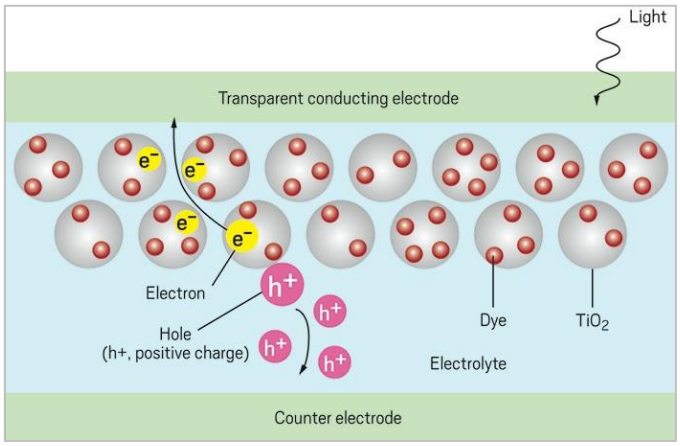

Figure (2.7): How DSSC work (American Chemical Society, 1998)**.**

The idea of concentrated PV (CPV) solar cells is to concentrate as much as possible of sun radiation on a small area where the PV cell is located. This will reduce the amount of semiconductor material which might be very expensive, so the cost will be reduced. CPV is a promising technology. Figures (2.8) and (2.9) show two different techniques used in CPV and their implementation.

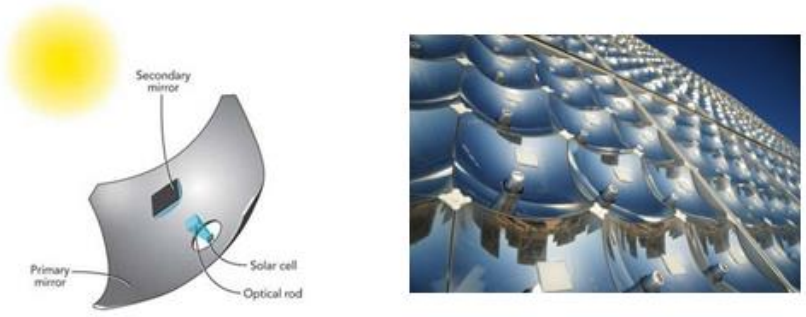

Figure (2.8): Reflection mirrors solar collectors (CBS Interactive, 1991).

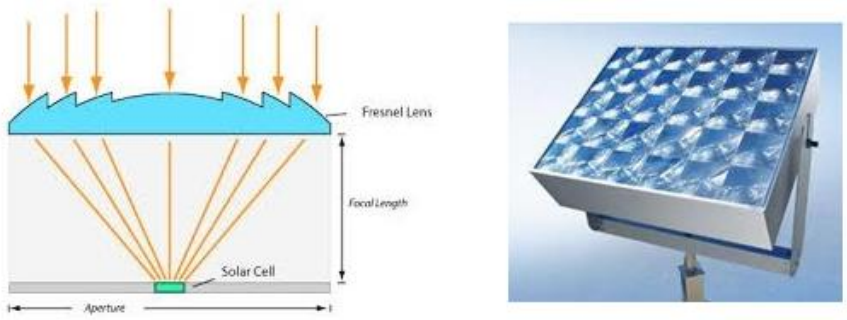

Figure (2.9): Fresnel lens solar collectors (D'Angelo, 2010).

2.2.3 Equivalent model of PV module

A PV cell can be represented as a current source in parallel with a single diode (Xue & Wang, 2013). In actual solar cells, the voltage loss on the way to the external contacts is observed. This voltage loss is expressed by a series resistance R_s. Furthermore, leakage currents are described by a shunt resistor R_{sh} (Mahammed, Bakelli, Oudjana, Arab, & Berrah, 2012). The equivalent circuit of a PV cell is shown in Figure (2.10).

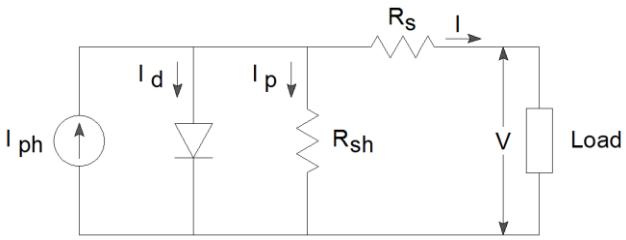

Figure (2.10): Equivalent circuit of a PV cell.

where I is the current through the load and V is the voltage across the load. By applying Kirchhoff's current law to the above circuit, the current I can be obtained by the following equation (Bellia, Youcef, & Fatima, 2014):

$$I = I_{ph} - I_d - I_p \tag{2.1}$$

where: I_{ph} is the photocurrent which is directly proportional to the amount of incident solar light on the PV cell, I_d is the diode current which is proportional to the reverse saturation or leakage current I_o, I_p is the current leak in the parallel resistor.

I_{ph}, I_d and I_d can be obtained using the following equations:

$$I_{ph} = I_{sc} + \frac{K_t(T_c - 298)G}{1000} \tag{2.2}$$

$$I_{sc} = \frac{G}{1000}\left[I_{sc-ref} + K_t(T_c - 298)\right] \tag{2.3}$$

$$I_d = I_o\left\{\exp\left[\frac{q(V + IR_s)}{AKT_c}\right] - 1\right\} \tag{2.4}$$

$$I_o = I_{o-ref}\left(\frac{T_c}{298}\right)^3 \exp\left[\frac{qE_g}{AK}\left(\frac{1}{T_c} - \frac{1}{298}\right)\right] \tag{2.5}$$

$$I_p = \frac{V + IR_s}{R_{sh}} \tag{2.6}$$

where: I_{sc} is the short-circuit current in ampere, K_t is the short-circuit current temperature coefficient, T_c is the cell temperature in kelvin, G is the light intensity in watt per square meter, I_{sc-ref} is the short-circuit current of a cell at a reference temperature (25 °C) and solar irradiation (1000 W/m^2) in ampere, I_o is the reverse saturation current in ampere, q is the electron charge in coulomb, A is the diode factor, K is Boltzmann's constant in joule per kelvin, I_{o-ref} is the reverse saturation current of a cell at a reference temperature and solar irradiation in ampere, E_g is the band gap energy in electron volt. The number 298 is the conversion of 25 °Celsius to Kelvin (Park et al., 2014).

The final analytical expression for the current in a PV cell according to the model is:

$$I = \frac{G}{1000}\left[I_{sc-ref} + K_t(T_c - 298)\right] + \frac{K_t(T_c - 298)G}{1000} - \left\{I_{o-ref}\left(\frac{T_c}{298}\right)^3 \exp\left[\frac{qE_g}{AK}\left(\frac{1}{T_c} - \frac{1}{298}\right)\right]\right\} \times \left\{\exp\left[\frac{q(V + IR_s)}{AKT_c}\right] - 1\right\} - \frac{V + IR_s}{R_{sh}} \quad (2.7)$$

Since the PV module consists of N_s cells connected in series and N_p cells connected in parallel, equation (2.7) can be generalized for a PV module as follows:

$$I_M = \frac{G}{1000}\left[I_{sc-ref-M} + K_t N_p(T_c - 298)\right] + \frac{K_t N_p(T_c - 298)G}{1000} - \left\{I_{o-ref-M}\left(\frac{T_c}{298}\right)^3 \exp\left[\frac{qE_g}{AN_sK}\left(\frac{1}{T_c} - \frac{1}{298}\right)\right]\right\} \times \left\{\exp\left[\frac{q(V_M + I_M R_{s-M})}{AN_sKT_c}\right] - 1\right\} - \frac{V_M + I_M R_{s-M}}{R_{sh-M}} \quad (2.8)$$

where, I_M and V_M are the current and voltage of the PV module, respectively. $I_{sc-ref-M}$ is the module short-circuit current at a reference temperature and solar irradiation $= N_p \times I_{sc-ref}$. $I_{o-ref-M}$ is the module reverse saturation current at a reference temperature and solar irradiation $= N_p \times I_{o-ref}$. R_{s-M} is the series resistance $= R_s \times \frac{N_s}{N_{sh}}$. R_{sh-M} is the shunt resistance $= R_{sh} \times \frac{N_s}{N_{sh}}$.

2.2.4 Characteristic curves of a PV module

Based on equation (2.8) the $I - V$ and $P - V$ characteristic curves of a PV module are as shown in Figure (2.11).

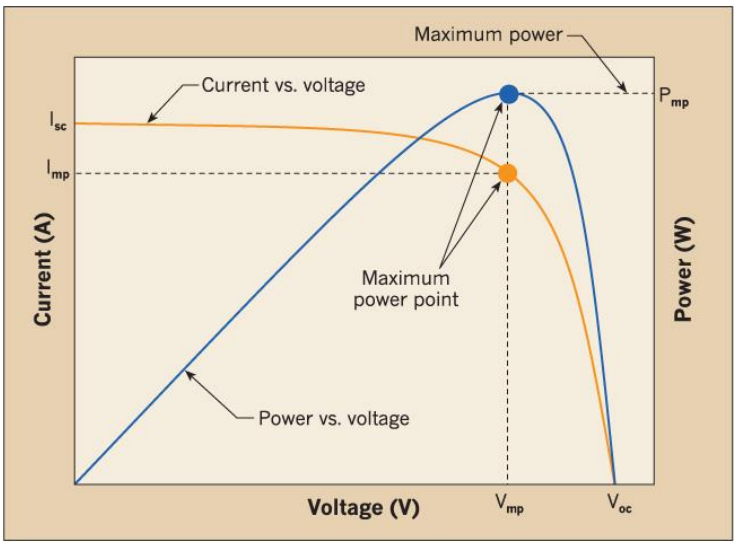

Figure (2.11): I-V characteristic curves of a PV module (Eby, 1995).

The span of the $I-V$ curve ranges from the short circuit current (I_{sc}) at zero volts to zero current at the open circuit voltage (V_{oc}). At the knee of a normal $I-V$ curve is the maximum power point (I_{mp}, V_{mp}), the point at which the module generates its maximum power (P_{mp}) (Solmetric, 2012).

The fundamental parameters related to a PV module are short circuit current (I_{sc}), open circuit voltage (V_{oc}), maximum power (P_{mp}), current at maximum power (I_{mp}) and voltage at maximum power (V_{mp}) (Mohammed, 2011). They are measured under standard test conditions (STC). The two important STC values are the temperature = 25 °C and the irradiance = 1000 W/m^2.

Effect of module temperature on the $I-V$ characteristic curve: The output voltage of a PV module is actually a variable value that is primarily affected by module temperature. The relationship between module voltage and module temperature is an inverse relationship. If the module temperature increases, the output voltage decreases and vice versa. Figure (2.12) shows the $I-V$ characteristic curves at different module temperature values.

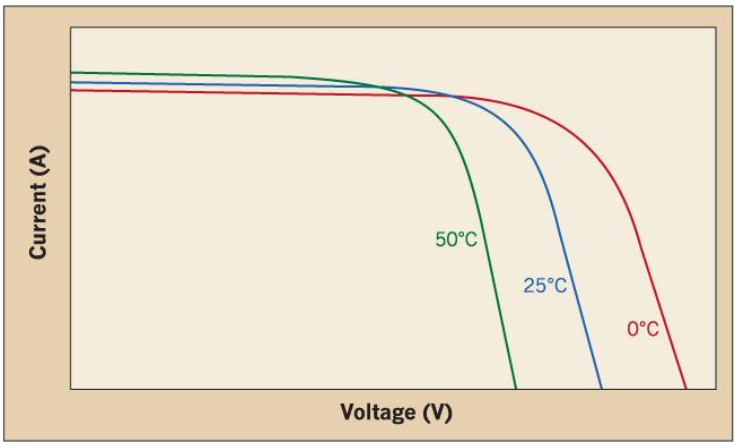

Figure (2.12): Effect of temperature on the I-V characteristic curve (Eby, 1995).

From the previous figure, it can be observed that the temperature linearly decreases the output voltage. The module temperature affects the short circuit current by a small amount in a proportional relationship. As the module temperature increases, the short circuit current slightly increases and vice versa (Jakhrani et al., 2014).

Effect of irradiance on the $I-V$ characteristic curve: The output current of a PV module is directly proportional to solar radiation (Foster, Ghassemi, & Cota,

2009). Actually the current increases linearly with increasing solar radiation while the output voltage increases logarithmically with increasing solar radiation. Figure (2.13) shows the $I-V$ characteristic curve under different irradiance levels.

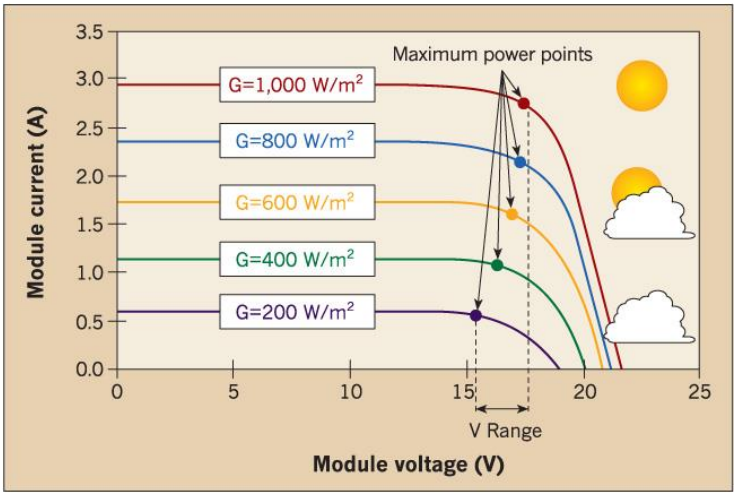

Figure (2.13): Effect of irradiance on the I-V characteristic curve (Eby, 1995).

2.3 Battery

The function of the battery is to store electrical energy in a form of chemical energy. The batteries are used in PV systems to provide the electrical loads with the required energy in night hours and in cloudy weather where the solar energy is insufficient.

2.3.1 Battery types

There are many types of batteries. Each type has a specific design which makes the battery suitable for a certain application. The most commonly used type of batteries in PV system is lead acid. Many researches are currently being carried out in the field of Li-ion batteries (Sumathi, Kumar, & Surekha, 2015).

2.3.2 Battery performance

Battery capacity: The capacity of the battery is defined as the amount of energy stored in the battery. The measuring unit of battery capacity is often ampere-hours (AH) which refers to the number of hours for which a battery can provide a current equal to the discharge rate at the nominal voltage of the battery.

Autonomy: It is the time period a battery can provide energy to the electrical load when there is no energy supplied from the PV array. Autonomy is measured either in hours or days.

Battery lifetime: The battery lifetime is equivalent to the number of cycles of charging/discharging stages. Battery lifetime is affected by several factors. Some of those factors are related to the battery design such as material type used in battery manufacture. Other factors are related to the operation condition such as ambient temperature, depth of discharge and average state of charge.

2.3.3 Battery charging

In general, the battery is charged in four charge modes. These modes are:

Bulk or normal charge: The charging current is kept constant and the voltage is left to increase. In this mode the battery is charged to about 80% of its capacity.

Absorption charge: the voltage is fixed at the peak value and the current is gradually reduced. In this mode the remaining 20% of battery capacity is returned.

Float or finishing charge: The charging current is reduced then kept constant at a certain value and the voltage is fixed at a constant value. The importance of this mode is to compensate the loss of battery capacity caused by its self-discharging.

Equalizing charge: A constant voltage is applied to the battery and the current is adjusted to a very low value. The purpose of the equalizing charge is to remove the sulphation from the lead plates and to eliminate the stratification of the electrolyte. The below figure illustrates charge modes.

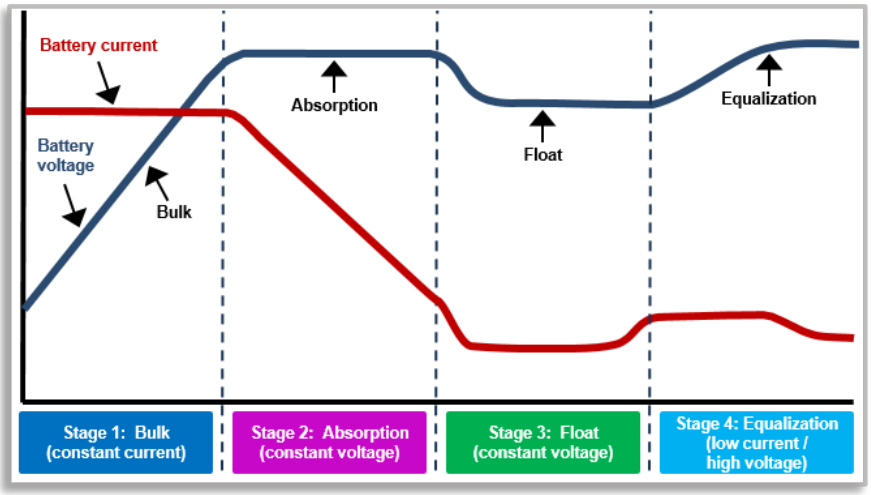

Figure (2.14): Charge modes (American battery charger company, 2015).

State of charge (SOC): Is the available capacity as percentage of the fully capacity. Discharging a battery resulting in decreasing of SOC while charging resulting in increasing SOC, that is when the battery is fully charged then the SOC is

100%. The relation between the SOC and the DOD is SOC+DOD=100%. Figure (2.15) shows the relation between SOC and DOD. The DOD will be defined later.

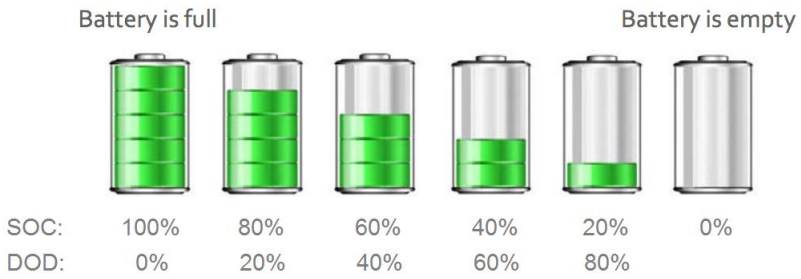

Figure (2.15): Relation between SOC and DOD.

2.3.4 Battery discharging

Discharge rate: The battery discharge current is changed depending on the changes of the load connected to the battery. Hence the battery is discharged in different discharge rates. Every battery is designed to a specific discharge rate which represents by the total capacity denoted as C and a number. For example C10, a discharge rate of C10 means that the battery is being discharged at a current equal to tenths the battery capacity. The battery discharge rate affects its capacity. The higher the discharge rate or current, the lower the capacity that can be withdrawn from a battery to a specific allowable DOD or cut off voltage.

Depth of discharge (DOD): Is referred to the percentage of the capacity drawn from the battery to its total capacity, the two qualifiers for depth of discharge in PV systems are the allowable or maximum DOD and the average daily DOD.

Allowable DOD: Is the maximum percentage of the capacity drawn from a battery. The DOD is dictated by the discharge rate and the cut off voltage. In PV systems the load low voltage disconnect (LVD) set point of the battery charge controller dictates the allowable DOD at a certain discharge rate. Based on the battery type used in PV system the design allowable DOD may be as high as 80% deep cycle.

Average daily DOD: Is the percentage of the full-rate capacity drawn from a battery with the average daily load profile. If the loads are constant, the average daily DOD will be greater in winter months, the reason is the long operation period of winter nightly loads. The average daily DOD is proportional inversely with autonomy. Figure (2.16) shows the allowable and average daily DOD as a percentage of the capacity.

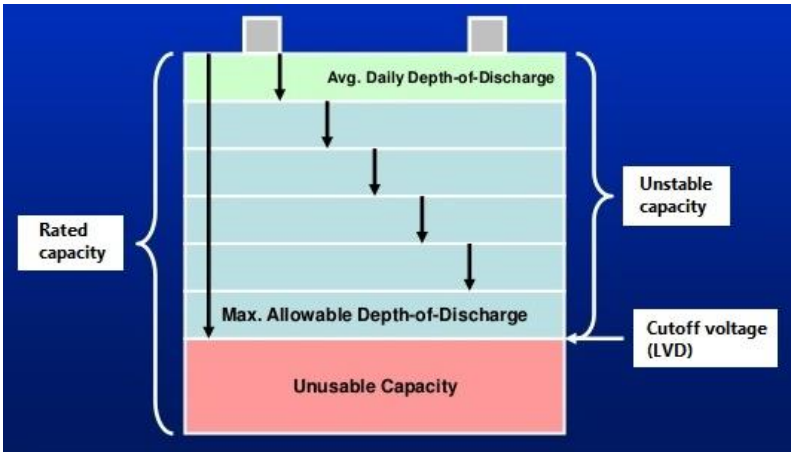

Figure (2.16): Allowable and average daily DOD as a percentage of the capacity (Dunlop, 2012).

Self-discharge rate: Self-discharge rate is defined as the charge loss of the battery without connecting to a load due to the battery internal chemical reactions. Self-discharge rate depends on battery type, state of charge, ambient temperature and other factors.

2.4 Maximum power point tracking (MPPT)

Improving PV array efficiency can be done either by material development or by optimization techniques. Optimization techniques are classified mainly into dynamic and static based techniques. Dynamic techniques use electro-mechanical equipment. This equipment works to keep the PV array in a position facing to the sun to collect the maximum possible solar radiation. This is why these techniques are known as sun trackers. Static techniques use control techniques which is often called maximum power point tracking techniques (Jaen, Moyano, Santacruz, Pou, & Arias, 2008).

The PV module has non-linear characteristics. The operating point of PV cells is influenced by solar radiation, solar cell temperature and load values. At a given irradiation and temperature, There is only one possible optimum operating point to extract the maximum available power from the PV module. The principle of MPPT is by adjusting the load impedance to make the PV power generation system always works near the maximum power point under different environmental conditions. Different possible techniques were proposed for MPPT in order to increase the PV's efficiency (Diab, Helw, & Talaat, 2012).

MPPT control techniques are classified into conventional and intelligent techniques. Conventional techniques are such as incremental conductance and perturbation and observation while intelligent techniques like fuzzy logic and neural networks. Methods used to increase the PV system efficiency is shown below.

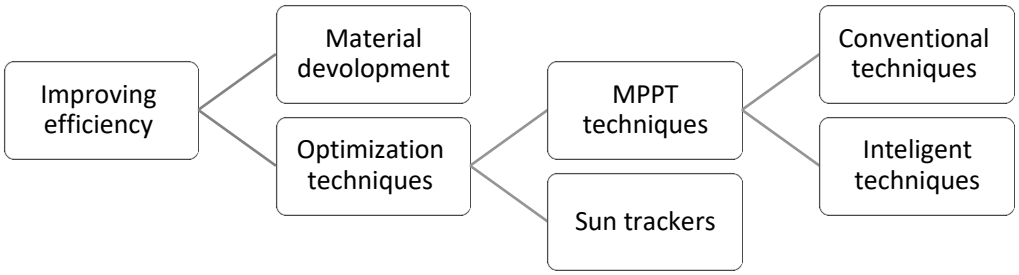

Figure (2.17): Methods used to increase PV system efficiency.

2.5 Charger

A charger is a solid state device that has an input voltage from the PV array and an output voltage equal to the battery bank voltage. As the battery charge modes require various current and voltage levels, the charger output voltage should be controlled to achieve optimal battery charging. Optimal charging process enhance battery performance and battery life.

The main part of a charger is a DC-DC converter. The charger also has integrated control circuits which have specific functions, e.g. preventing against overcharge and deep discharge. Most chargers use maximum power point tracking schemes to extract the maximum power from the PV array.

2.5.1 DC-DC converter

A DC-DC converter is a power electronic circuit which converts direct current of source from one voltage level to the required voltage. They are classified into linear and switched. linear DC/DC converter uses a resistive voltage drop to create and regulate a given output voltage. Switched-mode DC/DC converts by storing the input energy periodically and then releasing that energy to the output at a different voltage. Accordingly switched DC-DC converters have higher efficiency than liner ones.

The most used topologies for switched DC-DC converters in PV systems are step-down (buck converter), step-up (boost converter) and single unit of step-down and step-up (buck –boost) and cuk converters (Mahela & Shaik, 2017).

2.5.2 Charge controller types

Charge controllers have two basic types: shunt and series controllers. The following is a brief overview of charge controller types.

Shunt controllers: A shunt controller has a switch connected in shunt with the PV panel. When the battery reaches the voltage regulation set point the shunt switch will short circuit the PV array, thereby it will not feed the battery. The blocking diode prevents short-circuiting of the battery. Shunt controllers are limited to use in PV systems with PV module currents less than 20 A. Note that PV modules and arrays can be short-circuited without any harm. Figure (2.18) shows the basic circuit of a shunt controller.

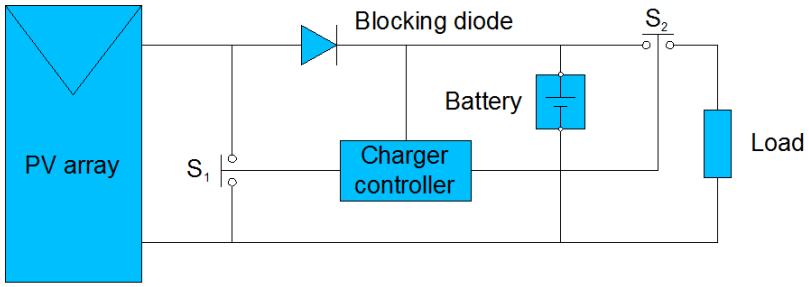

Figure (2.18): Basic circuit of a shunt controller.

Series controllers: In a series controller, a relay or a solid-state switch opens the circuit between the module and the battery to stop charging or limits the current in a series-linear manner to hold the battery voltage at high value. The major drawback in series controller is the additional losses associated with the series switch which passes the charging current. This type of controllers is commonly used in small PV systems. It is also preferred for using in large systems due to the current limitation of shunt controllers. Figure (2.19) shows the basic circuit of a series controller.

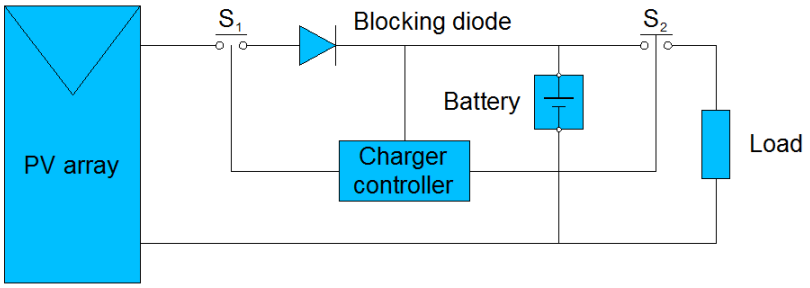

Figure (2.19): Basic circuit of a series controller.

2.6 Inverter

Inverters are used to convert DC current to AC current. They convert DC power from the batteries or the solar array into 50 or 60 Hz AC power. Inverters can be transformer based or high frequency switching types. High frequency switching based inverters have high efficiency compared with transformer based inverters. Inverters can be stand alone, utility interconnected or a combination of both.

2.6.1 Inverter types

Inverters are classified into: stand-alone and grid tie. An overview of inverter types is as follow.

Stand-alone inverters: Stand-alone inverters are designed to work in off-grid systems. Many stand-alone inverters incorporate integral battery chargers to replenish the battery from an AC source, when available. Normally, inverters of this type do not interface in any way with the utility grid.

Grid tie inverters: Grid-connected inverters convert the DC power to AC power in synchronization with electric utility grid. They are designed to quickly disconnect if the utility grid goes down. This is an NEC requirement. So all grid tie inverters are designed to be anti-islanding devices and the voltage on the AC side of the inverter must reduce to zero within two seconds of the gird going down. Grid-connected PV systems have three possible structure topologies of the inverters: string, multi-string and central inverter. See Figure (2.20).

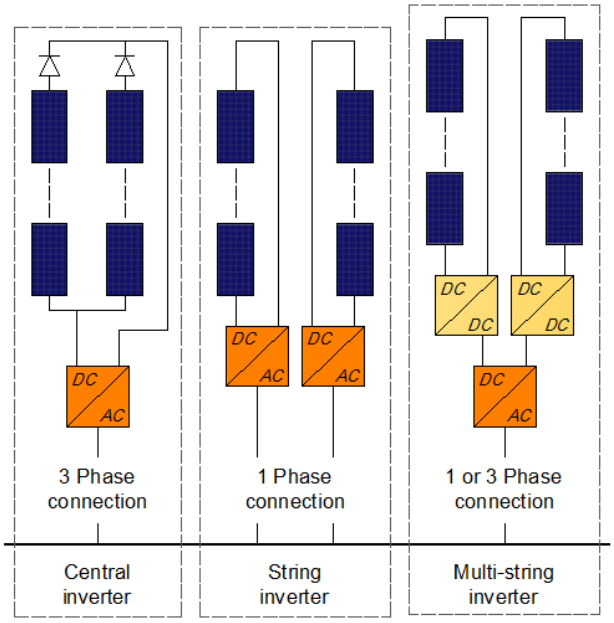

Figure (2.20): Grid-tied inverter topologies.

2.7 Mounting Structure

The PV modules mounting structure should be designed in such a way that it can withstand rain, hail, wind, load of the modules and other adverse conditions. When installing a PV array mounting structure, issues such as durability of the design, tilt angle, orientation and PV array shading should be taken into account. Different tilt angles lead to different efficiency values of the PV module. In fact, the optimum tilt angle changes according to the position of the sun in the sky. So, the optimal tilt angle should be chosen to guarantee falling of the maximum solar radiation on the PV module surface all over the year. Similarly, shading has a significant effect on the PV generation. It is essential that the PV arrays should be installed at shading-free locations. To mitigate the wind pressure on the PV array, the PV panels are separated by a small spacing. This separation will also work on cooling the PV panels. Moreover, dust accumulation on a PV module surface reduces the efficiency of the module, therefore, PV modules require cleaning from time to time. For this purpose a sufficient passing area should be left between the PV strings in order to serve the PV array. On the other hand, mounting structure item includes a battery rack. Battery companies often provide batteries with a suitable rack.

2.8 Energy Meters

Energy meters are used in some cases just for measuring the consumed electrical energy by the load from the PV system or the local electric utility. In other case, energy meters measure the consumed energy in two directions (export and import), so they are known as bidirectional meters. Bidirectional meters are used when the PV system and the electric utility are interconnected.

2.9 Cables and wires

Cables and wires are used to establish connection between PV system components. They must be appropriately sized to reduce power loss. Sizing cables and wires depends on type of the conducting material of the cable, the amount of current that passes through the cable and the length of the cable. In addition to the appropriate sizing, selection of relevant type of wire is also important in the case of solar PV application. For outdoor applications, ultraviolet stabilized cable must be used, while normal residential cables can be used in indoors. To install cables and wires, cable trays and/or ducts are required.

2.10 Protection devices

Protection devices are very important component in a PV system. They protect the system against electrical faults. AC and DC protection devices are used to prevent each component of a PV system. Protection devices include fuses and fuse holders, surge protective devices, miniature circuit breakers and molded case circuit breakers. Protection devices should be properly rated to provide the optimal protection. Protection devices item includes distribution boards and combiners boxes.

2.11 Grounding system

Grounding is important for safety considerations. Grounding equipment provides a well-defined, low-resistance path from PV system to ground. The importance of grounding is to protect a PV system from current surges, lightning strikes or equipment malfunctions. Moreover, grounding stabilizes voltages and provides a common reference point. PV systems operating under 50 V do not require grounding according to the electrical code. If the maximum system voltage of a PV system is greater than 50 V then one conductor must be grounded. Although chassis ground is required for all hardware even that operating under 50 V. Each company who works in the PV systems field has its own recommendation for grounding. In general, grounding of PV modules and their mounting structure is often made.

2.12 Monitoring and control

Monitoring and control of PV systems is essential for reliable functioning and maximum yield of any solar electric system. Monitoring and control can be performed via the LCD of different devices used in a PV system. For large systems which consist of many devices, a separate monitoring and control unit is used. Most of monitoring and control units enable remote monitoring and control through connecting to the Web using Ethernet connection. This implies that the system data can be accessed via the Internet from any location worldwide.

Chapter Three

PV System Design

3.1 Introduction

PV system yield is affected directly by the solar radiation that falls on the PV array surface. As it is known that the solar radiation is varying from time to time. Therefore, it is important to know the solar radiation concepts which deemed as an essential step in sizing a PV system, they also help to determine the optimal orientation of the PV array. In the other hand, PV system should be designed to provide a load with the required energy. So, accurate estimation of the load plays an important role in PV system design. Moreover, the losses associated with the components of the system should be taken into account in order to optimally design the PV system. In this chapter, PV systems types are mentioned firstly, then the solar radiation concepts are described and finally, components sizing and their associated losses are discussed.

3.2 PV system types

PV systems are generally classified based on whether they are connected to the local electric utility grid or not and their connection with other electrical systems and sources. The classification of PV system types is shown in Figure (3.1).

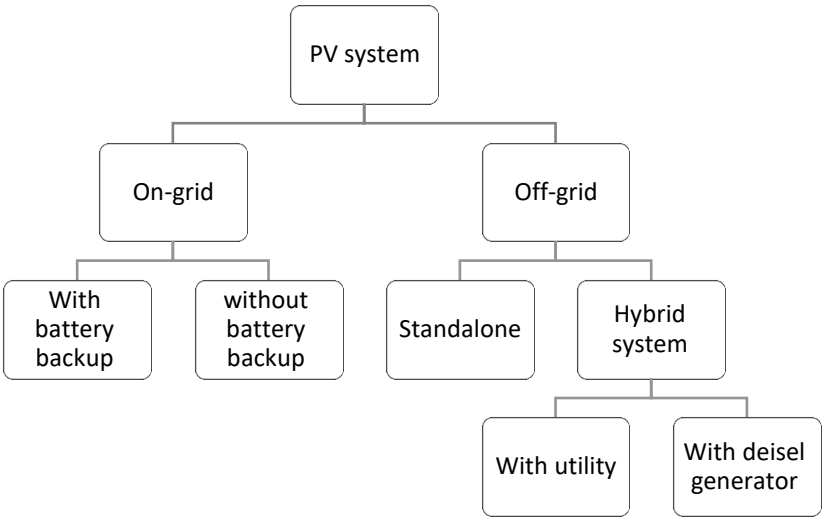

Figure (3.1): PV system types.

3.2.1 On-grid PV system

The primary component of on-grid PV systems is the power conditioning unit (PCU). The PCU converts the DC power produced by the PV array into AC power as per the voltage and power quality requirements of the utility grid. PCU is an electronic unit which consists of chargers and inverters. A bidirectional interface is

made between the PV system AC output circuits and the electric utility network. This allows the AC power produced by the PV system to either supply on-site electrical loads or to back-feed the grid when the PV system output is greater than the on-site load demand. On-grid PV system will not continue to operate and feed back into the utility grid when the grid is down for maintenance or during grid failure state. This safety feature is required in all on-grid PV systems. Inverters in on-grid system must have line frequency synchronization capability to deliver the excess power to the grid. Net meters have a capability to record consumed or generated power in an exclusive summation format. The recorded power registration is the net amount of power consumed that is the total power used minus the amount of power that is produced by the solar power cogeneration system. Figure (3.2) shows a block diagram of on-grid PV system without battery backup.

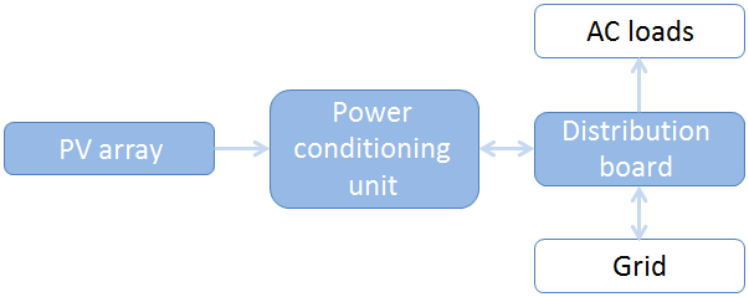

Figure (3.2): Block diagram of on-grid PV system without battery backup.

As was mentioned before that during grid outages, the PV system will automatically shut down. In order to keep the system working, a battery backup is required to supply the electrical loads with electricity. In this case, the system will work as an off-grid system. Battery backup has also the advantage of increasing self-consumption for the system. For more reliability and independence during long-term power outages, a backup generator could be incorporated. Figure (3.3) shows a block diagram of on-grid PV system with battery backup.

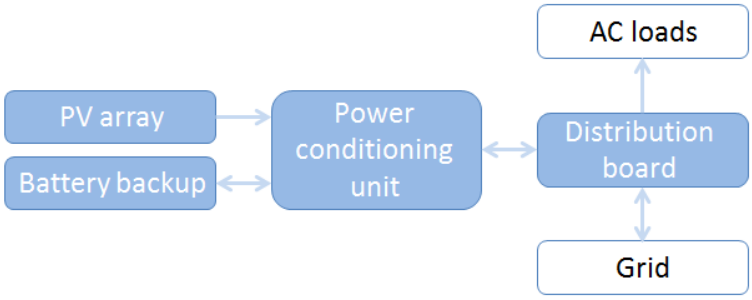

Figure (3.3): Block diagram of on-grid PV system with battery backup.

3.2.2 Off-grid PV system

Off-grid PV system is designed to operate independent of the electric utility grid. In this system, energy is stored in a battery bank then drawn as needed at night or on a cloudy day if the sun is insufficient. In remote areas, off-grid PV system is the best (or even the only) option. Actually off-grid PV systems are classified into standalone and hybrid off-grid systems. Figure (3.4) shows a block diagram of a standalone off-grid PV system.

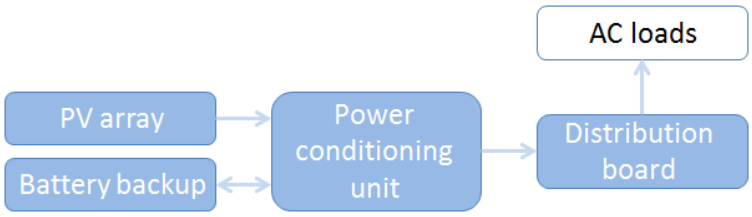

Figure (3.4): Block diagram of a standalone off-grid PV system.

Off-grid PV system may be powered by a generator or utility power as an auxiliary power source in what is called a hybrid system. Hybrid systems are considered as more reliable off-grid PV systems. Figure (3.5) shows a block diagram of hybrid off-grid PV system.

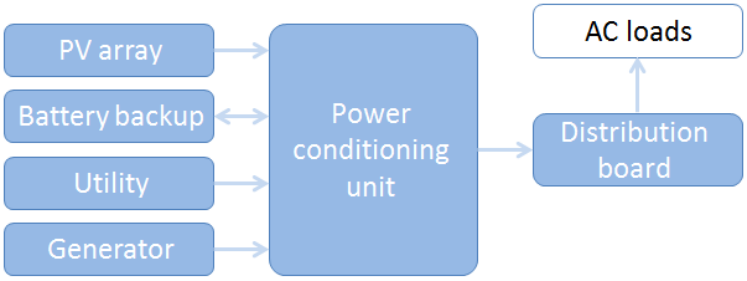

Figure (3.5): Block diagram of a hybrid off-grid PV system.

Power conditioning unit AC or DC coupling: There are two different approaches to integrating battery backup into an existing PV system. They are DC-coupling or AC-coupling. Both involve adding a battery bank and a battery based inverter or charger. In a DC coupled system, a charge controller regulates the output voltage of the PV array to the rated voltage of the battery bank. However in an AC coupled system, a battery inverter is used to connect the battery bank with the PV array inverter. DC-coupling and AC-coupling topologies are shown in the below figure. Examples of DC-coupling and AC-coupling will be presented in Chapter Four.

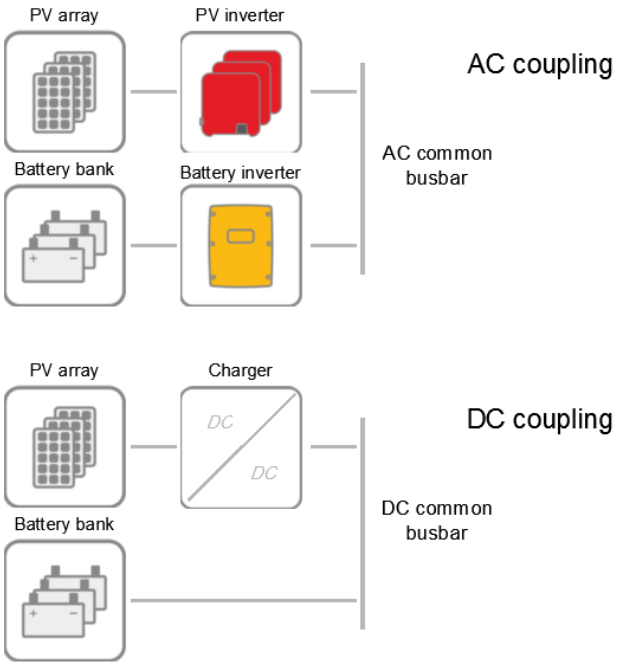

Figure (3.6): Block diagrams of DC coupling and AC coupling.

3.3 Solar irradiance and irradiation

The solar irradiance also known as solar power is an instantaneous power density in units of kW/m^2. It varies throughout the day from zero kW/m^2 at night to the maximum of about 1 kW/m^2. Due to atmospheric effects, typical peak values of terrestrial solar irradiance are on the order of 1 kW/m^2 on surfaces at sea level facing the sun's rays under a clear sky around solar noon. Consequently, 1 kW/m^2 is used as a reference condition for rating the peak output form PV modules and arrays. This value of solar irradiance is often referred to as peak sun. For south-facing fixed tilted surfaces on a clear day, the incident solar irradiance varies along a bell-shaped curve, peaking at solar noon when the surface faces most directly toward the sun. Local weather patterns and cloud cover affect the receivable radiation accordingly.

The solar irradiation also known solar energy is the total amount of solar energy received at a particular location during a specified time period, often in units of $kWh/m^2/day$. Graphically, solar irradiation (energy) is the area under the solar irradiance (power) curve. Solar irradiation can also be denoted by solar insolation.

Total solar insolation is composed of direct, diffuse and reflected radiation. All contribute to the overall radiation levels on earth (Mayfield, 2010).

Direct radiation: The direct radiation from the sun isn't intercepted as it travels from the sun to the earth's surface. It therefore makes the greatest

contribution to a PV array and has the biggest effect on the array's ability to convert sunlight into electrical energy. On clear, sunny days, the vast majority of the solar radiation experienced is in the form of direct radiation.

Diffuse radiation: The sun's diffuse radiation takes a more roundabout path to the earth. Typically clouds, water vapour, dust, and other small airborne particles block and scatter the diffuse radiation's path to the planet's surface. The diffuse component of solar radiation therefore plays a minor role in the power output of a PV module. However, on days when clouds cover the sky, all the radiation is in the form of diffuse light without any direct radiation component.

Reflected radiation: also called albedo radiation is part of the solar radiation at a site. It's light that's reflected from physical surroundings, such as a roof or the ground, and put back into the atmosphere as diffuse radiation. Figure (3.7) shows the direct, diffuse and reflected radiation.

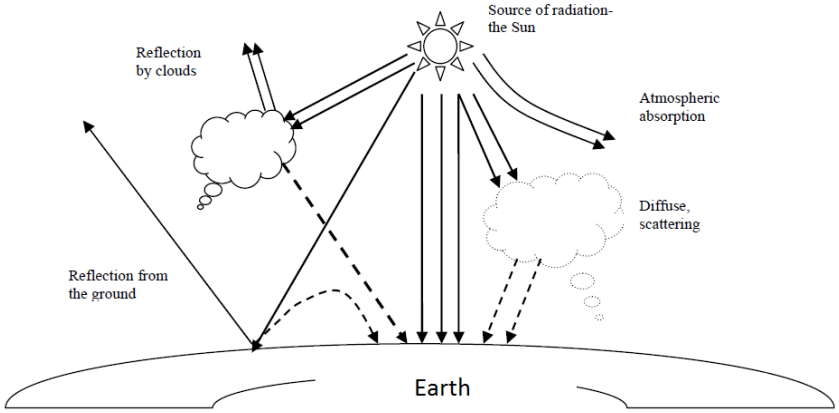

Figure (3.7): Direct, diffuse and reflected radiation on the surface of the earth (Mayfield, 2010).

It is clear that the insolation depends on many factors such as length of day, clouds, haze, pollution and elevation above sea level.

The average daily amount of solar energy received on a given surface is represented by peak sun hours; it is equivalent to the number of hours that the solar irradiance would need to be at a peak level of 1 kW/m^2 to accumulate the total amount of daily energy received. Peak sun hours (PSH) can be calculated using equation (3.1).

$$PSH\ \left(\frac{hrs}{day}\right) = \frac{Average\ daily\ irradiation\ (kWh/m^2/day)}{Peak\ sun\ (1\ kW/m^2)} \qquad (3.1)$$

As a general rule, the number of peak sun hours increases when moving from winter to summer and then begins to decrease again moving back towards winter. Figure (3.8) shows peak sun ours in a day.

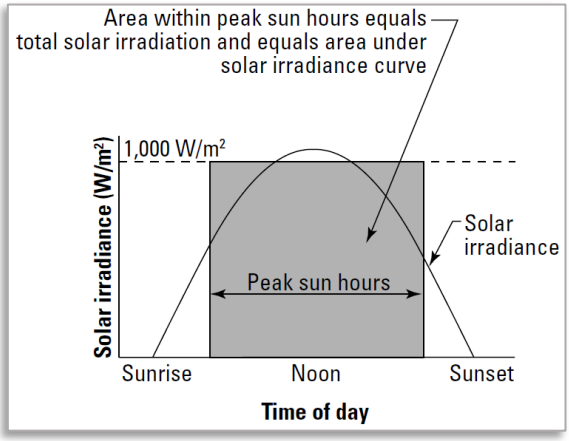

Figure (3.8): Peak sun hours in a day (Mayfield, 2010).

3.4 PV array design

3.4.1 Design parameters of a PV module

PV module input power: The input power is a function of the solar irradiance and the area of the PV module. The input power P_{in} is given by equation (3.2).

$$P_{in} = S_I \times A \tag{3.2}$$

where S_I is the solar irradiance in watt per square meter and A is the area of the PV module. The area of the module is calculated as the product of the module's physical dimensions (long and width) excluding the area which occupied by the module frame. The solar irradiance can be estimated by several methods include mathematical equation, solar maps, software tools and measuring instruments. Details on calculating the solar irradiance on tilt surfaces using mathematical equation can be found in (Klein, 1976) and (Jakhrani et al., 2012). Solar maps are quick sources to find out approximate solar irradiance estimation. Solargis is a website provides accurate solar maps for regions and locations through all over the world (Solargis, 2018). Software tools depend on solar resources to complete design requirements where solar irradiance estimation is an essential need in simulating PV systems. Similarly, solar irradiance can be estimated using measuring instruments such as a pyranometer which measures the direct and diffuse radiation on a horizontal surface.

Fill factor: It is essentially a measure of the solar cell quality. Fill factor can be calculated by comparing the maximum output power to the theoretical power that would be output at both the open circuit voltage and short circuit current together. The fill factor FF is given by following equation:

$$FF = \frac{P_{max}}{V_{oc} \times I_{sc}} \tag{3.3}$$

where P_{max} is the maximum output power in watt, V_{oc} is the open circuit voltage in volt and I_{sc} is the short circuit current in ampere. P_{max}, V_{oc} and I_{sc} values are provided in the datasheet of the PV module by the manufacturer.

Efficiency: The efficiency of the PV panel indicates the ability of a panel to convert sunlight into usable energy for electrical load consumption. Knowing the efficiency of a panel is important in order to choose the correct panels required for the PV system. For smaller roofs, more efficient panels are necessary, due to space constraints. The maximum efficiency of a solar PV cell is given by the following equation:

$$\eta = \frac{P_{max}}{P_{in}} \times 100 \tag{3.4}$$

where η is the module efficiency, P_{in} is the input power in watt and P_{max} is the maximum output power in watt.

PV module temperature: As discussed in Chapter Two, at a fixed solar radiation level, increasing temperature leads to decrease the open circuit voltage and slightly increase the short circuit current, eventually it reduces the power output. So, it is important to determine the cell temperature to take its effect into consideration. Many models are used to determine cell temperature. The preferred model for size optimization and design of PV systems is given by the following equation:

$$T_c = T_a + \frac{S_T}{S_{T,NOCT}} \left(\frac{9.5}{5.7 + 3.8 \times V_w}\right) \times (T_{Tc,NOCT} - T_{a,NOCT}) \times (1 - \eta) \tag{3.5}$$

where T_c is the cell temperature, T_a is the ambient temperature, S_T is the incident solar radiation, $S_{T,NOCT}$ is the incident solar radiation under nominal operating cell temperature (NOCT) conditions, V_w is the wind speed in meter per second, $T_{Tc,NOCT}$ is the temperature under NOCT conditions, $T_{a,NOCT}$ is the ambient temperature under NOCT conditions and η is the efficiency of the module. The values of varies parameters under NOCT conditions are generally provided by the manufacturers.

After determining the cell temperature the open circuit voltage can be amended by using the below equation:

$$V_{oc} = V_{oc,STC}(1 + \alpha_V \Delta T) + \frac{AN_s KT_c}{q} \ln(\frac{S_T}{S_{T,STC}}) \quad (3.6)$$

where V_{oc} is the open circuit voltage, $V_{oc,STC}$ is the open circuit voltage under STC, α_V is the voltage temperature coefficient and ΔT is the difference between cell and nominal temperature. A is the diode factor, N_s is the number of serial connected cells in a PV module, K is Boltzmann's constant in joule per kelvin, T_c is the cell temperature in kelvin, q is the electron charge in coulomb, S_T is the incident solar radiation, and $S_{T,STC}$ is the STC incident solar radiation.

The amount of power lost due to temperature increase can be calculated using maximum power temperature coefficient. This coefficient indicates how much power the module will lose when the temperature rises by 1°C. It is a negative number because the output power decreases as the cell temperature increases. Manufacturers of PV modules usually provide this coefficient in their product brochures.

Tolerance: It is the range a module can deviate from its specified maximum output power P_{max}. For example, if a 200 W PV module has a tolerance of ±3% then the panel could have an actual maximum output power within a range of 194 W to 206 W. Nowadays, and with the technical development of the PV modules, the module tolerance has been improved to be 0% negative power tolerance. Which means that the module will always has a rated maximum output power greater than or equal to the specification.

3.4.2 PV array losses

There are several factors affect the PV array production resulting in reducing the array output power than its nominal power. An overview of the PV array losses is as follow.

Soiling: Is the loss due to dirt and other foreign matter on the surface of the PV module that prevent solar radiation from reaching the cells. Soiling is location and weather dependent. There is greater soiling loss in high traffic and high pollution areas with infrequent rain.

Shading: Representing the reduction in the incident solar radiation from shadows caused by objects near the array such as buildings or trees. Shading analysis tools can determine a loss percentage of shading by nearby objects.

Snow: This is due to snow accumulation on a PV module surface. Snow reduces the energy production depending on the amount of snow and how long it remains on the surface of the PV module.

Mismatch: Is defined as the electrical losses due to slight differences caused by manufacturing imperfections between modules in the array that cause the modules to have slightly different current voltage characteristics.

Light induced degradation: Is the loss which arising after exposition the PV module to the sun due to nature of material used in the PV module manufacture.

Solar radiation loss: This loss results from the reflection of light after falling on the PV module glass surface**.**

Nameplate Rating: The power nameplate rating is the maximum power output under standard test conditions which the manufacturers indicate. In most cases, there might be an error between the actual field performance and nameplate rating. One reason of that is the measurement inaccuracy which is accounted as potential source of error that can happen by the manufacturers while testing.

Age: This loss is the degradation that occurs during lifetime.

3.4.3 Energy consumption and load assessment

Knowledge of electrical loads is an important consideration for designing a PV system. Electrical loads can be determined either by calculations or measurements. Loads calculations are performed based on the rated power of each load. A prepared calculations sheet is used to calculate the total energy of the loads, the sheet has columns for: load name, rated power in kW, operating hours and energy in kWh. Obviously, the sum of energy column values gives the total required energy. Loads calculations can be highly inaccurate. Actual measurement of the loads using electronic watt-hour meters is the most accurate method to determine the required energy. Another simple method of determining the energy consumption is to review the last electrical bills for the past year or longer and estimate the average energy consumption.

3.4.4 PV array sizing

Sizing the PV array firstly requires the estimation of the amount of electricity required by the load. To produce enough energy for the loads, losses within the system have to be considered (Solanki, 2013). The following equation gives the size of the PV array.

$$P_{array} = \frac{E_{load}}{(1 - A_{losses})(1 - B_{losses})(1 - W_{losses})(1 - I_{losses}) \times PSH} \quad (3.7)$$

where P_{array} is the rated array power, E_{load} is the load required energy in Wh, A_{losses} is the percentage of array losses, B_{losses} is the percentage of battery losses, W_{losses} is the percentage of wires losses, I_{losses} is the percentage of inverter losses and PSH is the peak sun hours. Array losses have been explained previously while battery bank, wires and inverter losses will be discussed later in this chapter. The number of PV modules needed to generate the PV array power calculated from the above equation can be determined based on the available PV module rated power in the market. The required number of modules can be given by the following equation.

$$N_{modules} = \frac{P_{array}}{P_{module}} \quad (3.8)$$

where $N_{modules}$ is number of the required PV modules, P_{array} is the PV array power in W, P_{module} is the PV module rated power. The number of PV module should be rounded to next higher integer number.

3.4.5 PV array orientation

The PV array orientation is defined by two angles, the array azimuth and tilt angles (Brooks & Dunlop, 2013). See below figure.

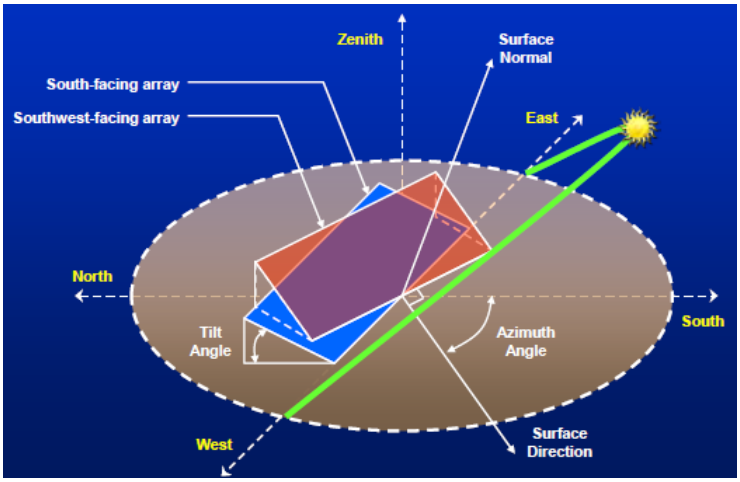

Figure (3.9): PV array orientation (Brooks & Dunlop, 2013).

The array azimuth angle is the direction an array surface faces relative to due south. The optimal azimuth angle for facing tilted PV array is due south in the northern hemisphere, and due north in the southern hemisphere. The tilt angle is the angle between the array surface and the horizontal plane. The exact tilt angle that maximizes the annual energy production varies based on the local climate. For most locations, the optimum tilt angle is approximately equal to latitude of the location.

3.4.6 PV array configuration

The PV array configuration or the number of PV modules to be connected in series or in string, and the number of parallel strings depend on the inverter (or charger) voltage ratings. The PV string V_{oc} and V_{mp} must be within allowable limits of the inverter ratings. Maximum I_{sc} of the PV array should also be within acceptable limit to the inverter. Final array configuration is selected based on the inverter input DC voltage window of operation. Inverter manufacturer specifies a range of V_{mp} values for its MPPT operation. Based on module tolerance and its minimum and maximum temperature of operation, a range of module V_{mp} output is determined. For a number of modules, connected in a series string, a range of string V_{mp} values is calculated. The number of modules in a series string is determined such that its range of V_{mp} output falls well within the permitted range of V_{mp} values of the inverter. This is demonstrated in Figure (3.10).

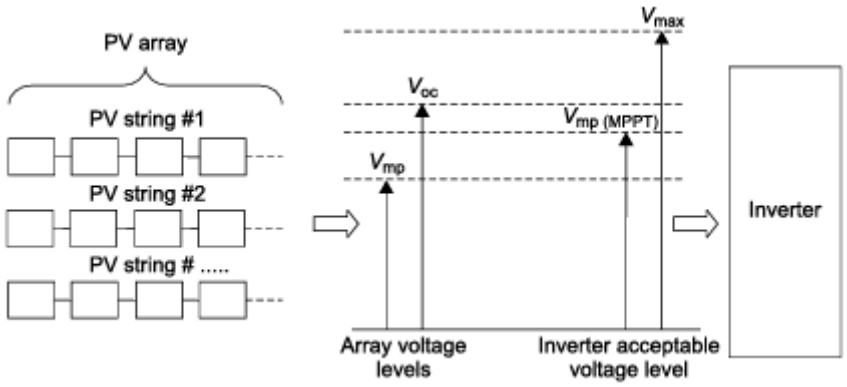

Figure (3.10): How to configure a PV array (Solanki, 2013).

Inverter manufacture also specifies maximum input DC voltage rating. Based on the modules tolerance and its minimum temperature of operation, maximum module V_{oc} output is determined. For a number of modules connected in a series string, maximum string V_{oc} output is equal to the maximum module V_{oc} multiplied by

the number of modules. The maximum array V_{oc} is equal to the maximum string V_{oc} for a number of strings connected in parallel to make an array. It is then verified that the maximum array V_{oc} is less than maximum input DC voltage rating of the inverter. It also verified that the maximum array I_{sc} is within the maximum input DC current rating of the inverter. The maximum module I_{sc} is determined based on module tolerance, maximum available solar radiation and maximum temperature of operation. The maximum string I_{sc} is equal to the maximum module I_{sc} for a series connected string, the maximum array I_{sc} is the string I_{sc} multiplied by the number of string in an array.

3.5 Inverter design

The inverter design considerations involve looking at the inverter electrical characteristics and matching these characteristics with the characteristics of other components of the system. That means, the rated output voltage of the inverter should be equal to the load appliances nominal operating voltage (often 230 V) and so on. Furthermore, it is good to choose an inverter which can take high input DC voltage. High voltage will require less current in the system for the same power flow. Less current means less power loss and thinner wires, this also means less cost of the system.

3.5.1 Inverter sizing

The capacity of the inverter depends on the total power of the connected load and the inverter losses. The desired output power of the inverter is equal to the total connected power of the load. In practice, it is preferred to choose an inverter having power capacity higher than the total connected load. For more precision, the cables power loss between the inverter and the load should be added to the load power. The inverter capacity can be obtained by the following equations:

$$P_{inv\ out} = P_{load} + P_{loss} \tag{3.9}$$

$$P_{inv\ in} = \frac{P_{inv\ out}}{I_{losses}} \tag{3.10}$$

$$P_{inv} \geq \frac{P_{inv\ in}}{P.F} \tag{3.11}$$

where $P_{inv\ out}$ is the inverter output power in W, P_{load} is the load power in W, P_{loss} is the cables power loss in W, $P_{inv\ in}$ is the inverter input power in W, I_{losses} is

percentage of the inverter losses, P_{inv} is the inverter power in VA and $P.F$ is the power factor of the load.

After estimating the capacity of the inverter, it should be matched with the available inverters capacities in the market, the capacity of the selected inverter which available in the market should be equal or slightly larger than the calculated capacity.

3.5.2 Inverter losses

The inverter power losses consist of MPPT tracking and DC to AC conversion losses. The inverter tracks the MPP within a specific voltage range, MPPT losses occurs when the inverter works outside the MPPT voltage range. The inverter has a different efficiency depending on the load. Usually, the manufacturers give the maximum efficiency, which is the weighting of the different efficiencies when the load is: 5, 10, 50 and 100%.

3.6 Battery design

The battery design considerations start with knowing the DC system voltage which is the DC input of the inverter. The battery voltage should be equal to the DC system voltage. Also the battery bank has to be chosen in such a way that it should not only supply the power and energy required by the load, but also be able to supply the loss of energy in inverter and cables.

3.6.1 Determine battery capacity

In order to size battery, we have to consider several parameters of batteries as well. These parameters are: Ampere-hour (Ah) capacity, depth of discharge (DOD) and number of days of autonomy. The equation of estimating the total capacity of batteries in Ah is presented below:

$$Ah_{total} = \frac{E_{load} \times A}{DOD \times V_{DC} \times \eta_{batt} \times \eta_{inv}} \tag{3.12}$$

where Ah_{total} is the capacity of the batteries in Ah, E_{load} is the required load energy in Wh, A is the number of the desired autonomy days, DOD is the depth of discharge, V_{DC} is the DC system voltage in V, η_{batt} is the battery efficiency and η_{inv} is the inverter efficiency.

From the above estimation and after choosing the appropriate batteries available in the market, the number of the required batteries is given by:

$$N_{batt} = \frac{Ah_{total}}{Ah_{batt}} \quad (3.13)$$

where N_{batt} is the required number of batteries (converted in round figure), Ah_{batt} is the capacity of the chosen battery in Ah.

3.6.2 Battery losses

The overall battery efficiency is specified in two efficiencies: the coulombic efficiency and the voltage efficiency.

The coulombic efficiency is the ratio of the number of charges that enter the battery during charging compared to the number that can be extracted from the battery during discharging. The losses reduce the coulombic efficiency are primarily due to the loss in charge due to secondary reaction, such as the electrolysis of water or other redox reactions in the battery. In general, the coulombic efficiency may be high, in excess of 95%.

The voltage efficiency is determined largely be the voltage difference between the charging voltage and voltage of the battery during discharging. The dependence of the battery voltage on SOC will therefore impact voltage efficiency. Other factors being equal, a battery in which the voltage varies linearly with SOC will have a lower efficiency than one in which the voltage is essentially constant with SOC (Honsberg & Bowden, 2013).

3.7 Cables and wires design

An appropriate choice of wires will reduce the electrical losses in wires. Also, help to avoid shock and fire hazard in PV systems.

3.7.1 Calculating voltage drop

The voltage drop in wires depends on the resistance of the wire and the current flowing through it. The resistance depends on resistivity of the material from it is made, length and cross-section area of the wire. Expressions of resistance and voltage drop are given in equation (3.14) and (3.15) respectively.

$$R = \frac{\rho \times L}{A} \quad (3.14)$$

$$\Delta V = I \times R \quad (3.15)$$

where R is the resistance in ohm, ρ is the resistivity in ohmmeter, L is the length in meter, A is the cross section in square meter, ΔV is the voltage drop in V and I is the

current in A. Usually, for the solar PV system wiring, the permitted voltage drop is 2% to 3% between two circuit nodes (from one equipment to other equipment).

3.7.2 Selecting a proper cross section

The cross section of a cable is determined by the maximum expected current of a branch. The following equation can be used to calculate the minimal required wire cross section.

$$A_{min} = \frac{2 \times P \times \rho \times L}{V.\Delta V_{max}} \tag{3.16}$$

where A_{min} is the minimal required wire cross section in square meter, P is the rated power in W, ρ is the resistivity in ohmmeter, L is the length in meter, V is the rated voltage in V. ΔV_{max} is the maximum allowed voltage drop in V.

Chapter Four

Cases of Study

4.1 introduction

Several types of PV solar system were installed in Gaza strip. In this work, Systems which represent the different types of PV system were selected as cases of study. Each selected system of the cases of study systems is considered as one of the large systems which are of the same type of that system. The selected systems were The Islamic University of Gaza (IUG), Al Azhar University (AAU) and Deir Elatin School (DES) PV systems. For all the cases of study, the specifications, rating and connection diagram of each component of the system components were fully described in this chapter.

4.2 Islamic University of Gaza (IUG) PV solar system

The system is a 140 kWP hybrid off-grid system. The main components of the system are: PV array, charge controllers, inverters and battery bank. Detailed information of the system is demonstrated as follow:

4.2.1 PV array

The PV module used in the system is a 315 WP module of type SUNTECH, model is STP315-24/Vem. The module specifications are listed in Table (4.1)

Table (4.1): SUNTECH (STP315-24/Vem) PV module specifications.

Electrical Characteristics	
STC	**Rating**
Maximum Power at STC (P_{max})	315 W
Optimum Operating Voltage (V_{mp})	36.8 V
Optimum Operating Current (I_{mp})	8.56 A
Open Circuit Voltage (V_{oc})	45.1 V
Short Circuit Current (I_{sc})	9.02 A
Module Efficiency	16.2%
Operating Module Temperature	-40 °C to +85 °C
Maximum System Voltage	1000 V DC
Maximum Series Fuse Rating	20 A
Power Tolerance	0 / +5 W
NOCT	**Rating**
Maximum Power at NOCT (P_{max})	229 W
Optimum Operating Voltage (V_{mp})	33.2 V
Optimum Operating Current (I_{mp})	6.91 A

Open Circuit Voltage (V_{oc})	41.5 V
Short Circuit Current (I_{sc})	7.30 A
Temperature Characteristics	**Rating**
Nominal Operating Cell Temperature (NOCT)	45 ± 2 °C
Temperature Coefficient of P_{max}	-0.41% / °C
Temperature Coefficient of V_{oc}	-0.33% / °C
Temperature Coefficient of I_{sc}	0.067% / °C

The total number of modules in the PV array is 450 modules with a peak power of 141.750 kWP. The array is divided into 30 sub-arrays. Each sub-array consists of five groups of PV modules connected in parallel, where the group contains three serially connected modules. The figure below shows the sub-array configuration.

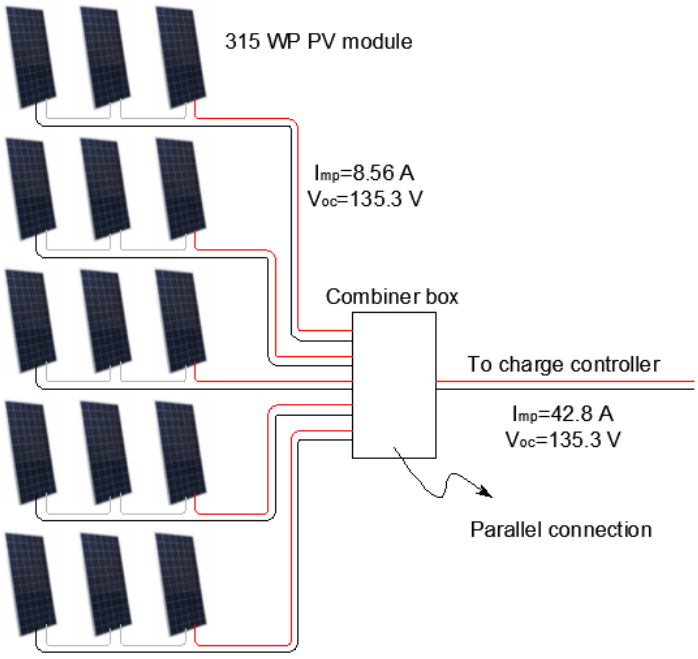

Figure (4.1): Sub-array configuration of IUG PV system.

The open circuit voltage of a sub-array is equal to the open circuit voltage of a group of modules while the optimal operating current of a sub-array is equal to the sum of the currents from all parallel groups. Consequently, the open circuit voltage and optimal operating current of a group of modules as shown in Figure (4.1) are 135.3 V and 8.56 A, respectively. The peak power of a sub-array is 4.725 kWP.

4.2.2 Charge controller

The system uses a charge controller of type STUDER, model is VT-80 with the following specifications:

Table (4.2): STUDER (VT-80) charge controller specifications.

Electrical characteristics PV array side	Rating
Maximum solar power recommended (@STC)	5000 W
Maximum solar open circuit voltage	150 V
Maximum solar functional circuit voltage	145 V
Minimum solar functional circuit voltage	Above battery voltage
Electrical characteristics battery side	**Rating**
Maximum output current	80 A
Nominal battery voltage	48 V
Operating voltage range	7-68 V
Power conversion efficiency	99%

The output of each sub-array mentioned previously is connected to the input of the charge controller. Therefor the total number of charge controllers is 30. The output of the charge controller is connected to a DC common busbar. The following figure shows the charge controller connections.

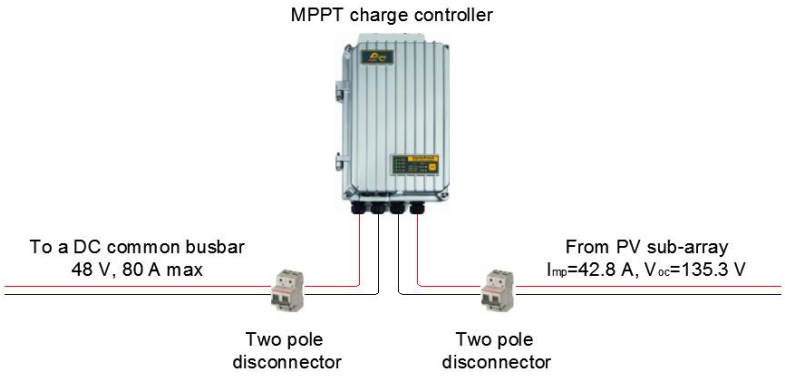

Figure (4.2): STUDER (VT-80) charge controller connections.

From Table (4.2), it can be notice that the open circuit voltage of a sub-array is less than the maximum solar open circuit voltage of the charge controller. Also, the recommended maximum solar power of the charge controller (5 kWP) is slightly higher than the sub-array peak power (4.725 kWP). That is a necessary condition for normal operation of the charge controller.

4.2.3 Inverter

The used inverter is a STUDER type inverter, model is XTH 8000-48. This device has an integrated charger to charge the battery bank, therefore the device is called inverter/charger. The input power source to the inverter when it operates as a

charger is either the utility grid or a backup generator, this makes IUG system a hybrid system. The device specifications are presented in Table (4.3).

Table (4.3): STUDER (XTH 8000-48) inverter/charger specifications.

Inverter	**Rating**
Nominal battery voltage	48 V
Continuous power @ 25 °C	7000 VA
Power 30 min. @ 25 °C	8000 VA
Maximum efficiency	96%
Output voltage	230 V
Battery charger	**Rating**
Maximum charging current	120 A
Temperature compensation	With BTS-01 or BSP 500/1200

The DC input of the inverter is connected to the DC common busbar and the AC input is connected to a common feeder from the utility grid or a backup generator while the AC output is connected to the loads distribution board. STUDER company provides each three inverters with an X-connect panel which contains DC circuit breakers and a Pre-installed DIN rails and other components in order to make installation process easier. Figure (4.3) shows inverter/charger connections.

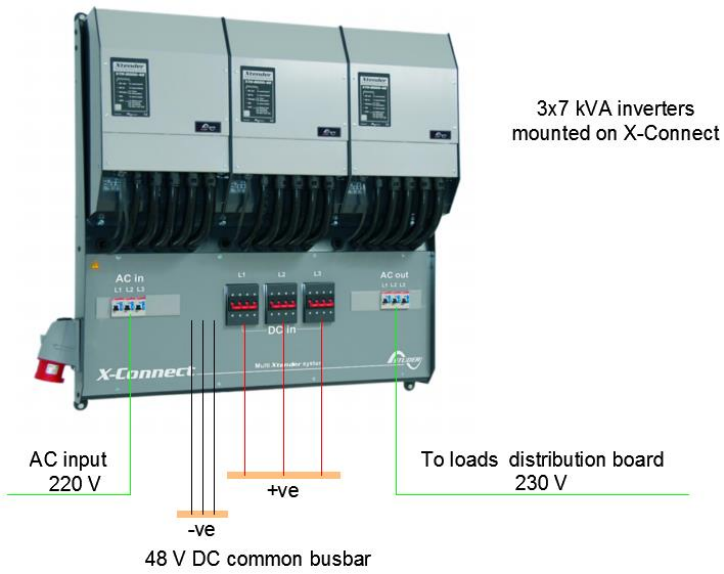

Figure (4.3): STUDER (XTH 8000-48) inverter/charger connections.

The IUG system has 18 inverters, making the total output power equals to 126 kVA. The inverters total output power represents approximately 90% of the PV array total power. Certainly, the designer took into account the losses of the PV array. As it

is clear in Table (4.3), the inverter has the ability to supply 8 kVA of power for a period of 30 minutes. Hence, for the total number of inverters, the output power for 30 minutes will be 144 kVA.

4.2.4 Battery bank

The battery used in the system is of BEA type, model is 22 PVV 4180 with capacity of 3210 Ah @ C_{10h}. Table (4.4) presents the battery specifications.

Table (4.4): BEA (22 PVV 4180) battery specifications.

Technology	Valve regulated (VRLA)
Nominal voltage	2 V
Positive electrode	Tubular lead calcium
Electrolyte	Gel
Charge voltage at cyclic operation (V/cell)	2.3-2.4

The type of coupling of the system power conditioning unit is DC coupling type. Thus the charge controller output, inverter DC input and battery bank are connected to a common DC busbar. Referring to nominal battery voltage in the specification of the charge controller and the inverter/charger, it will be found that it is 48 V so the rated voltage of the battery bank should be 48 V. However, the nominal voltage of the battery used in the system is 2 V. In order to establish the required rated voltage of the battery bank, 24 batteries must be connected in series as a battery string. To increase the battery bank capacity in order to have longer backup time, six battery strings were used in the system.

4.2.5 System accessories

Remote control and programming centre (RCC-02): It offers unlimited access to the various functions of the devices used in the system. Devices in the system in addition to RCC-02 unit are equipped with a proprietary communication bus for data exchange, configuration and updating of the system. Series connection is obtained by linking the devices with communication cables.

Battery status processor (BSP): The BSP offers a highly precise measuring and an extremely efficient algorithm that calculates the state of charge in the most accurate way. The BSP offers voltage measurement for 12, 24 and 48 V batteries as well as current measurement with a resistive shunt. By using the communication bus,

the BSP is able to communicate with the other devices in the system. It is possible to configure the BSP and to display its values with the RCC-02.

Battery temperature sensor (BTS-01): It enables the inverter/charger to correct the battery voltage and guarantee an optimum charge whatever the battery temperature. This is clear in the specifications of the inverter/charger.

Communication set by internet with Xcom-LAN: The set includes Xcom-232i and Ethernet port. It allows a constantly controlled of the system devices from any remote terminal, computer, tablet or smartphone by connecting these terminals to Web sites via internet connection over a local network.

Figure (4.4) shows a schematic diagram of IUG system. Actually, the IUG system is divided into two identical blocks. Each block has the same components and quantities of the other block.

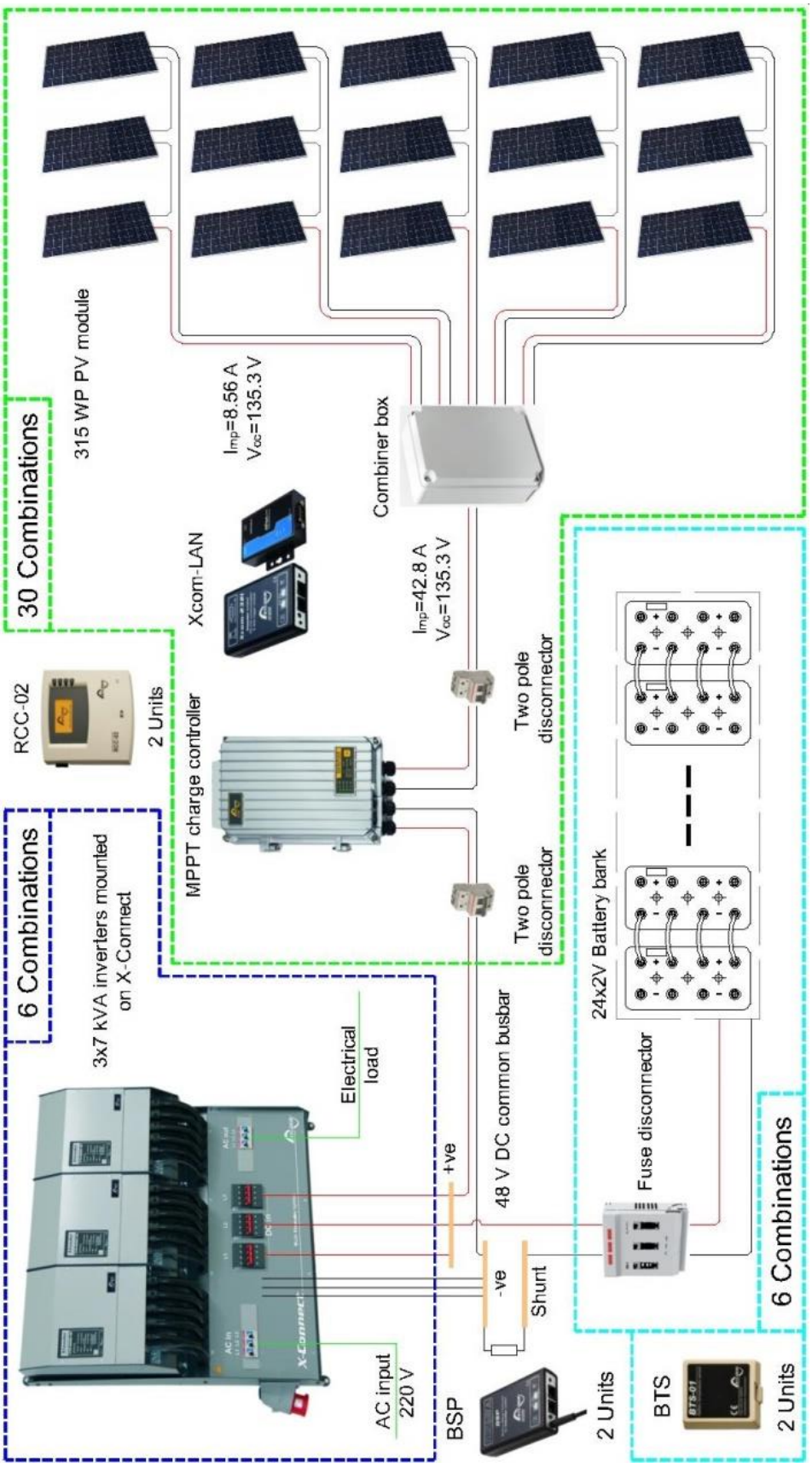

Figure (4.4): Schematic diagram of IUG PV system.

4.3 Al Azhar University (AAU) PV solar system

The system is a 75 kWP on-grid with a backup battery. The system components include: PV array, solar inverters, battery inverters, battery bank and multicluster unit. The multicluster unit is the basic component in the grid tie. The following is a detailed view of each component of the system.

4.3.1 PV array

The type of the PV modules used in the system is CanadianSolar, model is CS6X-320P. The module specifications are listed in Table (4.5).

Table (4.5): CanadianSolar (CS6X-320P) PV module specifications.

Electrical Data	
STC	**Rating**
Nominal Max. Power (P_{max})	320 W
Opt. Operating Voltage (V_{mp})	36.8 V
Opt. Operating Current (I_{mp})	8.69 A
Open Circuit Voltage (V_{oc})	45.3 V
Short Circuit Current (I_{sc})	9.26 A
Module Efficiency	16.68%
Operating Temperature	-40 °C to +85 °C
Max. System Voltage	1000 V DC
Max. Series Fuse Rating	15 A
Power Tolerance	0 ~ +5 W
NOCT	**Rating**
Nominal Max. Power (P_{max})	232 W
Opt. Operating Voltage (V_{mp})	33.6 V
Opt. Operating Current (I_{mp})	6.91 A
Open Circuit Voltage (V_{oc})	41.6 V
Short Circuit Current (I_{sc})	7.50 A
Temperature Characteristics	**Rating**
Temp. Coefficient (P_{max})	-0.41% / °C
Temp. Coefficient (V_{oc})	-0.31% / °C
Temp. Coefficient (I_{sc})	0.053% / °C
Nominal Operating Cell Temperature (NOCT)	45 ± 2 °C

The PV modules (with a total of 235 modules) are divided into five sub-arrays. Each sub-array consists of three groups. Two of the three groups contain 16 modules

connected in series and the third group contains 15 modules connected also in series. Regarding the peak power, the array peak power is 75.2 kWP while the sub-array peak power is 15.04 kWP. Figure (4.5) shows the configuration of the sub- array.

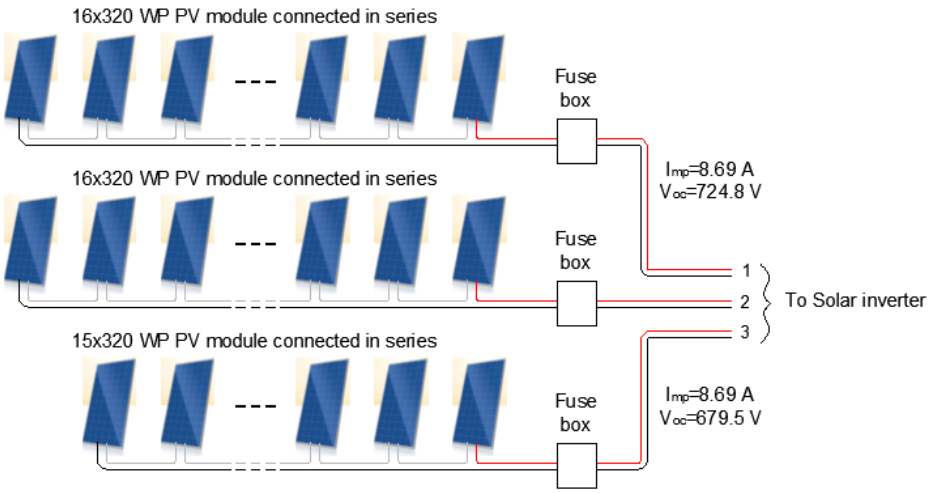

Figure (4.5): Sub-array configuration of AAU PV system.

As it is known from electrical circuits theory that the terminal voltage of electrical elements connected in series equals to the sum of voltages of all elements. While the flowing current through a series connected elements has the same value of the flowing current through each element. Therefore, the terminal open circuit voltages of 16, 15 PV modules connected in series are 724.8 V, 679.5 V, respectively and the current flow through the last series connected modules is 8.69 A.

4.3.2 Solar inverter

The solar inverter type is SMA, model is SUNNY TRIPOWER 15000TL. The inverter specifications are as in the following table.

Table (4.6): SMA (SUNNY TRIPOWER 15000TL) solar inverter specifications.

Technical Data (Input DC)	**Rating**
Max. DC power (at cos φ = 1) / DC rated power	15340 W / 15340 W
Max. input voltage	1000 V
MPP Voltage range / rated input voltage	360 V to 800 V / 600 V
Min. input voltage / initial input voltage	150 V / 188 V
Max. input current per string input A1 / input B1	40 A / 12.5 A
Technical Data (Output AC)	**Rating**
Rated power (at 230 V, 50 Hz)	15000 W
Nominal AC voltage	3 / N / PE; 230 / 400 V
Max. output current / Rated output current	24 A / 24 A

Efficiency	Rating
Max. efficiency / European efficiency	98.2% / 97.8%

Comparing the total power, voltage and current for both the sub-array output and the solar inverter DC input side, it will be found that there is matching between them. This matching is required for optimal operation of the system.

An important point to consider is that when configuring the PV array, the initial input voltage, maximum input voltage and MPP voltage range of the solar inverter must be taken into account. In the sense that the sub-array voltage must fall between the initial and maximum input voltage of the inverter, also, the sub-array voltage should fall within the MPP voltage range in order to operate the system with a higher efficiency.

There are five solar inverters in the system with a total power of 75 kW. The inputs of the solar inverter are the outputs (1, 2 and 3) of the PV sub-arrays. The outputs of the solar inverters are assembled in a distribution board. This board contains electrical faults protection devices for the outputs of the solar inverters. The coupling type in the board is an AC coupling type, which means that all the solar inverters outputs are connected to a common AC busbar. Figure (4.6) shows the solar inverter connections.

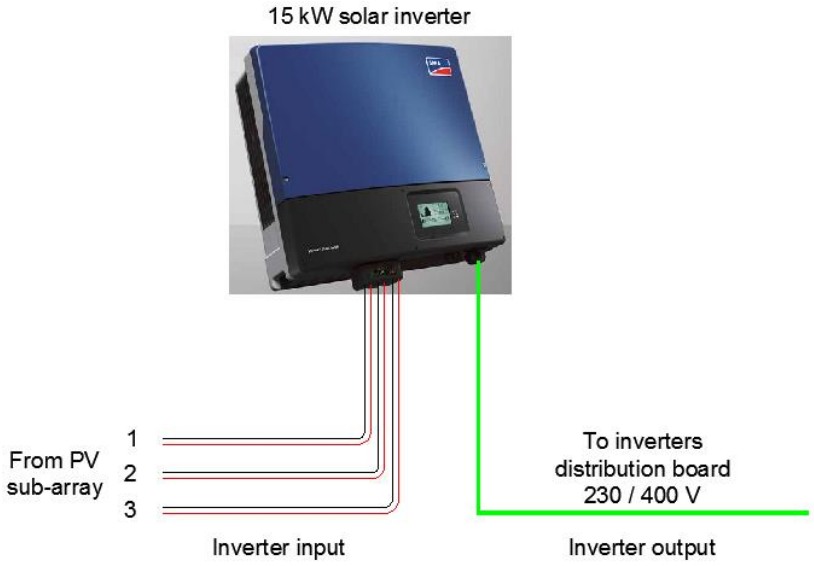

Figure (4.6): SMA (SUNNY TRIPOWER 15000TL) solar inverter connections.

In general, AC coupling should be done under specific conditions such as the same value of voltage, frequency and phase also the same phase sequence of the

connected devices. These conditions are satisfied by the inverters themselves. For this purpose (and for other purposes too) the inverters communicates with each other via Modbus protocol.

4.3.3 Battery bank

A SUNLIGHT type battery, model is 2V 24 RES OPzV 4245 is used in the system. The capacity of the battery is 3357 Ah @ C_{12} (at 20 °C and to 1.75 volt per cell). The specifications of the battery are listed in the following table.

Table (4.7): SUNLIGHT (2V 24 RES OPzV 4245) battery specifications.

Technology	Valve regulated (VRLA)
Nominal voltage	2 V
Positive electrode	Tubular
Electrolyte	Gel
Number of cycles (60% DoD)	2500

The total number of batteries used in the system is 96 batteries. The batteries are divided into four battery strings (24 batteries per string) with a terminal voltage of 48 V. Certainly, The connection topology of the battery string is a serial connection topology. Each battery string was connected to a group of three battery inverters. Figure (4.7) shows the connections of the battery string.

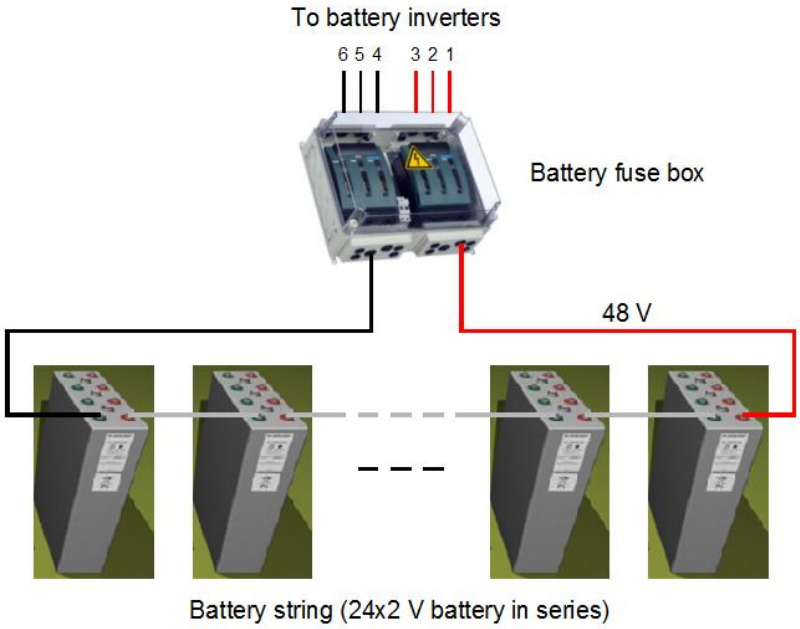

Figure (4.7): Battery string connections.

The total energy stored in the battery bank is 644.544 kWh. For 50% DOD and 70 kW load, the backup time will be about 4 hours (if no solar energy is available).

4.3.4 Battery inverter

A battery inverter of type SMA, model is SUNNY ISLAND 8.0H is used in the system. The difference between the solar inverter and the battery inverter is clear from the naming. In other words, the DC input of the solar inverter is connected to the DC output of the PV array, while the DC input of the battery inverter is connected to the DC terminals of the battery string. The specifications of this device are presented in Table (4.8).

Table (4.8): SMA (SUNNY ISLAND 8.0H) battery inverter specifications.

Operation on the utility grid or generator	**Rating**
Rated grid voltage / AC voltage range	230 V / 172.5 V to 264.5 V
Maximum AC current for increased self-consumption	26 A
Maximum AC power for increased self-consumption	6 kVA
Maximum AC input current	50 A
Maximum AC input power	11500 W
Stand-alone or emergency power operation	**Rating**
Rated grid voltage / AC voltage range	230 V / 202 V to 253 V
Rated power (at U_{nom}, f_{nom} / 25 °C / cos φ = 1)	6000 W
Rated current / maximum output current (peak)	26 A / 120 A
Battery DC input	**Rating**
Rated input voltage / DC voltage range	48 V / 41 V to 63 V
Maximum battery charging current	140 A
rated DC charging current	115 A
DC discharging current	130 A
Efficiency / self-consumption of the device	**Rating**
Maximum efficiency	95,8%
No-load consumption / standby	25,8 W / 6,5 W

As mentioned previously, that each battery string is connected to a group of three battery inverters. In the time that there are four battery strings, there will be four groups of battery inverters. The total power of all the battery inverters is 72 kW. Therefore, the battery inverters have the ability to handle the designed system power. The figure below shows the connections of a group of battery inverters.

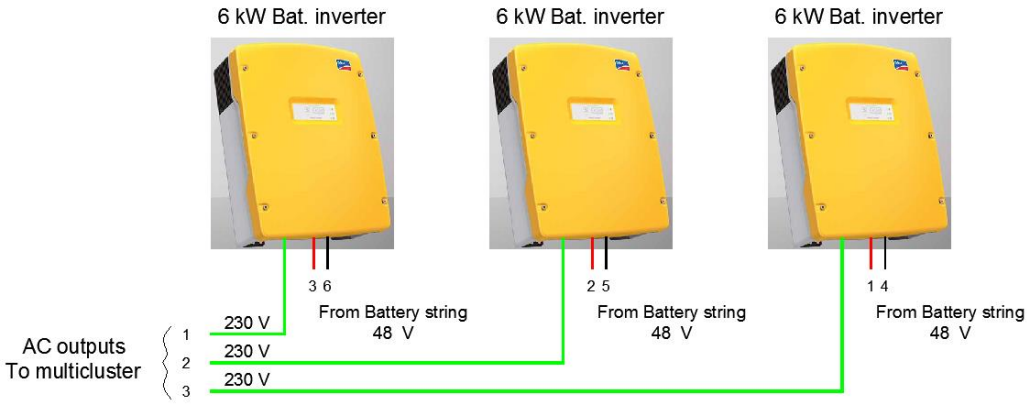

Figure (4.8): SMA (SUNNY ISLAND 8.0H) battery inverters connections.

The battery inverter works as an inverter and as a battery charger too. The inverter is equipped with an integrated battery management algorithm. The inverter is also provided with a temperature sensor. The battery management algorithm monitors the state of charge and the battery temperature. As a matter of fact, he battery charging process is dependent on the temperature. Therefore, the battery management algorithm has a feather of automatic temperature compensation in order to prevent overcharging and insufficient charging of the battery. the battery management algorithm works on decreasing the charging voltage when the temperature is above 20 °C, while it works on increasing the charging voltage when the temperatures is below 20 °C.

4.3.5 Multicluster

A Multicluster system 12 for sunny island of type SMA is used in the system. It consists of multicluster-Box 12 (model is Mc-Box-12.3-20) and NA-Box 12 (model is NA-Box-12.3-20). The specifications of the multicluster system 12 are presented in the following table.

Table (4.9): SMA (Mc-Box-12.3-20) multicluster-Box 12 specifications.

Load connection	**Rating**
Rated power	138 kW
Rated grid voltage	230 V / 400 V
Current at rated values	3 × 200 A
Sunny Island connections	**Rating**
Maximum number of devices	12
AC rated power / AC current at rated values	72 kW / 12 × 26 A
Rated operating voltage	230 V / 400 V

Generator connection	Rating
Rated grid input power	138 kW
Nominal voltage	230 V / 400 V
AC input current	3 × 200 A
PV system connection	**Rating**
Rated power	138 kW
Rated operating voltage	230 V / 400 V
AC current at rated values	3 × 200 A
NA-Box / Grid-Connect-Box connection	**Rating**
Rated input power	138 kW
Rated operating voltage	230 V / 400 V
Rated current / AC input current	3 × 200 A

The NA-Box is an automatic transfer switch which enables the operation of an SMA multicluster system on a utility grid. In the event of a grid failure, the NA-Box disconnects the SMA multicluster system from the utility grid via a redundant tie switch. The Multicluster-Box is a main AC distribution board. It allows connecting up to four clusters. Each cluster is made up of three battery inverters. The multicluster-Box has the following functions:

- Main AC distribution board for Sunny Island inverters, one generator, one load and one PV system.
- Load shedding.
- Automatic bypass and reverse current monitoring for the generator.
- Active anti-islanding.

4.3.6 System accessories

SMA cluster controller: The SMA Cluster Controller is the central communication unit for system monitoring, recording data and controlling PV systems. It is combined with SMA inverters. The cluster controller primarily performs the following tasks:

- Reading out, provision and administration of PV system data.
- Configuring device parameters.
- Feedback on current total active power of the system.
- Implementation and feedback of grid operator set points for active power limitation and reactive power operation under grid management services.

- Implementation and feedback of set points for active power limitation when PV electricity is directly marketed.
- Sending the system data to an FTP server and/or the Sunny Portal Internet Portal. Also sending e-mail alarms in the event of critical system statuses.
- Performing updates for the Cluster Controller and the inverters.

Sunny remote control: Battery inverters configure and control can be done remotely using sunny remote control. The display of the remote control shows operating data, events, warnings and errors on the battery inverter. A convincing feature of the remote control is the simplicity of installation. Only one cable is needed for the electrical connection and communication.

The schematic diagram of the AAU complete system is shown in Figure (4.9).

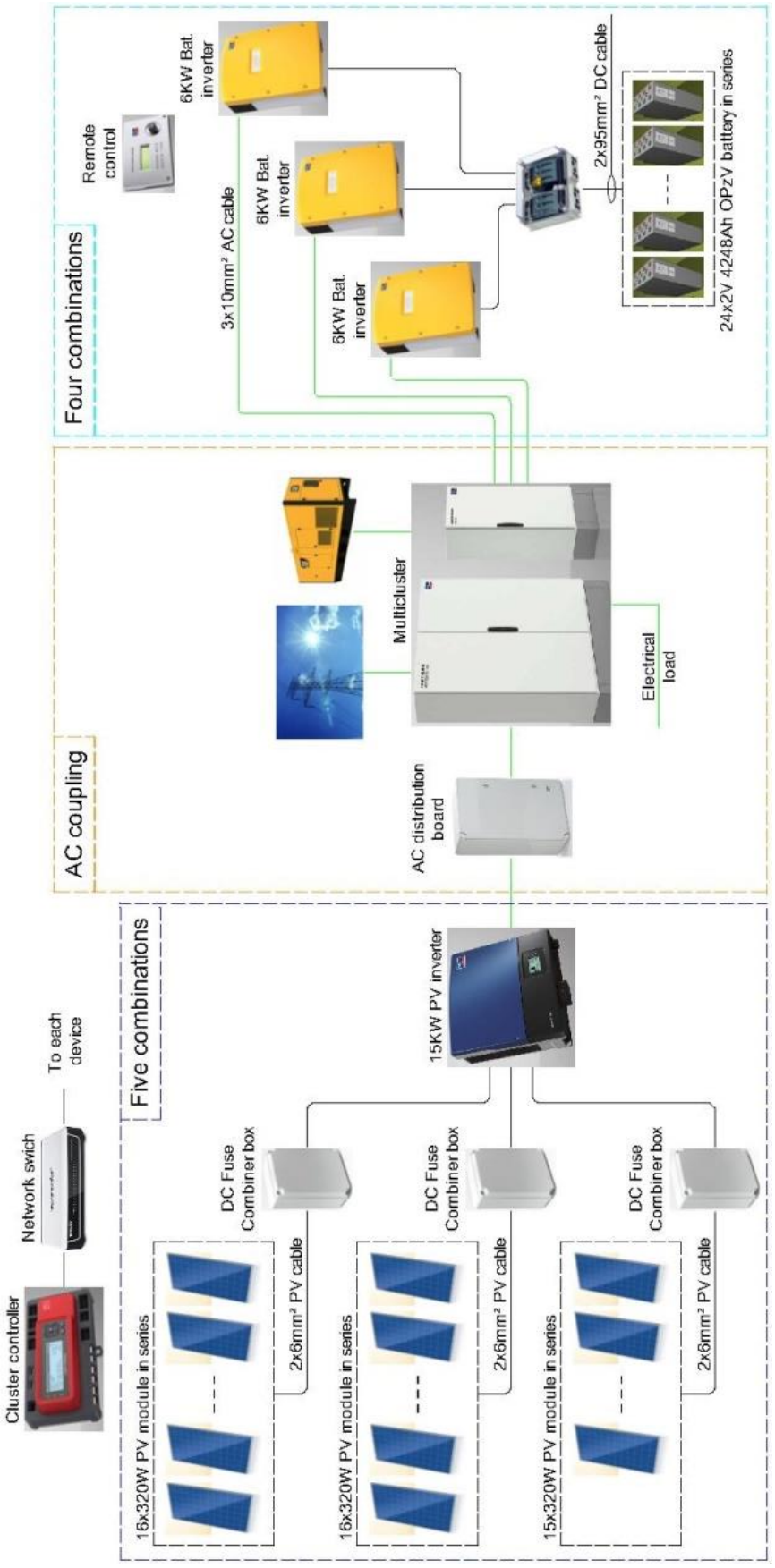

Figure (4.9): Schematic diagram of AAU PV system.

4.4 Deir Elatin School (DES) PV solar system

The system is a 100 kWP on-grid without battery backup. The system has two components. These are the PV array and the solar inverters. Detailed information of the system is presented below.

4.4.1 PV array

The PV modules used in the system are of the same type of the modules used in IUG PV system which is SUNTECH, but with a rated power of 325 WP. The model of the module is STP325S-24/Vem. The module specifications are listed in the table below.

Table (4.10): SUNTECH (STP325S-24/Vem) PV module specifications.

Electrical Characteristics	
STC	**Rating**
Maximum Power at STC (P_{max})	325 W
Optimum Operating Voltage (V_{mp})	37.1 V
Optimum Operating Current (I_{mp})	8.77 A
Open Circuit Voltage (V_{oc})	45.8 V
Short Circuit Current (I_{sc})	9.28 A
Module Efficiency	16.7%
Operating Module Temperature	-40 °C to +85 °C
Maximum System Voltage	1000 V DC
Maximum Series Fuse Rating	20 A
Power Tolerance	0 / +5 W
NOCT	**Rating**
Maximum Power at NOCT (P_{max})	236 W
Optimum Operating Voltage (V_{mp})	33.3 V
Optimum Operating Current (I_{mp})	7.09 A
Open Circuit Voltage (V_{oc})	41.6 V
Short Circuit Current (I_{sc})	7.52 A
Temperature Characteristics	**Rating**
Nominal Operating Cell Temperature (NOCT)	45 ± 2 °C
Temperature Coefficient of P_{max}	-0.41% / °C
Temperature Coefficient of V_{oc}	-0.34% / °C
Temperature Coefficient of I_{sc}	0.060% / °C

The PV array is formed of four sub-arrays. Three of the sub-arrays are identical. Each sub-array of the identical sub-arrays contains six strings. The string consists of 13 module connected in series. The fourth sub-array also contains six string, three of the strings are similar to the strings of the identical sub-arrays. Each string of remaining three strings of the fourth sub-array consists of 12 module connected in series. The total number of PV module is 309 modules with a peak power of 100.425 kWP. As well the peak power of the three identical sub-arrays is 25.35 kWP and for the fourth sub-array the peak power is 24.375 kWP. The figure below shows the PV array configuration of one of the identical sub-arrays.

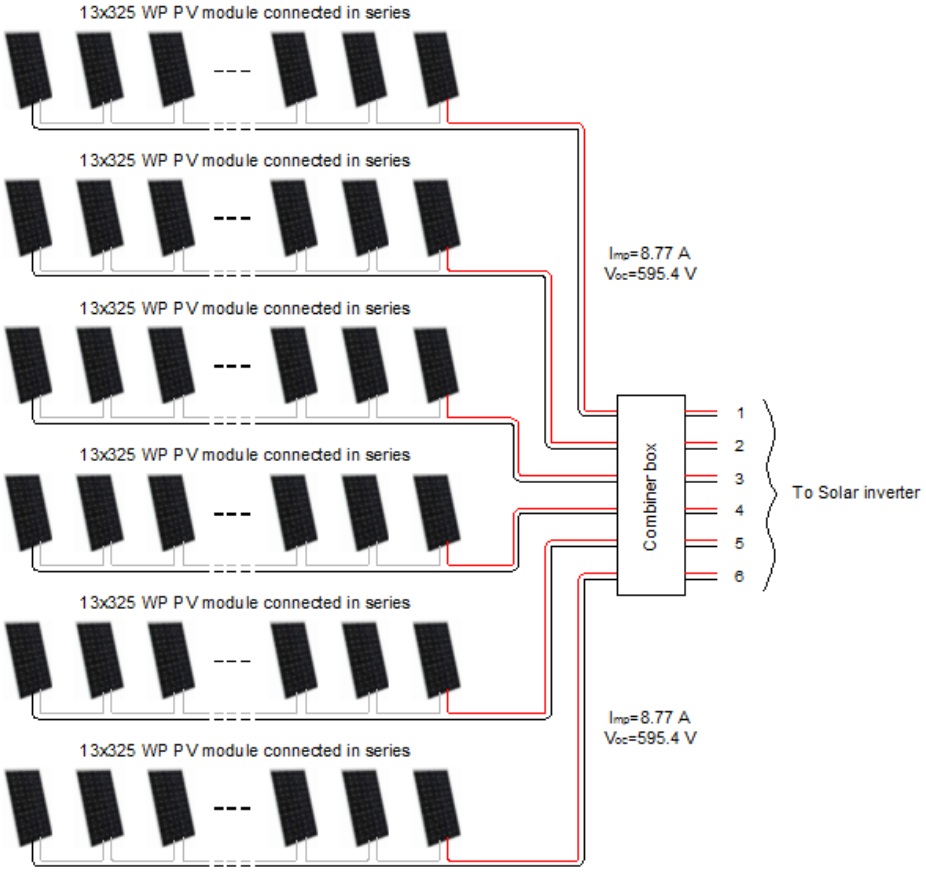

Figure (4.10): Sub-array configuration of DES PV system.

As shown in Figure (4.10) the open circuit voltage of a PV string is 595.4 V and the optimal operating current is 8.77 A.

4.4.2 Solar inverter

The solar inverter type is SMA, model is SUNNY TRIPOWER 25000TL. It is of the same solar inverter type used in AAU PV system. Therefore, the specifications of the two inverter models are similar to each other except some items such as the

power and current. The following table presents the rating values that differ than those mentioned in table (4.6).

Table (4.11): SMA (SUNNY TRIPOWER 25000TL) solar inverter specifications.

Technical Data (Input DC)	**Rating**
Max. DC power (at cos φ = 1) / DC rated power	25550 W / 25550 W
Max. input voltage	1000 V
MPP Voltage range / rated input voltage	360 V to 800 V / 600 V
Min. input voltage / initial input voltage	150 V / 188 V
Max. input current per string input A / input B	33 A / 33 A
Technical Data (Output AC)	**Rating**
Rated power (at 230 V, 50 Hz)	25000 W
AC nominal voltage	3 / N / PE; 230 / 400 V
Max. output current / Rated output current	36.2 A / 36.2 A
Efficiency	**Rating**
Max. efficiency / European efficiency	98.3% / 98.1%

The inputs of the inverter are the outputs of the sub-array. The coupling of the inverters outputs is an AC coupling. The load is tied to the common AC busbar. The figure below shows the connections of an inverter.

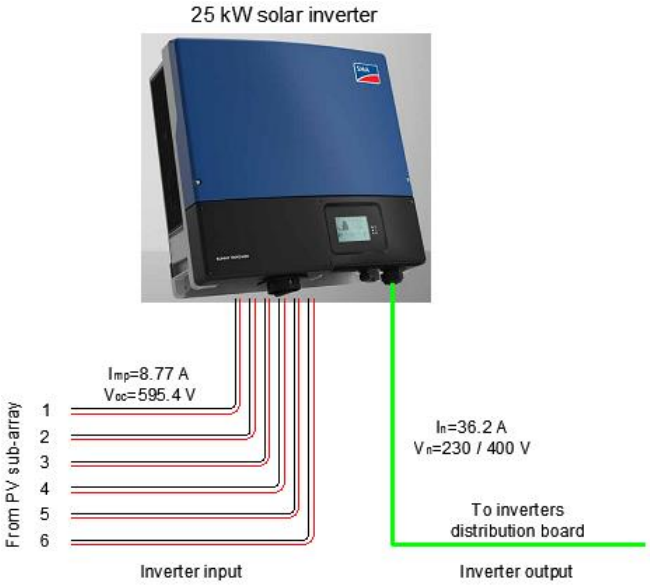

Figure (4.11): SMA (SUNNY TRIPOWER 25000TL) solar inverter connections.

4.4.3 System accessories

SMA cluster controller: The same as in AAU PV system.

Bidirectional meter: A bidirectional meter of type HOLLEY is used in the system. The model of the meter is DTSD545-G. This model uses the cellular

network's GPRS service to allow any of the meter readings or associated usage information to be read remotely by the electric utility. In general the meter can measure active and reactive (imported/exported) electrical energy, also the real time active/reactive/apparent power, voltage, current, power factor and frequency.

The DES project is implemented in two construction phases. The two phases are identical unless that the number of PV modules in one phase is less than the number of modules in the other phase by three module. A schematic diagram of DES is shown in Figure (4.12).

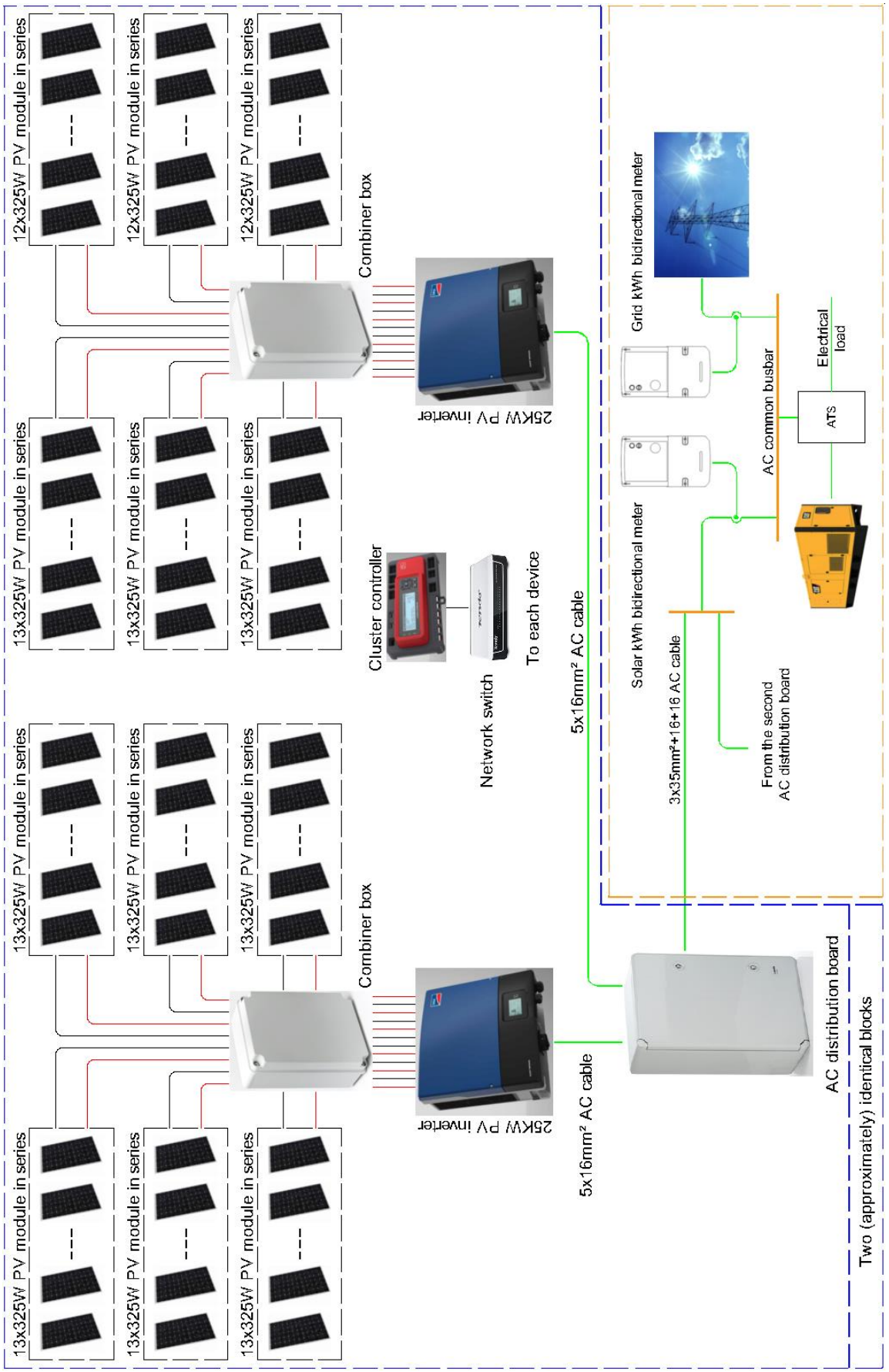

Figure (4.12): Schematic diagram of DES PV system.

Chapter Five

Simulation Using HOMER Software

5.1 Introduction to HOMER software

HOMER is an abbreviation for (Hybrid Optimization of Multiple Electric Renewables). It was developed by National Renewable Energy Laboratory (NREL) in 1993. HOMER has the ability to simulate, optimize and analyse both off-grid and grid connected power systems. HOMER generates results in a list of feasible configurations sorted by net present cost. The simulation results can be displayed in a wide variety of tables and graphs that help in comparing and evaluating configurations based on their economic and technical merits.

5.2 IUG PV solar system simulation

5.2.1 Solar radiation and temperature data

To obtain the solar radiation and temperature data, a location must be firstly chosen. The location can be selected by clicking on the map in the home page of HOMER software or simply typing the location name then clicking on the "Location Search" button. Figure (5.1) shows IUG location.

Figure (5.1): IUG location.

Solar radiation and temperature data can be downloaded from the HOMER website, entered manually month by month or imported as a time series data form a file. HOMER software will synthesize hourly data from monthly averages.

Downloading solar radiation and temperature data from HOMER website can be performed by clicking on the "Resources" button then selecting solar and temperature and finally clicking on the "Download" button. This will automatically

fill in the twelve monthly average values based on the latitude and longitude of the selected location.

HOMER software downloads solar radiation and temperature data from NASA surface meteorology and solar energy database. The global horizontal irradiation (GHI) resource is used to calculate flat panel PV array output. GHI is the sum of beam radiation (also called direct normal irradiance or DNI), diffuse irradiance and ground reflected radiation (HOMEnergyLLC, 2018). Figure (5.2) shows the monthly average solar GHI data of IUG location.

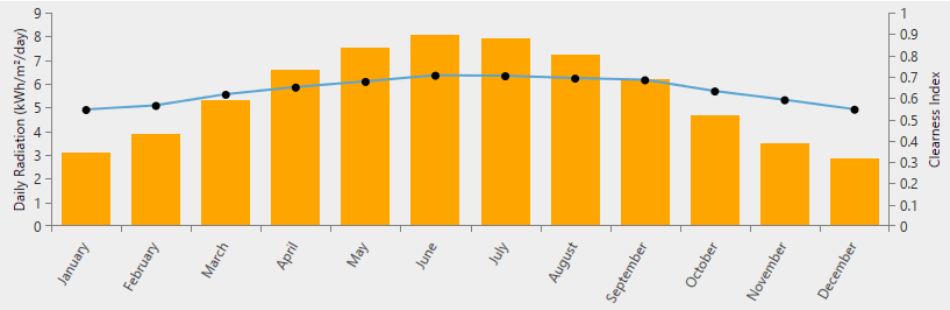

Figure (5.2): Solar GHI data of IUG location.

The annual average solar GHI of IUG location is equal to 5.57 kWh/m^2/day. The blue coloured curve with black dots in the previous figure represents the clear index which is a fraction of the radiation on the horizontal surface of the earth to the extra-terrestrial radiation. The value of the clearness index depends on the atmospheric conditions such as water vapour content and clouds distribution. The clearness index is a dimensionless value between 0 and 1. Higher values of clearness index occur in clear sky. HOMER software calculates the clear index from the global horizontal irradiance.

HOMER software uses the ambient temperature to calculate the PV cell temperature. The annual average temperature of IUG location is 19.82 °C. Figure (5.3) shows the monthly average temperature data of IUG location.

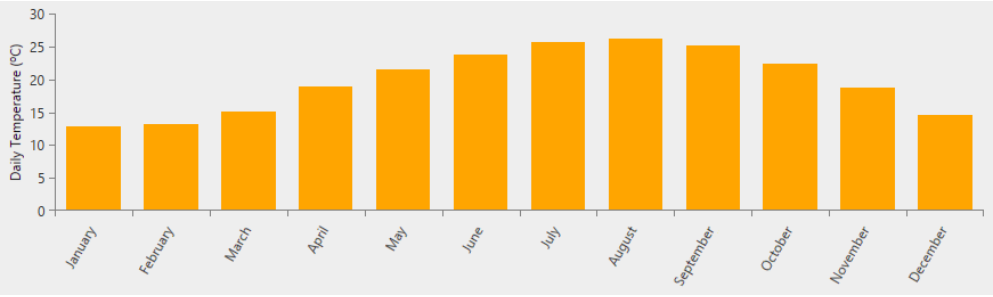

Figure (5.3): Temperature data of IUG location.

5.2.2 Electric load

The electrical loads connected to the PV system of IUG include around 70% of the building lighting (about 30 kVA) work as long as there are lectures for students, almost form 8:00 AM to 5:00 PM, main servers devices (about 10 kVA) work for 24 hours a day and air conditioning units of the main servers room (about 18 kVA) also work for 24 hours controlled by a thermostat to keep the temperature within an acceptable set point. In fact the electrical loads are connected directly to the inverters so the inverters data represents the actual electrical loads.

A very useful feature in the remote control RCC-02 is the data logger function. The data logger function, integrated in the remote control, records the data of the system. STUDER Innotec offers a free analysis tool (Xtender Data Analysis Tool) in the form of a file type Microsoft Excel allowing all recorded data to be collected and displayed graphically. The data are then easy to read and understand at a glance. This enables the follow up on the system's energy consumption evolution, to check the power cuts, to monitor the input currents and voltages, etc...

The main electrical values are saved on the SD card in the remote control as CSV file. After requesting these files from the supervisor of the PV system in IUG, the July-2017 files were obtained. The data has taken every minute. This means that for the 31 days of July month, there will be 44640 values of data for each electrical parameter. The files are imported into the analysis tool. On the 15th of July, the total AC input power, the total AC output power and the total solar power are found to be as in the following figure.

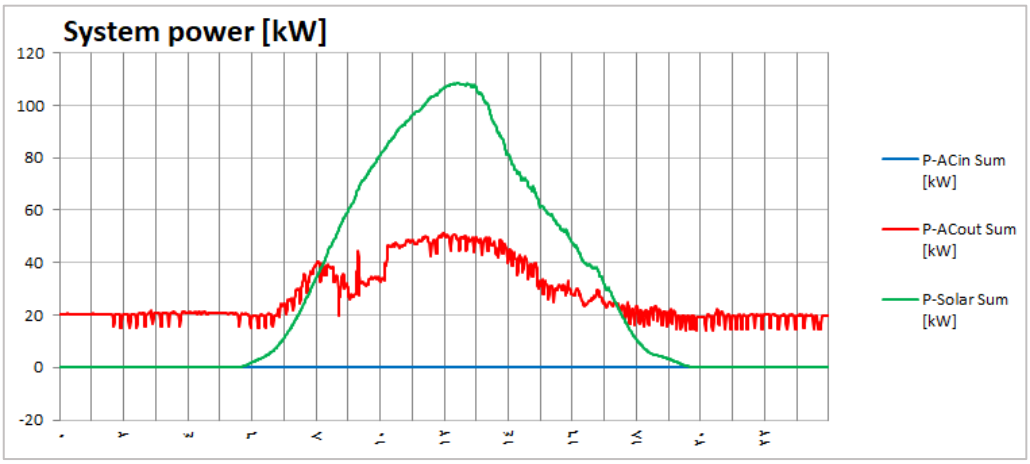

Figure (5.4): System power on the 15th of July.

Note: IUG system is under the guarantee of the project contractor. Due to technical issues, only the data of the July-2017 files were obtained.

The total AC output power represents the consumed power of the electrical loads. Actually it is the load power. The values of the total AC output power will be used to prepare a load profile file (a text file with .dmd extension) for July month in order to import the file to HOMER software.

HOMER software has the ability to add randomness to the load data of July month. Thereby, a more realistic load data of the rest months can be obtained after adding the randomness. Random variability is defined with two values, "Day-to-day" and "Timestep". Day-to-day variability causes the size of the load profile to vary randomly from day to day, although the shape stays the same while the timestep to timestep variability disturbs the shape of the load profile without affecting its size.

HOMER software calculates the average load value of all the weekdays load values, also calculates the average load value of all the weekends load values in each month for 24 hours of the day, these average values are tabulated in a table shown by clicking on the "Show All Months" button. The daily profile of July month is shown in the below figure.

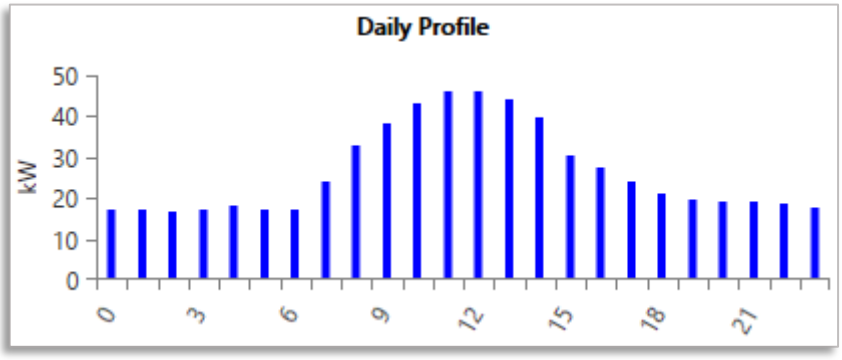

Figure (5.5): Daily profile of July month.

The maximum, average maximum, average, average minimum, minimum values of all the days in the month are represented for all months in the seasonal profile which shown in Figure (5.6). For each month, the top line corresponds to that month's overall maximum. The bottom line corresponds to the overall minimum. The top of the box is the average of the daily maximum of all the days in the month, and the bottom of the box is the average daily minimum. The middle line is the overall average for the whole month.

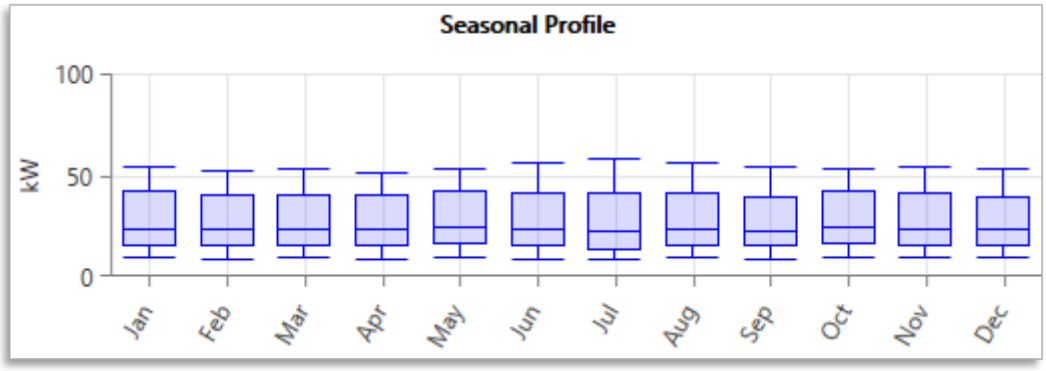

Figure (5.6): Seasonal profile of IUG load.

The load demand can be summarized in Table (5.1). Note that, the load factor is a dimensionless number equal to the average load divided by the peak load. The baseline data represents the real values of the load while the scaled data represents the baseline data after scaling by a factor. The value of this factor is equal to the value that specify in "Scaled Annual Average" input variable divided by the baseline annual average. The scaled data retains the seasonal shape of the baseline data, but may differ in magnitude. The default value for the scaled annual average is the baseline annual average.

Table (5.1): Load demand of IUG.

Metric	Baseline	Scaled
Average (kWh/d)	574.3	574.3
Average (kW)	23.93	23.93
Peak (kW)	58.77	58.77
Load Factor	.41	.41

5.2.3 System modelling

HOMER software has the ability to model any PV system component and store it in the software library, therefore the IUG solar system components such as PV module, charge controller, inverter and battery were modelled in HOMER software, the required data of modelling a specific components was obtained from the specifications of that component which considered in the previous chapter. The capital and replacement costs of a component were obtained from the final payment of the project. The operation and maintenance costs are assumed to be 1% of the capital cost. Figure (5.7) shows the complete model of the system.

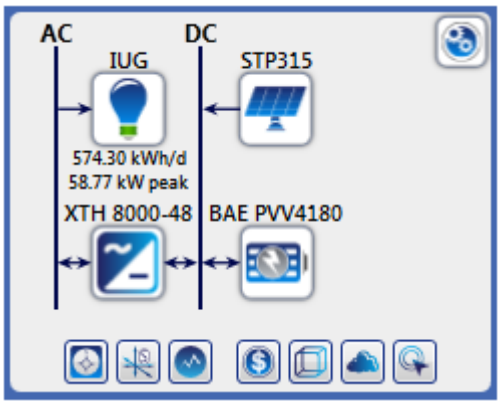

Figure (5.7): IUG PV system model.

Other required data to complete the design using HOMER software is listed in Table (5.2). This data is a standard data, an expected data or an actual data of the current system.

Table (5.2): Required input data of IUG system design.

Battery input data	**Value**
Round trip efficiency (%)	90
Minimum state of charge (%)	50
Float life (years)	20
Capital cost ($/battery)	1174.4
Replacement cost ($/battery)	1009
Initial state of charge (%)	100
PV module input data	**Value**
Life time (years)	25
Derating factor (%)	80
DC to DC Converter capital cost ($/kW)	389.3
DC to DC Converter replacement cost ($/kW)	170
DC to DC Converter lifetime (years)	15
PV module capital cost ($/kW)	1324.4
PV module replacement cost ($/kW)	825.4
Ground reflectance (%)	20
Panel slope (degree)	30
Panel azimuth (degree West of South)	0
DC to AC Converter input data	**Value**
Capital cost ($/kW)	1243.3
Replacement cost ($/kW)	1000
Life time (years)	15

Design constraints	Value
Annual capacity shortage (%)	0
Project life time (years)	25
Load in current time step (%)	0
Solar power output (%)	21

The round trip efficiency of the storage bank is the fraction of energy put into the storage that can be retrieved. HOMER software assumes the storage charge efficiency and the storage discharge efficiency are both equal to the square root of the round trip efficiency.

The float life of the storage is the length of time that the storage will last before it needs replacement. HOMER software gives the choice of storage replacement either by a fixed length of time (float life, years), or a fixed quantity of energy cycles through it (throughput, kWh), or whichever of those two happens first.

The maximum annual capacity shortage is the maximum allowable value of the capacity shortage fraction, which is the total capacity shortage divided by the total electric load. HOMER software considers infeasible (or unacceptable) any system with a higher value of the capacity shortage fraction.

The derating factor of the PV array represents all the array losses as a percentage. PV array losses include soiling, shading, snow and so on. From the data obtained from the supervisor of the system, the PV power was compared with the solar power. It is found that the average value of the array derating factor is 80%.

5.2.4 Simulation results

After set the parameters mentioned in the Table (5.2) and run the simulation, the result was that no feasible solution found, i.e. the system model (with the installed components ratings) was infeasible due to the capacity shortage constraint. This concerned that the system cannot be able to be standalone off-grid system. That was what the system supervisor confirmed, where he stressed that the system is sometimes connected to another source of energy other than the solar generator. Therefore, the system is deemed as a hybrid off-grid system. It is thought that the system capacity shortage takes place during winter months where the amount of solar radiation is low.

To determine the amount of capacity shortage that makes the system feasible, sensitivity variables were added to the annual capacity shortage with a range from 1 to 9. The results showed that there was a feasible solution with 9% capacity shortage. The simulation results are represents in Tables (5.3) and (5.4).

Table (5.3): System architecture with 9% annual capacity shortage.

Sensitivity	Architecture							
Capacity Shortage (%)					STP315 (kW)	STP315-MPPT (kW)	BAE PVV4180	XTH 8000-48 (kW)	Dispatch
9.00					142	150	144	126	LF

Table (5.4): Electrical prodution and quality with 9% annual capacity shortage.

Production	kWh/yr	%
SUNTECH STP315 - 24/Vem	232,698	100
Total	232,698	100

Quantity	kWh/yr	%
Excess Electricity	23,171	9.96
Unmet Electric Load	16,593	7.92
Capacity Shortage	17,454	8.33

The annual energy production is 232698 kWh. The excess electricity which defines as the surplus produced energy is 23171 kWh per year. The unmet electrical load is the load which the system was unable to supply, it is 16593 kWh per year. The capacity shortage is the difference between the required capacity by the loads and the available capacity, the capacity shortage has an annual value of 17454 kWh.

Here, a question is raised, which is, how much is the annual average (kWh/d) that the system model can handle without capacity shortage? To answer the question a scale annual average input variable were defined. The scale annual average input variable was used to scale the baseline data by a factor. Using an input range of scaled annual average which is between 290 - 295 kWh/d, the result was as in the follow table.

Table (5.5): Electrical quality with 292 kWh/d scaled annual average.

Quantity	kWh/yr	%
Excess Electricity	116,856	50.2
Unmet Electric Load	103	0.0967
Capacity Shortage	104	0.0974

Now, the answer of the question is that the system model can support 51% ($\frac{292\times100}{574.3}$) of the baseline average (kWh/d) without capacity shortage. It can be concluded that the load is reduced by about 49% in each month. But due to the

higher value of excess electricity which was 116856 kWh/yr, represents 50.2% of the total production, the system is considered inefficient.

The revised model of the system includes adding the electrical utility grid and the a backup diesel generator. The system is now a hybrid off-grid PV system. The system model is typically the same as the actual one. Figure (5.8) shows the revised model of the system. Be careful, not to confuse between the system model on its form and on-grid systems. In fact, the system inverters are connected to the local electrical grid of the IUG as described in Chapter Four. The local grid is fed from the utility grid or a backup generator via an automatic transfer switch.

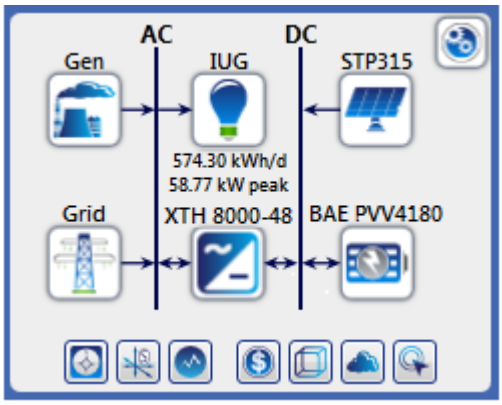

Figure (5.8): Revised model of the IUG PV system.

For simplicity, the external power source were restricted to the grid only in order to find out the intervals of the capacity shortage and to check the previous expectation that the capacity shortage take place in winter months or not. Figure (5.9) shows the monthly average electrical production of both the PV array and the utility grid.

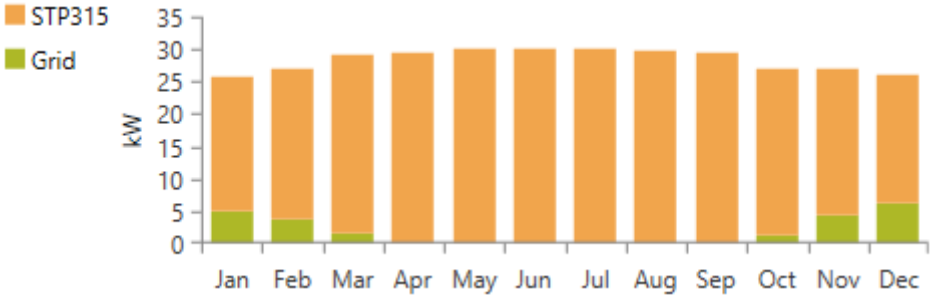

Figure (5.9): PV array and utility grid monthly average electrical production.

Referring to the above figure, it is obvious that the capacity shortage spreads over six months includes winter season months. One more note, the calculated

monthly average production is equal to the total hourly production in a certain month divided by the number of hours in that month.

The modelling parameters of the grid are the price of the energy where it was set to $0.17 per kWh and the reliability of the grid where it is assumed to be 4 hours "on" and 12 hours "off" schedule. A time schedule file of the grid reliability was prepared and imported to HOMER software. While the backup generator supplies all the electrical loads in the IUG include those which connected to the inverters output. So only the fuel price parameter of the backup generator modelling parameters was used to model the backup generator. The price was set to the fuel price in the fuel stations which is $1.47 per litter ($1=NIS 3.5). The revised system model is ready now to simulate.

The simulation is performed and as a part of the results, the system architecture with items ratings is represented in Table (5.6) also the system cost is represented in Table (5.7).

Table (5.6): IUG system architecture.

Architecture											
						STP315 (kW)	STP315-MPPT (kW)	Gen (kW)	BAE PVV4180	Grid (kW)	XTH 8000-48 (kW)	Dispatch
						142	150	59.0	144	999,999	126	LF

Table (5.7): IUG system cost.

Cost				System
COE ($)	NPC ($)	Operating cost ($/yr)	Initial capital ($)	Ren Frac (%)
$ 0.211	$ 1.12M	$ 21,742	$ 574,450	92.2

where the initial capital cost of the system is defined as the cost of supplying and installing the system components at the beginning of the project. While the operating cost is defined as the annualized value of all costs and revenues other than the initial capital. As well the total net present cost (NPC) of a system is defined as the present value of all the costs that it incurs over its lifetime minus the present value of all the revenue that it earns over its lifetime. Costs include capital costs, replacement costs, operation and maintenance costs, fuel costs, and the costs of buying power from the grid. Revenues include salvage value and grid sales revenue.

The cost of energy (COE) is the cost of production 1 kWh of energy from the system. For the currently installed system, the COE is $0.211 per kWh. This means that the cost of energy produced by the system is more than the utility grid COE which is $0.17 per kWh.

The last column of Table (5.7) represents the renewable fraction (abbreviated Ren Frac) of the system. The renewable fraction is the fraction of the energy delivered to the load that originated from renewable power sources. It equals to 92.2%, the remaining 7.8% represents the energy delivered to the load either from the grid or from the backup generator.

The monthly average electrical production of the PV array, the utility grid and the backup generator are shown in Figure (5.10).

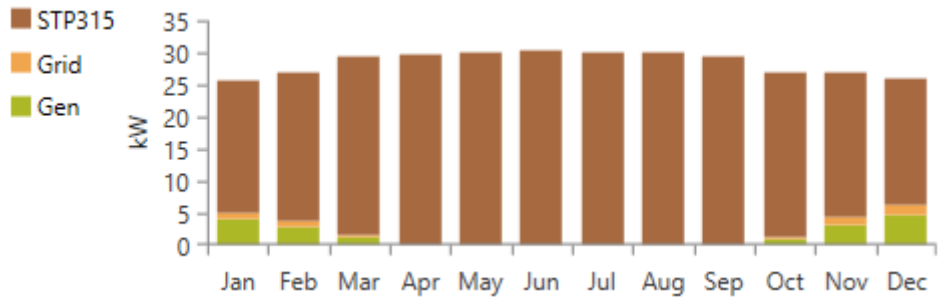

Figure (5.10): Monthly average electrical production.

The simulation results of the PV array output power, the load power and the power delivered by the grid on the 15th of July are shown in Figure (5.11).

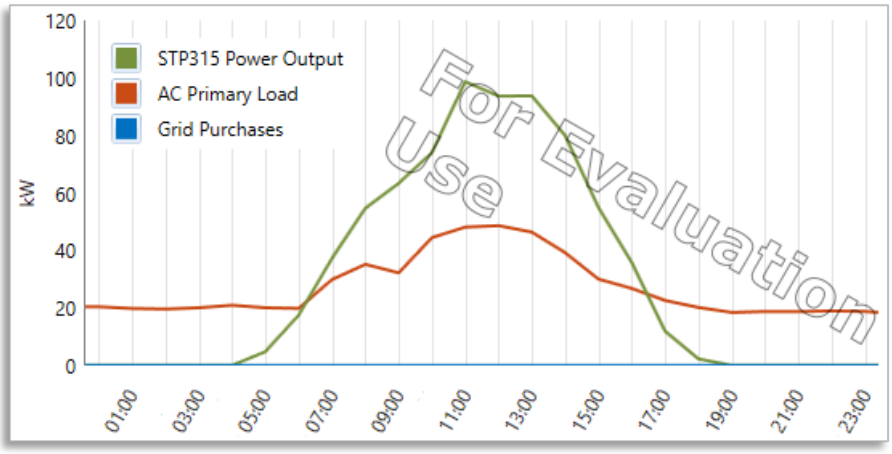

Figure (5.11): Simulated system power on the 15th of July.

From the previous figure, it seems that a large amount of the PV output power is unused. The results were checked to find out the amount of excess power in order

to interpret the unused amount of power production. Figure (5.12) illustrates the excess power.

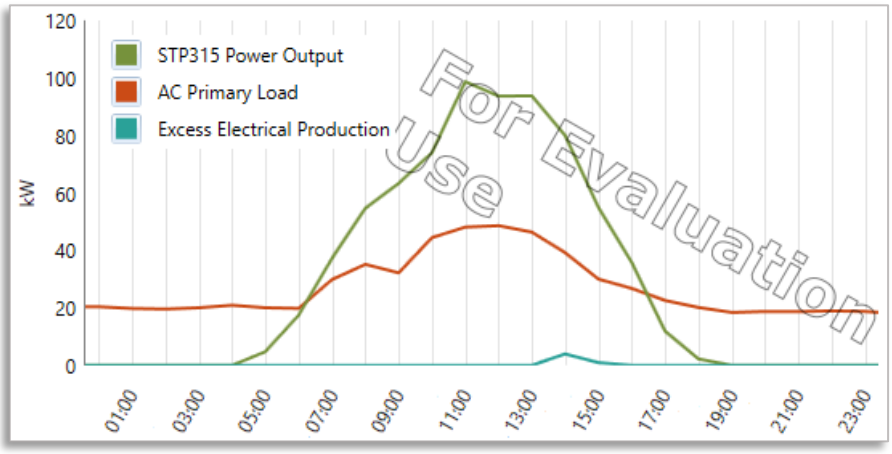

Figure (5.12): System power with illustrating excess power.

The excess power has a little amount and that is good because there is not loss of power. By the way, the yearly amount of excess electricity is 20400 kWh. This amount represents 8.18% of the total yearly production. Certainly the SOC of the battery bank will interpret the unused amount of power production. Figure (5.13) illustrates the battery bank charge power.

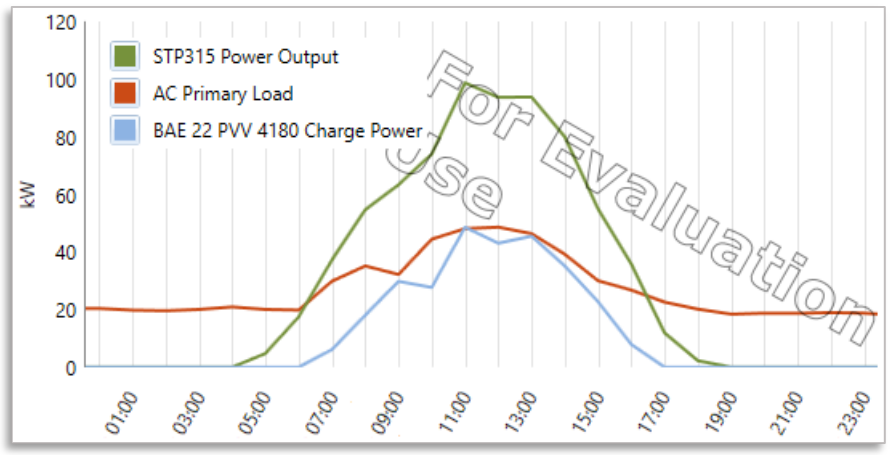

Figure (5.13): System power with illustrating battery bank charge power.

It is clear now that the PV output power is used to serve the load and charge the battery bank. It is also observed that the priority of consuming the generated energy from the PV array is for the load.

Remember the data CSV files of the IUG PV system, these files contains data about the battery bank SOC. The data was used to confirm the battery charge power

curve already considered. Figure (5.14) shows the actual charge power curve of the system battery bank on the 15th of July.

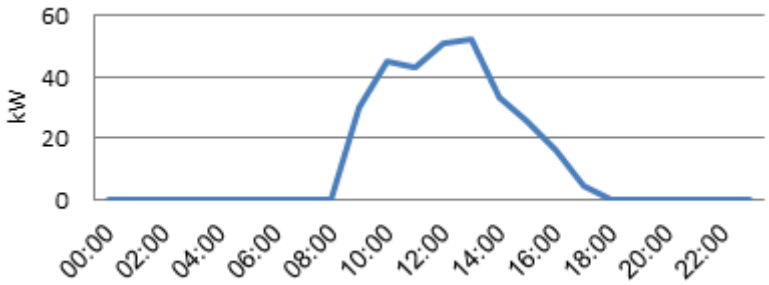

Figure (5.14): Actual charging power curve of the battery bank.

The previously charge curve slightly differs from the simulated curve, this is because of the difference between the actual solar radiation and the synthetic solar data created by HOMER software.

Referring to Table (5.2), the battery bank minimum state of charge is 50% equivalent to 50% depth of discharge. To optimize the SOC and the batteries number, a sensitivity variable was added to the SOC (from 20% to 60% with 10% increasing step) and the search space of batteries number was expanded (from 96 to 144). The search space is defined as the set of decision variable values that HOMER searches to locate the optimal system. As well the decision variable is defined as a variable whose optimal value is determined during the course of the optimization process. The system configuration result is as in Table (5.8).

Table (5.8): Battery bank SOC with batteries number optimization results.

Sensitivity			Gen	Grid
Minimum State Of Charge (%)	BAE PVV4180	Autonomy (hr)	Production (kWh)	Energy Purchased (kWh)
20.0	120	33.3	10,688	3,270
30.0	144	34.9	10,349	3,228
40.0	144	30.0	11,354	3,507
50.0	144	25.0	12,718	3,874
60.0	144	20.0	14,243	4,713

It can be noted from the last table that the required number of batteries with 20% DOD is 120 batteries. Worth mentioning here that the generator and the grid will keep the systems configurations in the previous results without capacity shortage by maintaining the generator energy production and the energy purchased from the grid within sufficient values.

5.2.5 System optimization

The system model is optimized according to the search space represented in Table (5.9). In the search space, different sizes or quantities are assigned to the system components. The chosen sizes for both the inverters and the charge controllers are multiples of one unit size of each of them. The number of batteries strings is changed by adding one string each time, begins with one string. The changing step of the PV array rated values is 4.725 kW which equals to the sub-array rated power connected to one charge controller. HOMER will simulate all combinations of the search space values to determine the most efficient system configuration.

Table (5.9): System model optimization search space.

XTH 8000-48 Capacity (kW) Optimizer	Gen Capacity (kW)	Grid Purchase Capac (kW)	STP315 DC Capacity (kW)	STP315 Size (kW) Optimizer	BAE PVV4180 Strings (#) Optimizer
21	59	999999	90	118.125	3
42			100	122.85	4
63			110	127.575	5
84			120	132.3	6
105			130	137.025	
126			140	141.75	
			150		

The optimal configuration architecture and cost are presented in Table (5.10) and Table (5.11) respectively. Knowing that the renewable fraction is 92%, the annual generator energy production is 12965 kWh, the annual energy purchased from the grid is 4008 kWh and the autonomy of the battery bank is 25 hours.

Table (5.9): Optimal configuration of the system.

Architecture										
						STP315 (kW)	STP315-MPPT (kW)	Gen (kW)	BAE PVV4180	Grid (kW)	XTH 8000-48 (kW)	Dispatch
						142	100	59.0	144	999,999	63.0	LF

Table (5.10): Optimal configuration cost.

Cost			
COE ($)	NPC ($)	Operating cost ($/yr)	Initial capital ($)
$ 0.180	$ 950,478	$ 18,953	$ 476,657

By comparing the optimal configuration with the installed system from an economic aspect, it was found that, the initial cost of the optimal configuration ($476657) is less than the installed system initial cost ($574450) by about $98000. Also the annual operating cost of the optimal configuration ($18953) is less than the annual operating cost of the installed system ($21742) by $2789. Finally the net present cost of the optimal configuration ($950478) is less than the installed system net present cost ($1120000) by $169522.

The optimality of the optimal configuration over the installed system occurs in the cost of energy where it was $0.18 and $0.211, respectively per kWh of energy. The cost of energy in the optimal configuration is close to the cost of energy delivered by the utility grid.

For the installed system, the load baseline is scaled (from 130% to 160% with 10% increasing step) in attempting to match the load power with the inverters rated power. In the same time the PV array power is increased to match the charge controller input power (which equals to the PV array power minus the losses) with its rated power. The result were as in the below table.

Table (5.11): System architecture after load scaling.

Sensitivity	Architecture												
IUG Scaled Average (kWh/d)							STP315 (kW)	STP315-MPPT (kW)	Gen (kW)	BAE PVV4180	Grid (kW)	XTH 8000-48 (kW)	Dispatch
747							220	130	95.0	144	999,999	63.0	LF
804							220	130	95.0	144	999,999	63.0	LF
861							240	140	95.0	144	999,999	84.0	LF
919							240	150	95.0	144	999,999	84.0	LF

As seen in Table (5.12), the inverters rated power did not match the load even with scaling the load up to 160% (919 kWh/day). This means that the inverters are too much oversized. In the same load scaling, the PV array power should be 240 kWP to match the charge controller input power with the charge controller rated power.

5.3 DES PV solar system simulation

5.3.1 Solar radiation and temperature data

DES is located not far from the IUG, so the location of DES has the same solar radiation and temperature data of the IUG location. .

5.3.2 Electrical load

The electrical loads of DES are the conventional electrical loads which can be found in any school such as the class rooms lighting, computer devices in computer labs, limited number of refrigerators and air conditioning units. The night electrical loads are restricted to the lighting and appliances of the guard room and few residents' rooms and the refrigerators.

As considered in Chapter Four, a net meter of type HOLLY is used for connecting the system to the utility grid. Actually there are three net meters used, one is connected to the solar output called the solar meter, the second is connected to the utility grid called the main meter, the third is connected parallel to the second one, the third meter called the monitoring meter. The net meters data is send via GSM grid and stored in the servers devices of the IT department of GEDCO. The data was requested from GEDCO, and they were thankful to provide it. The obtained data was scheduled as in the following table.

Table (5.12): HOLLY meter data.

		Meter No:	main		Meter Type:	DTSD545		
		CT Radio:	200A/5A		PT Radio:	1V/1V		
No.	Time	Import			Export			PF
		Active	Reactive	Apparent	Active	Reactive	Apparent	
19	01/04/2017 18:00	0	0.021	0.021	0.565	0	0.565	0
20	01/04/2017 19:00	0	0.006	0.006	0.099	0	0.099	0
21	01/04/2017 20:00	0.267	0.087	0.281	0	0	0	0.95
22	01/04/2017 21:00	0.218	0.095	0.238	0	0	0	0.916

The data in the previous table is the data of the main meter. The current transformer turns ratio (CT Ratio) is 200 A/5 A. So the imported and exported data should be multiplied by the CT ratio which equals to 40 in order to obtain the real values. It is obvious that the main meter has an imported or exported data i.e. if there is an imported data then there would not be an exported data and voice vies, while the solar meter has an exported data only. Only the active data will be used in calculating the load.

The load power can be calculated from the main meter imported and exported data and the solar exported data according to the following: if the main meter exported data equals to zero then the load power equals to the solar meter exported data plus the main meter imported data and if the main meter imported data equals to

zero then the load power equals to the solar meter exported data minus the main meter exported data.

The load profile file was prepared (a text file with .dmd extension) and imported to HOMER software. The average daily energy consumption of the load is 248.26 kWh/d. The seasonal profile is shown the Figure (5.15).

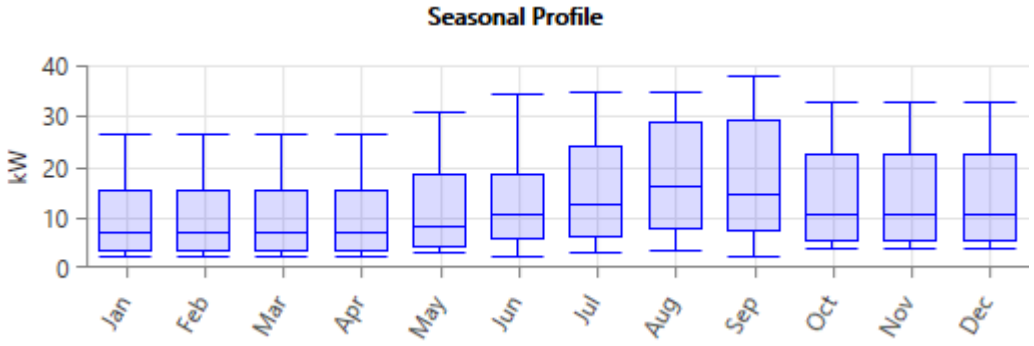

Figure (5.15): Seasonal profile of DES load.

The Sunny Portal is another source of data, but that data is for the solar generated power only. So it cannot be used alone to calculate the load power. The Sunny Portal data was used to confirm the solar meter data and the grid outage intervals during daytime. Figures (5.16) and (5.17) show the Sunny Portal data and the solar meter data on the 24th of May respectively.

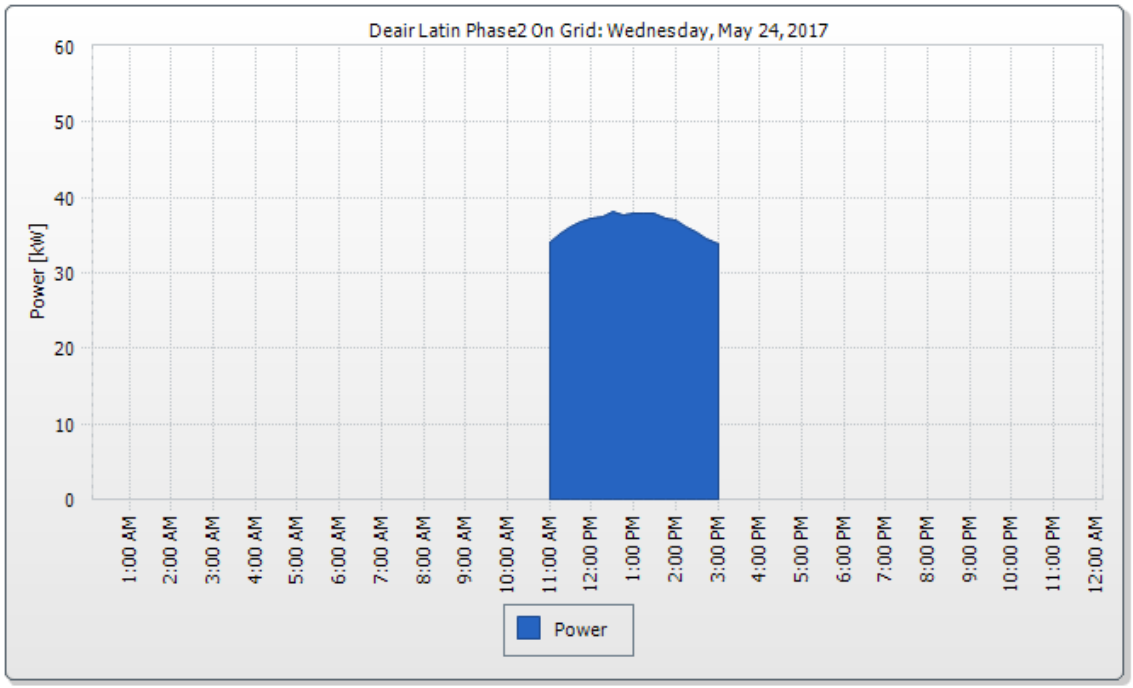

Figure (5.16): Sunny portal data on the 24th of May.

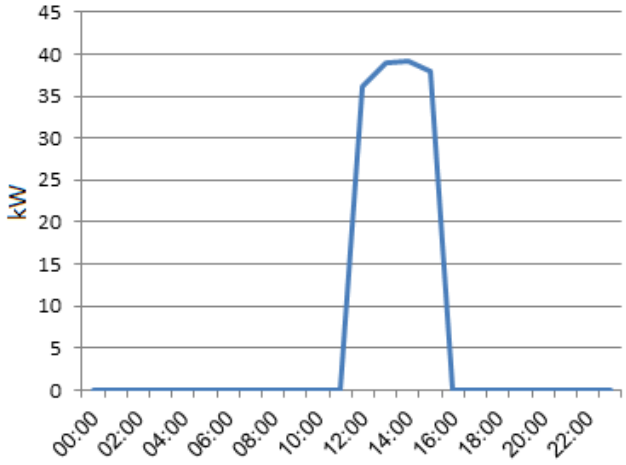

Figure (5.17): Solar meter data on the 24th of May.

As mentioned in Chapter Four that DES system was implemented upon two consecutive phases. Sunny Portal data shown in Figure (5.16) is for the second phase.

5.3.3 System modelling

The required data for modelling the PV module and the solar inverter was taken from their data sheets. The grid energy price was set to $0.17 per kWh and the sellback price was set to $0.17 per kWh, this was based on the contract between DES and GEDCO. The time series grid outage file was prepared depending on the main meter data, where the main meter works on or off according to the utility grid on or off states. The backup generator was modelled and the fuel price was set to $1.47 per litter. Figure (5.18) shows the DES PV system model also Table (5.13) repersent the required input data for the design.

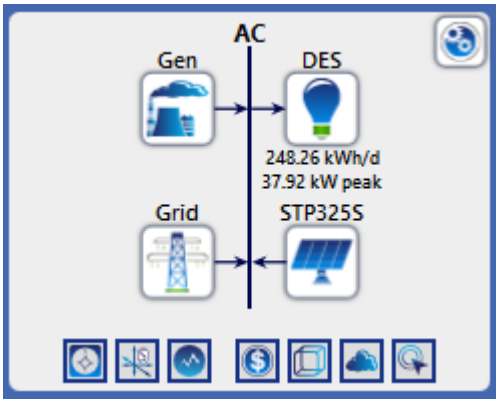

Figure (5.18): DES PV system model.

Table (5.13): Required input data of DES system design.

PV module input data	Value
Life time (years)	25
Derating factor (%)	80
Converter capital cost ($/kW)	288.7
Converter replacement cost ($/kW)	182.1
Converter lifetime (years)	15
PV module capital cost ($/kW)	950.80
PV module replacement cost ($/kW)	602.6
Life time (years)	25
Ground reflectance (%)	20
Panel slope (degree)	30
Panel azimuth (degree West of South)	0
Design constraints	**Value**
Annual capacity shortage (%)	0
Project life time (years)	25
Load in current time step (%)	0
Solar power output (%)	25

5.3.4 Simulation results

The power rating of the required generator to serve the loads is 38 kW. The COE is $0.102 per kWh. It is less than the COE of the utility grid. The renewable fraction of the system is 68.4%, it has a low value due to the effect of grid outage periods which resulting in automatic inverters shutdown. The annual PV array production is 163452 kWh. The initial and NPC cost of the system is $123440 and $377816 respectively.

The economic effect of the permanent availability of the utility gird on the system is valuable where after the life time of the project, the NPC is -$141371 and the COE is -$0.0269 per kWh. The minus sign indicates that previous financial values should be paid to the PV system owner by GEDCO.

The purpose of the simulation is to compare the system model with and without grid outage from an economic point of view. The disadvantage of DES PV system is that the system does not work unless the grid is available. Therefore the grid reliability plays an important role in determining the feasibility of the system. The load is fed from the backup generator during grid outage. The energy

(purchased, sold and charge) with and without grid outage are presented in Tables (5.15) and (5.16) respectively.

Table (5.14): Energy (purchased, sold and charge) with grid outage.

Month	Energy Purchased (kWh)	Energy Sold (kWh)	Energy Charge ($)
January	2,265	6,645	$744.59-
February	1,878	6,744	$827.17-
March	1,798	9,597	$1,325.91-
April	1,705	9,745	$1,366.80-
May	983	3,969	$507.64-
June	1,585	4,082	$424.47-
July	2,190	4,484	$389.90-
August	2,287	1,842	$ 75.55
September	1,879	3,119	$210.72-
October	1,524	3,097	$267.40-
November	1,577	2,348	$131.11-
December	1,939	2,346	$69.18-
Annual	21,611	58,019	$6,189.35-

From the previous table, 58019 kWh of energy was sold to GEDCO while 21611 kWh was purchased and 36408 kWh was considered as a balance for DES. This balance is equivalent to $6189.35 annually.

Table (5.15): Energy (purchased, sold and charge) without grid outage.

Month	Energy Purchased (kWh)	Energy Sold (kWh)	Energy Charge ($)
January	2,838	8,340	$935.31-
February	2,258	8,473	$1,056.58-
March	2,313	11,544	$1,569.31-
April	2,162	12,041	$1,679.44-
May	3,006	12,437	$1,603.19-
June	3,930	11,349	$1,261.21-
July	5,017	11,097	$1,033.68-
August	6,246	9,700	$587.03-
September	5,387	9,574	$711.92-
October	4,342	9,752	$919.74-
November	4,425	8,096	$624.08-
December	5,000	7,358	$400.81-
Annual	46,925	119,762	$12,382.28-

In the case of permanent availability of grid, the energy balance is 72837 kWh which equivalent to $12382.28 annually over the project life time, this balance is equivalent to $309549 after the end of the project life time. And if it is known that

the capital cost of the system is $123440.22, it will be found that the system is economically feasible.

An electricity bill of the consumed energy of DES is attached below. In June-2017, the consumed and produced energy were 1085, 3983 kWh respectively. The cumulative energy balance for the last months until the bill date is 24176 kWh.

Table (5.16): Electricity bill of DES in June month.

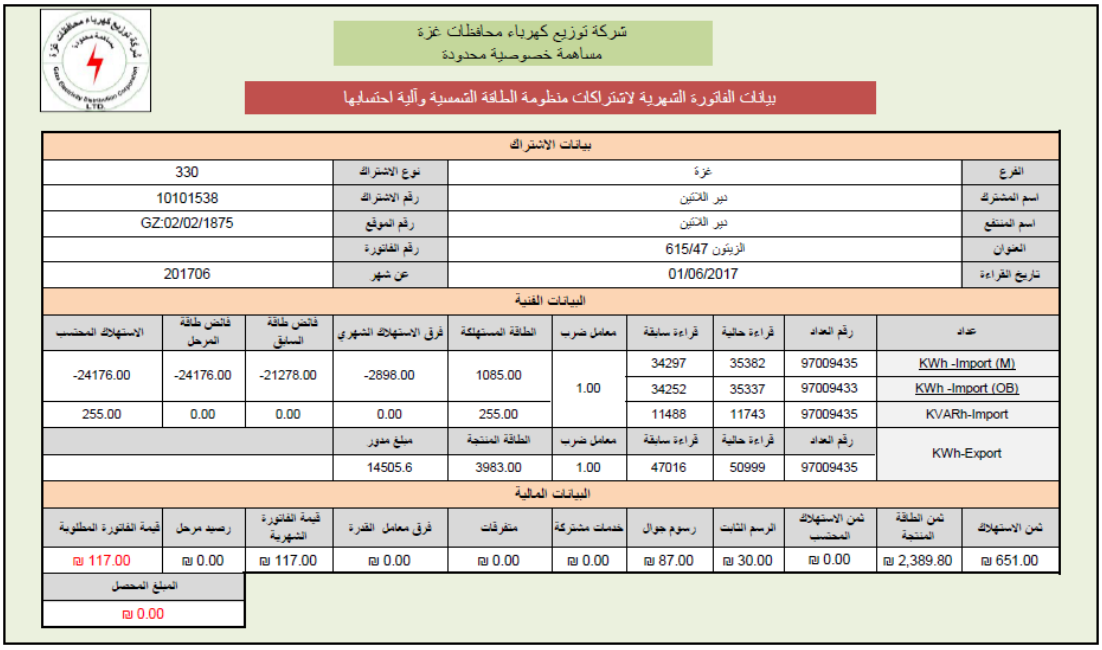

شركة توزيع كهرباء محافظات غزة
مساهمة خصوصية محدودة

بيانات الفاتورة الشهرية لاتتزاكات منظومة الطاقة الشمسية وآلية احتسابها

بيانات الاشتراك			
الفرع	غزة	نوع الاشتراك	330
اسم المشترك	دير الثنين	رقم الاشتراك	10101538
اسم المنتفع	دير الثنين	رقم الموقع	GZ:02/02/1875
العنوان	الزيتون 615/47	رقم الفاتورة	
تاريخ القراءة	01/06/2017	عن شهر	201706

البيانات الفنية

عداد	رقم العداد	قراءة حالية	قراءة سابقة	معامل ضرب	الطاقة المستهلكة	فرق الاستهلاك الشهري	فائض طاقة السابق	فائض طاقة المرحل	الاستهلاك المحتسب
KWh -Import (M)	97009435	35382	34297	1.00	1085.00	-2898.00	-21278.00	-24176.00	-24176.00
KWh -Import (OB)	97009433	35337	34252						
KVARh-Import	97009435	11743	11488		255.00	0.00	0.00	0.00	255.00
KWh-Export	رقم العداد	قراءة حالية	قراءة سابقة	معامل ضرب	الطاقة المنتجة	مبلغ مدور			
	97009435	50999	47016	1.00	3983.00	14505.6			

البيانات المالية

ثمن الاستهلاك	ثمن الطاقة المنتجة	ثمن الاستهلاك المحتسب	الرسم الثابت	رسوم جوال	خدمات مشتركة	متفرقات	فرق معامل القدرة	قيمة الفاتورة الشهرية	رصيد مرحل	قيمة الفاتورة المطلوبة
₪ 651.00	₪ 2,389.80	₪ 0.00	₪ 30.00	₪ 87.00	₪ 0.00	₪ 0.00	₪ 0.00	₪ 117.00	₪ 0.00	₪ 117.00

المبلغ المحصل
₪ 0.00

5.4 On-grid and off-grid solar PV systems comparison

As considered that the IUG system PV system is an off-grid system and the DES PV system is an on-grid system, comparing the two systems can be generalized to represent comparing On-grid and off-grid systems. The comparison parameters are the cost of energy yield from the two systems and the excess energy produced. The comparison includes the advantages and disadvantages of both systems.

In the IUG system the cost of energy is $0.211 per kWh, while for the DES system the cost is $0.102 per kWh. That means the cost of energy produced from the IUG system is about double the cost of one kWh produce form the IUG system. The reason of that is the higher cost of the battery bank. It is noted that there is no excess energy in the DES because the surplus energy is fed to the local utility grid, but mostly there will be a certain amount of excess energy that would not be consumed in the IUG system. The excess energy in the IUG system can be utilized to avoid waste of energy by optimal control of the electrical loads but this method could be

somewhat difficult to implement. The advantage of DES system is the excess energy usage in the opposite to the IUG system where the excess energy is a drawback of the system. The advantage that distinguishes the IUG system is the reliable energy production of the system. The major drawback of the DES is the synchronized shutdown of the system with grid outage.

5.5 AAU PV solar system simulation

The load data did not obtained because there was not a practical method that gives an accurate load data. So, the system simulation will not be conducted and deemed as future work.

Chapter six

Simulation Using PVsyst Software

6.1 Introduction to PVsyst software

PVsyst is a software package for studying, sizing, simulating, and analysing PV systems. This software was developed by Swiss physicist Andre Mermoud and electrical engineer Michel Villoz. Using PVsyst, different types of PV systems such as grid tie, standalone, pumping and DC grid can be modelled. PVsyst has the ability to predict the performance of different system configurations, evaluate the results and identify the best approach for energy production.

6.2 IUG solar system simulation

6.2.1 Solar radiation and temperature data

Designing using PVsyst software begins by defining the geographical site where the PV system will be installed. The IUG is located on 31.51 latitude, 34.44 longitude and 45m altitude above sea level. The standard time zone of Gaza Strip is UTC/GMT + 2 hours.

Importing meteo data in PVsyst software can be either from NASA or meteonorm resources (MeteotestAG, 2018). PVsyst software states that NASA resource is not always the best data resource but, because of using NASA resource in HOMER software, NASA resource will be used as a meteo data resource in PVsyst software. Table (6.1) presents the solar radiation (global and diffuse) and the temperature of IUG location. The data is typically the same as the data obtained from HOMER software.

Table (6.1): Solar radiation and temperature data of IUG location.

	Global [kWh/m².day]	Diffuse [kWh/m².day]	Temper. [°C]
January	3.08	1.01	12.9
February	3.90	1.26	13.1
March	5.29	1.48	15.1
April	6.58	1.68	18.9
May	7.50	1.79	21.5
June	8.07	1.73	23.8
July	7.90	1.69	25.8
August	7.23	1.56	26.2
September	6.22	1.33	25.1
October	4.67	1.21	22.3
November	3.50	1.00	18.7
December	2.87	0.92	14.6
Year	**5.58**	**1.39**	**19.8**

A comparison between meteonorm and NASA data is shown in Figure (6.1). The global horizontal average of NASA data is equal to 2006 kWh/y while for

meteonorm data the global horizontal average is equal to 1969 kWh/y. Actually there in no effective difference between the two meteo data resources.

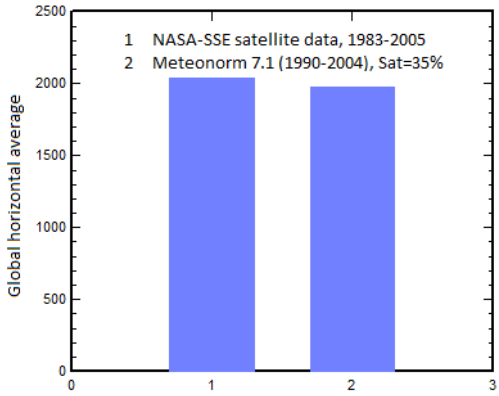

Figure (6.1): Meteonorm and NASA data comparison.

6.2.2 Orientation

PVsyst software has the ability to optimize the orientation of the PV module. Really the optimization can be performed with respect to three cases: Yearly, summer (Apr-Sep) and winter (Oct-Mar) irradiation yield. The preferred choice of the previous three cases is the yearly case. The optimized tilt and azimuth angles are 30°, 0° respectively.

A transposition Factor, abbreviated FTranspos. is defined as the difference (loss) with respect to the optimum orientation and the available irradiation on this tilted plane. The value of this factor should be as low as possible. PVsyst indicates the global yield on collector plane due to the selected orientation. In our case the global yield in the optimized orientation equals to 2287 kWh/m^2 (PVsystSA, 2018). Figure (6.2) shows the optimized orientation according to yearly irradiation level.

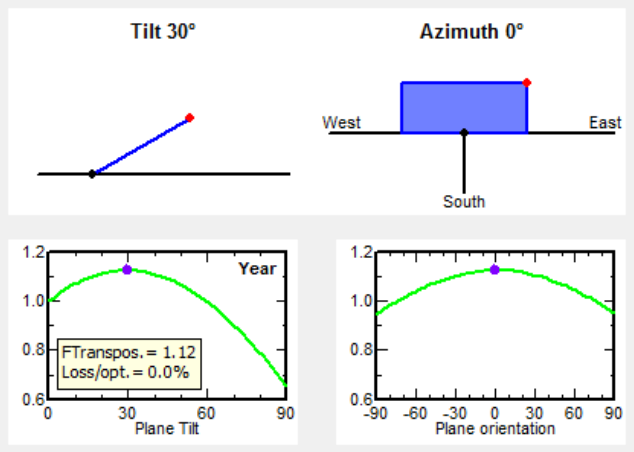

Figure (6.2): Optimized orientation of PV modules in Gaza strip.

6.2.3 User's needs

The same created load profile file which was imported to HOMER software was used to import IUG load profile data to PVsyst software but after converting to CSV file because this is the file type that PVsyst software supports. Figure (6.3) shows the load power on the 15th of July.

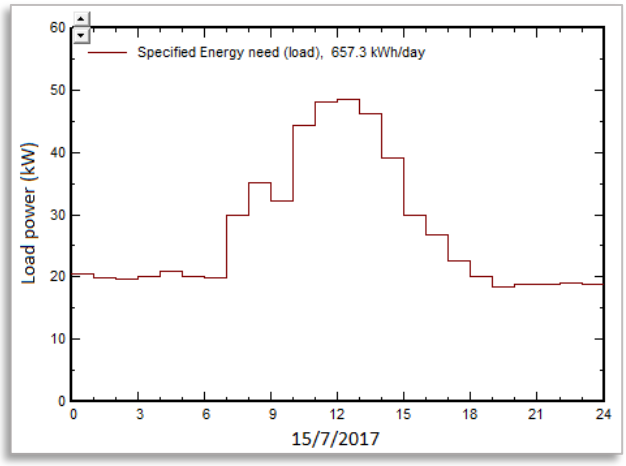

Figure (6.3): Load power on July 15, 2017.

PVsyst calculates average load energy of each month of the year based on the entered load profile data. It can be noted here, that PVsyst uses monthly average energy representation of the user's need while HOMER uses monthly average power representation to define the load demand. The energy value obtained from PVsyst in a certain month equals to the average power value in that month obtained from HOMER software multiplied by number of days in the month multiplied by 24 hours. Figure (6.4) shows the monthly average energy all over the year.

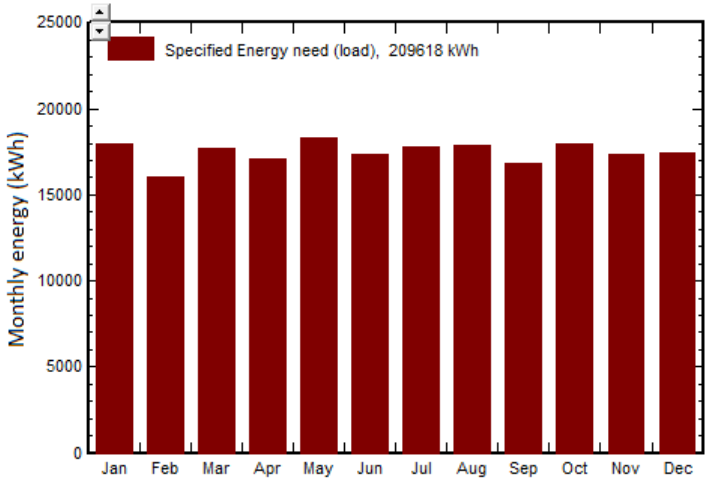

Figure (6.4): Monthly average energy.

The load demand is presented in Table (6.2). Certainly the load demand is typically the same as the load demand in HOMER software.

Table (6.2): User's needs of IUG.

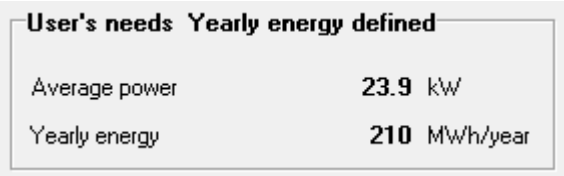

6.2.4 System modelling

PVsyst software offers presizing suggestions of the system. A presizing is a rough estimation of the PV system energy yield and user's needs satisfaction, based on a few very general parameters. Its aim is to determine the size of the optimal PV array power and battery pack capacity required to match the user's needs. Table (6.3) presents the pre-sizing data.

Table (6.3): Pre-sizing data.

Note that, LOL is an abbreviation of "loss of load" and is defined as the probability that the user's needs cannot be supplied. The pre-sizing LOL is 5%. LOL is equivalent to capacity shortage in HOMER software which was 9%.

The wonderful in PVsyst software is the wide database of PV systems components which stored in the software. The battery, PV module and charge controller types are selected from the software database. Other required data for modelling is entered manually. The modelling data are presented in Table (6.4).

Table (6.4): IUG system components modelling data.

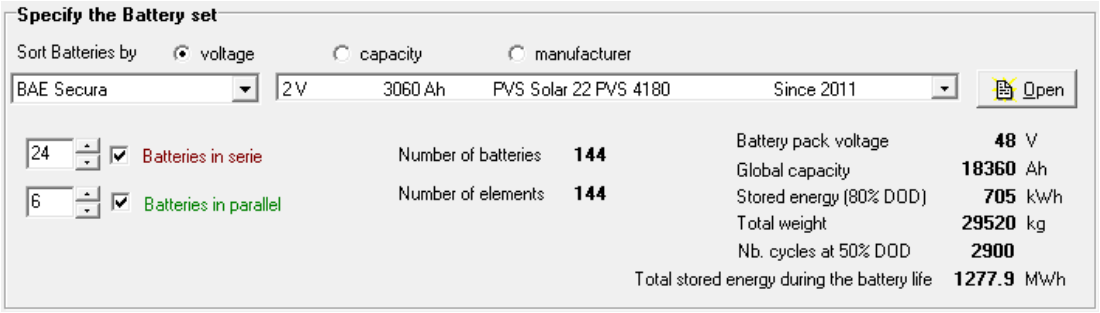

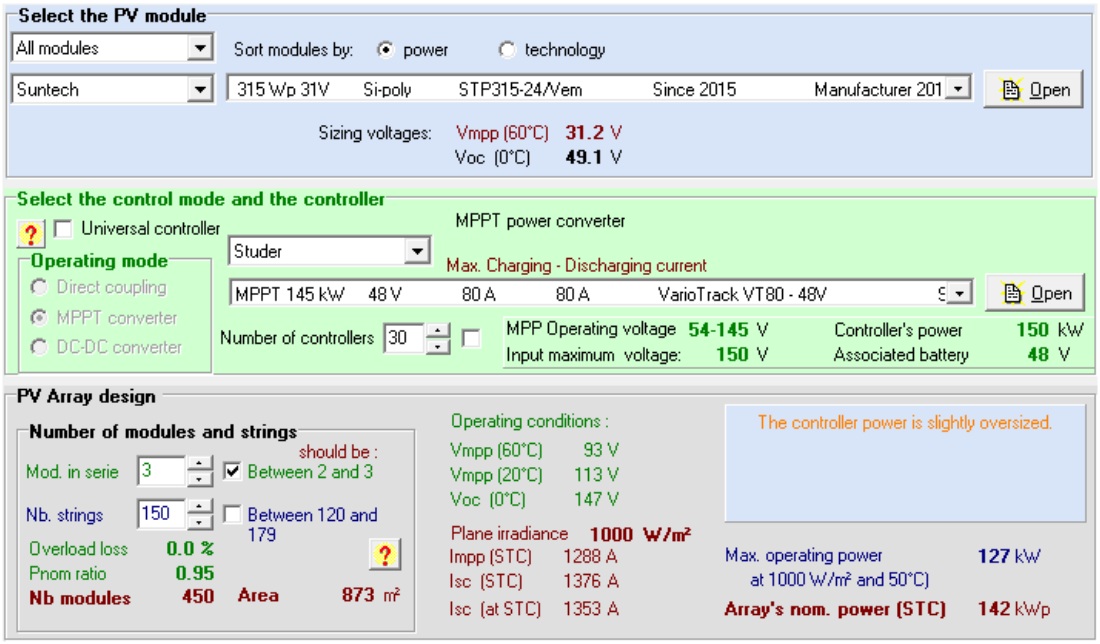

6.2.5 Simulation results

The balances and main results of the simulation are presented in Table (6.5). The annual available solar energy (E Avail) is 252.38 MWh/yr. The unused energy (E Unused) is 23.061 MWh/yr. The unused energy is equivalent to the excess electricity in HOMER software which was 23.171 MWh/yr. The missing energy (E Miss) is 10.512 MWh/yr. The equivalent of missing energy in HOMER software is the capacity shortage which has a value of 16.593 MWh/yr. The solar fraction (SolFrac) is defined as the present of the energy supplied to the user (E User) to the energy need of the user (E Load). It has a value of 95%. Note that the actual value of the LOL rather than the pre-sizing value is 4.7%.

Table (6.5): Balances and main results of IUG system.

	GlobHor kWh/m²	GlobEff kWh/m²	E Avail MWh	EUnused MWh	E Miss MWh	E User MWh	E Load MWh	SolFrac
January	95.5	140.7	16.94	0.000	2.775	15.18	17.96	0.845
February	109.2	143.5	17.15	0.130	1.422	14.58	16.00	0.911
March	164.0	189.1	22.25	2.290	0.805	16.92	17.73	0.955
April	197.4	199.0	22.99	3.013	0.000	17.07	17.07	1.000
May	232.5	209.3	23.94	3.002	0.000	18.28	18.28	1.000
June	242.1	206.3	23.34	3.355	0.000	17.35	17.35	1.000
July	244.9	213.7	23.96	3.492	0.000	17.79	17.79	1.000
August	224.1	215.4	24.05	3.489	0.000	17.89	17.89	1.000
September	186.6	204.8	22.92	3.397	0.000	16.79	16.79	1.000
October	144.8	183.6	20.93	0.891	0.000	17.98	17.98	1.000
November	105.0	151.2	17.59	0.000	1.989	15.35	17.34	0.885
December	89.0	136.2	16.32	0.002	3.520	13.92	17.44	0.798
Year	2035.1	2192.9	252.38	23.061	10.512	199.11	209.62	0.950

6.3 DES PV solar system simulation

6.3.1 Solar radiation and temperature data

DES has the same solar radiation and temperature data of the IUG, where DES locates not far from IUG.

6.3.2 User's needs

A CSV file was prepared to import into the software. The data of that file is the same as the data of the load profile file which was imported to HOMER software. The annual required energy is 90615 kWh to serve the user's need.

6.3.3 System modelling

In PVsyst, the DES solar PV system can be easily modelled. The PV module and the solar inverter types are stored in the database of the software. The note that should be mentioned is that the total number of modules in the system is 309 modules, but, in fact the modelled number of PV modules is 312 modules because of the inability of assigning 39 modules to first MPPT input and 36 modules to the second MPPT input of the fourth array inverter. So three modules are added to the fourth sub-array, this makes the total number of modules 312 modules instead of 309 modules. Table (6.6) presents the system modelling data.

Table (6.6): DES system components modelling data.

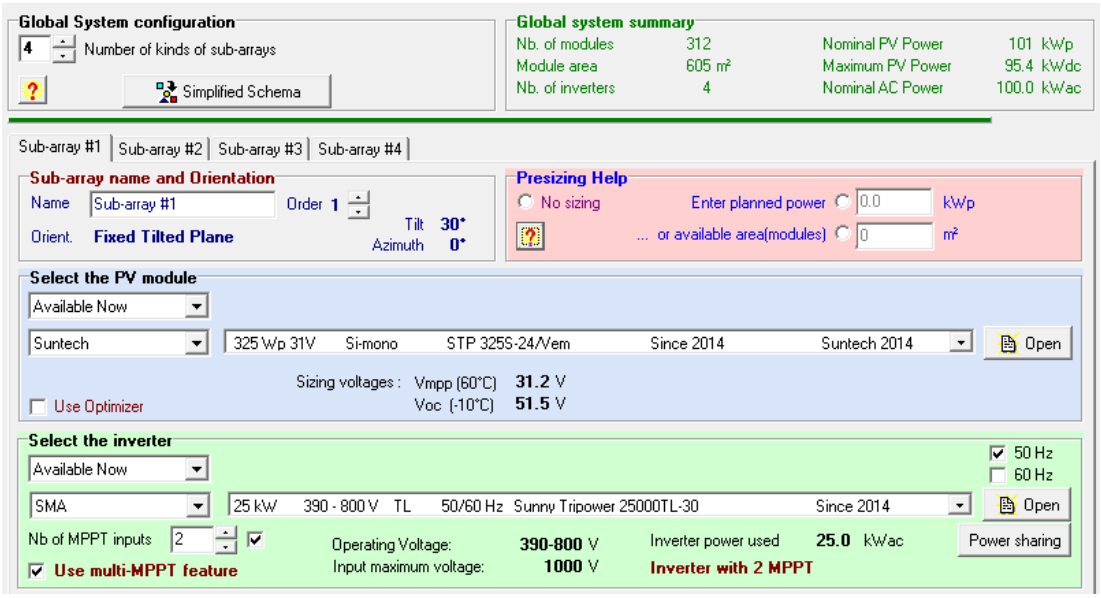

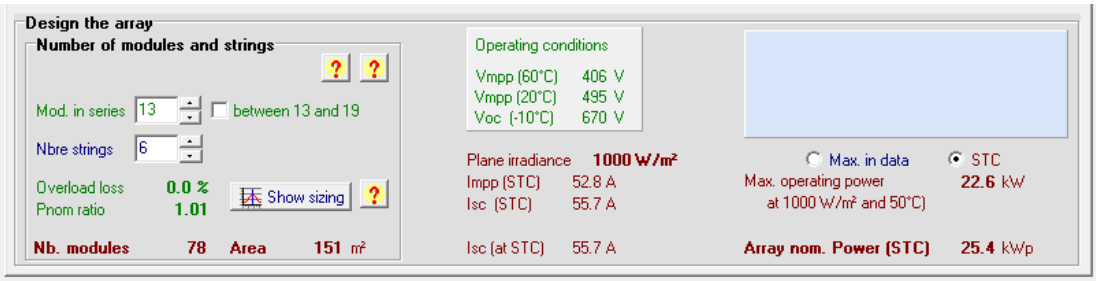

6.3.4 Simulation results

The balances and main results of the simulation are presented in Table (6.7). Comparing the data in Table (6.7) with the corresponding data in Table (5.16) which presented the results obtained from HOMER software, it will be noted that the data in Table (6.7) has values slightly more than those of the data in Table (5.16), this is due to the considered reason in the system modelling which is the three extra added modules to the fourth sub-array.

Table (6.7): Balances and main results of DES system.

	GlobHor kWh/m²	DiffHor kWh/m²	T Amb °C	GlobInc kWh/m²	GlobEff kWh/m²	E Load MWh	E User MWh	E_Grid MWh
January	95.5	31.30	12.89	145.6	142.7	5.28	2.596	8.76
February	109.2	35.30	13.10	148.5	145.5	4.71	2.428	9.04
March	164.0	45.90	15.10	195.6	191.8	5.28	2.853	11.98
April	197.4	50.40	18.87	206.7	202.3	5.08	2.849	12.48
May	232.5	55.50	21.48	218.1	213.2	6.20	3.126	12.85
June	242.1	51.90	23.81	215.4	210.3	7.84	3.854	11.72
July	244.9	52.40	25.75	222.9	217.8	9.65	4.561	11.41
August	224.1	48.40	26.24	223.9	219.1	12.15	5.817	10.16
September	186.6	39.90	25.08	211.9	207.7	10.67	5.178	10.00
October	144.8	37.50	22.34	189.9	186.2	8.02	3.643	10.29
November	105.0	30.00	18.68	156.2	153.2	7.71	3.119	8.61
December	89.0	28.50	14.54	141.0	138.1	8.02	3.139	7.78
Year	2035.1	507.00	19.86	2275.7	2227.8	90.61	43.161	125.09

Chapter Seven

Conclusion, Recommendations and Future Work

7.1 Conclusion

Solar energy as a renewable energy resource has many merits over conventional energy resources. The disadvantage of the solar energy usage is the high capital cost of installing a PV solar system. But, for the long run time, PV systems have a verified economic feasible. There is an orientation toward installing PV system all over the world. PV systems have become the focus which the researchers care about.

In this thesis, PV system components were discussed in details, their types, characteristics and categories were clearly explained. The solar radiation and its related concepts were presented including how to estimate the incident solar radiation on tilted surface facing the sun. In one hand, the PV solar system design principles and sizing of each component were mathematical formulated. In the other hand, PV system components losses were also mentioned.

The selected cases of study were fully described. Those cases were: the Islamic University of Gaza, Al Azhar University and Deir Elatin School PV solar systems. Furthermore, the specifications of each component were explained and the connection diagram of each component was depicted in an illustration figure.

From the results of IUG simulation, it was found that the system can operate as a standalone system in certain months which have a monthly average amount of solar radiation higher than the annual average amount of solar radiation, while in the remaining months, the system operate as a hybrid system. The results showed that the load percentage where the system able to be a standalone system throughout the year was 51% of the actual load connected to the system. But, in this case, the excess electricity was 50.2%, this implies that the system had poor efficiency, therefore it is not recommended to operate the system as permanently standalone. The results also showed that during the sun light hours, the PV array generates power to serve the load and to charge the battery bank, therefore it is recommend taking the required battery charging power into account when designing a standalone PV system. A sensitivity analysis was performed to determine the adequate required number of batteries in different SOC values of the battery bank, it is found from the results that 144 batteries were required for normally operation when the SOC is adjusted to 50%. This is verified in the installed system.

The important results were the system optimization results, where it was found that the rated power of: the PV array was 141.75 kW, the charge controller power was 100 kW and the inverter power was 63 kW also the number of batteries was 144 batteries. Therefore, there is an essential quantum difference between the optimized system and the current system. From the economic point of view, the NPC cost of the optimized and current installed systems were $950478, $1120000, respectively with a difference of $169522.

Regarding DES PV system, the results showed that the system exports annual surplus electricity to the utility grid with an amount equivalent to $6189.35 in the case of grid outage periods. While the amount of exported annual surplus electricity when the utility grid permanently available is equivalent to $12382.28. This shows that the on-grid PV system has promising future and is recommended to install if it is assumed that the utility grid is permanently available in Gaza Strip.

PVsyst is a powerful tool in design PV system. The software gives the ability to accurately model any component of PV system and adjust the parameters and characteristics of that component as needed. As HOMER software allows more flexibility in optimization options, this encourages usage of HOMER in PV systems optimization. PVsyst results were used to confirm HOMER results, in fact the results of both software tools were close to each other.

7.2 Recommendations

Regarding the IUG PV system, taking this research results into consideration is recommend for the concerned parties. The results will help managers to take the suitable decision especially the decision related to the inverters where 63 kW of the inverters was not used.

Installing on-grid PV systems could contribute to solve the problem of electricity shortage in Gaza strip, providing that the utility grid is available through the hour where PV systems will produce the shortage amount of energy during the daytime periods.

Using software tools when designing PV systems is recommend for PV system designers to due to the benefit in obtaining a perfect design. Furthermore, when sizing the components of PV systems, it is recommended for the designers to take the power required to charge the battery bank into account.

7.3 Future work

The future work of this thesis is the simulation of the AAU PV system. The AAU system has the merits of both the IUG and DES systems. The AAU system overcomes the drawbacks of the synchronized shutdown with grid outage as the battery bank keeps the continuity of the power and the excess energy production where AAU is an on-grid system. Also the AAU system has the advantage of reliable energy production.

If it is possible to obtain the yearly load profile of IUG system, the simulation results will be more close to the actual data and the system optimization will give the most optimal configuration of the system.

References

American battery charger company. (2015). *http://www.chargetek.com/basic-information.html*. Retrieved 2018, from Chargetek.

American Chemical Society. (1998). *https://cen.acs.org/articles/94/i18/future-low-cost-solar-cells.html*. Retrieved 2018, from Chemical & Engineering News.

Bellia, H., Youcef, R., & Fatima, M. (2014). A detailed modeling of photovoltaic module using MATLAB. *NRIAG Journal of Astronomy and Geophysics, 3*(1), pp. 35-61.

Brooks, W., & Dunlop, J. (2013). *NABCEP PV Installation Professional Resource Guide.*

CBS Interactive. (1991). *https://www.zdnet.com/article/on-the-us-mexico-border-a-massive-cpv-solar-project-will-rise/*. Retrieved 2018, from ZDNet.

Çelik, Ö., Teke, A., & Yıldırım, B. (2015). Survey of Photovoltaic (PV) Technologies, PV Module Characteristics, Connection Forms and Standards. *Çukurova University Journal of the Faculty of Engineering and Architecture, 2*(30), pp. 137-150.

D'Angelo, A. (2010). *https://www.quora.com/To-increase-the-power-can-we-use-a-magnifying-glass-over-each-solar-cell-panel-to-concentrate-the-sun-beam*. Retrieved 2018, from Quora.

Diab, H., Helw, H., & Talaat, H. (2012). Intelligent Maximum Power Tracking and Inverter Hysteresis Current Control of Grid-connected PV Systems. *International Conference on Advances in Power Conversion and Energy Technologies* (pp. 1 - 5). Mylavaram, Andhra Pradesh, India: IEEE.

Dunlop, J. (2012). *Photovoltaic Systems.* Illinois: American Technical Publishers.

Eby, M. (1995). *http://www.ecmweb.com/green-building/highs-and-lows-photovoltaic-system-calculations*. Retrieved 2018, from Electrical Construction & Maintenance.

Foster, R., Ghassemi, M., & Cota, A. (2009). *Solar Energy: Renewable Energy and the Environment.* CRC Press.

HOMEnergyLLC. (2018). *https://www.homerenergy.com/support/docs/3.11/index.html*. Retrieved 2009, from HOMER energy.

Honsberg, C., & Bowden, S. (2013). *http://pvcdrom.pveducation.org/BATTERY/effic.htm*. Retrieved 2018, from PVEducation.

Jaen, C., Moyano, C., Santacruz, X., Pou, J., & Arias, A. (2008). Overview of maximum power point tracking control techniques used in photovoltaic systems. *International Conference on Electronics, Circuits and Systems* (pp. 1099 - 1102). St. Julien's, Malta: IEEE.

Jakhrani, A., Othman, A.-K., Rigit, A., Samo, S., & Kamboh, S. (2012). Estimation of Incident Solar Radiation on Tilted Surface by Different Empirical Models. *International Journal of Scientific and Research Publications, 2*(12), pp. 1-6.

Jakhrani, A., Samo, S., Kamboh, S., Labadin, J., & Rigit, A. (2014). An Improved Mathematical Model for Computing Power Output of Solar Photovoltaic Modules. *International Journal of Photoenergy, 2014*, 1-9.

Kibria, M., Ahammed, A., Sony, S., Hossain, F., & Shams-Ul-Islam. (2015). A Review: Comparative studies on different generation solar cells technology. *5th International Conference on Environmental Aspects of Bangladesh*, (pp. 51-53). Dhaka, Bangladesh.

Klein, S. (1976). Calculation of monthly average insolation on tilted surfaces. *Solar Energy. 4*, pp. 325-329. Great Britain: Elsevier.

Mahammed, I., Bakelli, Y., Oudjana, S., Arab, A., & Berrah, S. (2012). Optimal Model Selection For PV Module Modeling. *2012 24th International Conference on Microelectronics* (pp. 1-4). Algiers, Algeria: IEEE.

Mahela, P., & Shaik, A. (2017). Comprehensive overview of grid interfaced solar photovoltaic systems. *Renewable and Sustainable Energy Reviews, 68*(1), pp. 316-332.

Mayfield, R. (2010). *Photovoltaic Design and Installation For Dummies.* Indianapolis, Indiana: Wiley Publishing, Inc.

MeteotestAG. (2018). *http://www.meteonorm.com/*. Retrieved from Meteonorm.

Mohammed, S. (2011). Modeling and Simulation of Photovoltaic module using MATLAB/Simulink. *International Journal of Chemical and Environmental Engineering, 2*(5).

Morshed, S., Ankon, S., Chowdhury, T., & Rahman, A. (2015). Designing of a 2kW Stand-alone PV System in Bangladesh Using PVsyst, Homer and SolarMAT. *2015 3rd International Conference on Green Energy and Technology (ICGET)* (pp. 1-6). Dhaka, Bangladesh: IEEE.

Nand, R., & Raturi, A. (2013). Feasibility Study of a Grid Connected Photovoltaic System for the Central Region of Fiji. *Applied Solar Energy, 49*(2), pp. 110-115.

Okedu, K., Uhunmwangho, R., & Ngang, N. (2015). A Comparative Study of on and off Grid Tied Integrated Diesel Solar PV Generation System. *International Journal of Engineering Technologies*, *1*(1), pp. 19-25.

Park, J., Kim, H., Cho, Y., & Shin, C. (2014). Simple Modeling and Simulation of Photovoltaic Panels Using Matlab/Simulink. *Advanced Science and Technology Letters*, *73*, pp. 147-155.

Prasetyaningsar, I., Setiawan, A., & Setiawan, A. (2012). Design Optimization of Solar Powered Aeration System for Fish Pond in Sleman Regency, Yogyakarta by HOMER Software. *International Conference on Sustainable Energy Engineering and Application*, *32*, pp. 90-98. Indonesian.

ProEnerga company. (2016). *http://proenerga.ma/photovoltaics/*. Retrieved 2018, from ProEnerga Technology.

PVsystSA. (2018). *http://files.pvsyst.com/help/index.html*. Retrieved 2012, from PVsyst.

Singh, A., Baredar, P., & Gupta, B. (2015). Computational Simulation & Optimization of a Solar, Fuel Cell and Biomass Hybrid Energy System Using HOMER Pro Software. *International Conference on Computational Heat and Mass Transfer. 127*, pp. 743-750. Cracow, Poland: Elsevier.

Solanki, C. (2013). *Solar Photovoltaic Technology and Systems: A Manual for Technicians, Trainers and Engineers.* India: PHI Learning Private Limited.

Solargis. (2018). *https://solargis.com/?_ga=2.206580880.2062552318.1518847025-1845478521.1518847025*. Retrieved from SOLARGIS.

Solaris Technology Industry. (2014). *https://www.solaris-shop.com/blog/crystalline-vs-thin-film-solar-panels/*. Retrieved 2018, from Solaris.

Solmetric. (2012). *Guide To Interpreting I-V Curve Measurements of PV Arrays.* Solmetric Corporation.

Sumathi, S., Kumar, L., & Surekha, P. (2015). *Solar PV and Wind Energy Conversion Systems.* Springer International Publishing.

Ventura, C. (2011). Theoretical and Experimental Development of a Photovoltaic Power System for Mobile Robot Applications.

Vijay, G. (2014). *http://solar-energy-tech.blogspot.com/2014/08/construction-of-solar-panel_20.html*. Retrieved 2018, from Green Solar Energy.

Wolinsky, J. (2010). *ValueWalk*. Retrieved 2018, from https://www.valuewalk.com/2017/02/solar-panels-explained/.

Xue, Y., & Wang, S. (2013). Photovoltaic Cell Modeling and The Maximum Power Point Tracking Simulation. *2013 International Conference on Materials for Renewable Energy and Environment* (pp. 119-123). Chengdou, China: IEEE.